Hindawi
Advances in Polymer Technology
Volume 2020, Article ID 6187048, 41 pages
https://doi.org/10.1155/2020/6187048

Review Article

3D *In Vitro* Human Organ Mimicry Devices for Drug Discovery, Development, and Assessment

Aida Rodriguez-Garcia,[1,2] Jacqueline Oliva-Ramirez,[3] Claudia Bautista-Flores,[4] and Samira Hosseini [4,5]

[1]*Universidad Autónoma de Nuevo León, Facultad de Ciencias Biológicas, Instituto de Biotecnología, Ave. Pedro de Alba S/N, Ciudad Universitaria, CP 66455, San Nicolás de los Garza, NL, Mexico*
[2]*Laboratorio Nacional de Manufactura Aditiva y Digital (MADiT), Apodaca, NL, Mexico*
[3]*Tecnológico de Monterrey, Escuela de Ingeniería y Ciencias, Ave. Lago de Guadalupe Km 3.5, Cd López Mateos, Atizapán, Estado de Mexico, Mexico*
[4]*Tecnologico de Monterrey, Escuela de Ingeniería y Ciencias, Ave. Eugenio Garza Sada 2501, Monterrey, 64849 NL, Mexico*
[5]*Tecnologico de Monterrey, Writing Lab, TecLabs, Vicerrectoría de Investigación y Transferencia de Tecnología, Monterrey, 64849 NL, Mexico*

Correspondence should be addressed to Samira Hosseini; samira.hosseini@tec.mx

Received 17 April 2020; Accepted 30 June 2020; Published 10 August 2020

Academic Editor: Mona Semsarilar

The past few decades have shown significant advancement as complex *in vitro* humanized systems have substituted animal trials and 2D *in vitro* studies. 3D humanized platforms mimic the organs of interest with their stimulations (physical, electrical, chemical, and mechanical). Organ-on-chip devices, including *in vitro* modelling of 3D organoids, 3D microfabrication, and 3D bioprinted platforms, play an essential role in drug discovery, testing, and assessment. In this article, a thorough review is provided of the latest advancements in the area of organ-on-chip devices targeting liver, kidney, lung, gut, heart, skin, and brain mimicry devices for drug discovery, development, and/or assessment. The current strategies, fabrication methods, and the specific application of each device, as well as the advantages and disadvantages, are presented for each reported platform. This comprehensive review also provides some insights on the challenges and future perspectives for the further advancement of each organ-on-chip device.

1. Introduction

Prior to testing a new drug in a clinical trial, principal phase analysis on the pharmacodynamics and pharmacokinetics takes place using animal models and/or two-dimensional (2D) *in vitro* models. Such analyses could prevent adverse drug events and predict organ toxicity and drug mechanisms prior to testing on human beings [1], while offering economic benefits and time reduction between drug discovery and clinical trials [2]. Despite the technological advancements in animal or 2D drug testing, the development and application of new therapeutic products face multiple barriers prior to clinical trials. While various animal models are genetically altered to mimic the human body for drug testing and screening, the inability to replicate key facets of the human body makes such trials limited with respect to drug efficacy and safety assessments. *In vitro* studies, on the other hand, allow a certain degree of progress, although as yet they cannot replace clinical trials on humans [3]. In particular, traditional *in vitro* analysis is incapable of mimicking the human body due to the lack of surrounding stimulations each organ undergoes in a living body or in some cases the studies are performed in different species [3, 4].

In the past few decades, more complex *in vitro* humanized systems have replaced animal studies and 2D *in vitro* analysis as they closely mimic the organ of interest and can

incorporate the necessary stimulations (physical, electrical, chemical, and mechanical) that an organ can experience. Since the advent of cell culture systems and microfabrication techniques, the organ-on-chip technology has gained momentum as one of the pioneering technologies for drug metabolism analysis [1]. Organ-on-chip devices fall under the category of microfluidics or biomicroelectromechanical system (Bio-MEMS) with main components including cells, media, tissues, and scaffolds [1, 5]. The principal approaches in in vitro organ-specific tissue modelling include three-dimensional (3D) organoids or spheroids, 3D microencapsulation within microgels, bioprinted organ platforms (e.g., cell-seeded scaffolds), and bioreactor-incorporated devices [6–8].

In vitro modelling including 3D organoids, 3D microfabrication, and 3D bioprinted platforms for several organs was presented. Such platforms fabricate human mimicry systems including the heart, kidney, lung, intestinal tract, liver, retina, bone, and brain [9]. Organ-on-chip devices facilitate drug testing on different cell lines, while multiple-organ-chip platforms study the pathways of different drugs and their efficacy on one organ in correlation with others [2]. Human-on-chip devices provide a deeper understanding of drug metabolism, pharmacokinetics, and toxicity on the human body as a unified physiological entity. Moreover, the addition of one or more biosensors for continuous monitoring of biomarkers has led to further comprehension of the metabolic changes *in situ*. The personalized medicine, in turn, could be highly promoted by organ-on-chip devices as they require a small tissue sample from the patient to replicate the organ [10]. Nonetheless, organ-on-chip and human-on-chip platforms also suffer from certain shortcomings, including the complexity of the operation due to the device size and the inconsistency of the results from one laboratory to another [11]. Undoubtedly, the microenvironmental control and monitoring to maintain the long-time cell culture without changing the microorgan's physiology and morphology are some of the major challenges yet to overcome. Moreover, the variability of the organogenesis throughout tissue development has to be carefully controlled in order to meet the expected objectives of an organ-on-chip device [12]. This review article concentrates on the latest updates of in vitro human mimicry systems for drug assessment. In that perspective, we narrow down the focus of this article to the advances of the organ physiology mimicry in on-chip devices with respect to drug discovery, development, and assessment for the selected organs: liver, kidney, lung, gut, heart, skin, and brain. Moreover, the review article provides some insights on human-on-chip devices and the application of such devices for drug assessment and screening.

2. Organ-on-Chip Strategies

2.1. Liver-on-Chip. The liver plays a critical role in drug metabolism, body homeostasis, digestion, and the elimination of toxic substances. *In vitro* human liver models are used to evaluate the metabolism and toxicity of chemical compounds and drugs and for the evaluation candidate drugs in cancer research and genetic studies [13]. Experiments can be carried out using primary cells isolated from patients or using cells from cell banks, such as the American Type Culture Collection (ATCC) [14]. Furthermore, cell culture systems allow researchers to understand drug absorption, distribution, metabolism, and excretion and to assess their pharmacokinetic and pharmacodynamic parameters. Human liver cells lose many functions in normal culture, including drug-metabolizing and drug transport activities, which are basic for drug discovery. 2D cultures have other limitations, including the alteration of cell morphology, the loss of polarity and phenotype, and the change in gene expression [15].

Current *in vitro* systems evaluate the toxicity of new drugs using different human hepatic cell lines, such as hepatocytes, liver sinusoidal endothelial cells (LSEC), human liver cells (HepG2), and a hepatic stem cell line (HepaRG). Hepatocytes are the main parenchymal cells that comprise the cell plates of the lobule, carrying out most of the metabolic functions of the liver [16]. LSEC are thin, elongated cells that are part of the reticuloendothelial system (RES) and play a role in maintaining the homeostasis and hepatic immunity [17]. HepG2 and HepaRG cells are immortalized cell lines that can be used as an alternative to primary cells for drug screening and toxicological studies. HepG2 are derived from a hepatocellular carcinoma and are frequently used for the evaluation of drug toxicity due to the expression of liver-specific enzymes and nuclear transcription factors, including p53 and Nrf2, which are essential for drug metabolism [18]. HepaRG are also derived from a hepatocellular carcinoma. These cells have two different cell morphologies; however, they can be differentiated on treatment with dimethyl sulfoxide (DMSO). Therefore, under appropriate cell culture conditions, HepaRG represents the most suitable cell line for long-term studies of a slowly metabolized drug and for determining the mechanisms associated with exposure to xenobiotics [19]. Another concept that must be considered in the evaluation of the metabolism and toxicity of drugs is drug-induced liver injury (DILI), which is associated with acute liver failure and is the main reason for the subsequent market withdrawal of approved drugs [20]. The major advances in molecular pharmacology and toxicology, hand in hand with novel strategies for development of 3D liver models, allow for the improved recreation of cell-cell interactions within their own microenvironment, as well as endowing a more permissive, tissue-like, microenvironment for long-term culture that can improve hepatotoxicity predictions [21]. Some of the latest examples of liver-on-chip platforms for drug discovery, development, and analysis are thoroughly reviewed in this article (Table 1).

2.1.1. Analysis of Drugs in Liver-on-Chip Devices. The liver plays a key role in all metabolic processes in the human body, such as body homeostasis, drug metabolism, and the detoxification of blood; therefore, an adequate liver model is a necessity for drug development [22]. Hepatocytes cultured within 2D *in vitro* models lose many functions and activities, limiting their modelling function. For that reason, 3D liver-on-a-chip models are an excellent option for *in vitro* liver analysis. The engineered hepatic tissues in 3D devices, however, should closely mimic the natural functions of the organ.

Table 1: Summary of recent advancements hepatotoxicity testing including the type of drug, the application, the applied cell lines, and the kinetics.

Drug type	Application	Applied cell lines	Kinetics	Ref(s)
Acetaminophen, clozapine, olanzapine, fialuridine, entecavir, aminophenol	Biotransformation, hepatotoxicity	Human hepatocytes from donors	7 days of culture, 48 hr stimuli	[32]
Amiodarone, acetaminophen	Hepatotoxicity due to mitochondrial respiration analysis	HepG2/C3	28 days	[39]
Acetaminophen-omeprazol, acetaminophen-rifampicina, acetaminophen-ciprofloxacin	Drug-drug interaction	HepG2, HUVEC EA.hy926, stellate, U937		[38]
Acetaminophen	Hepatoxicity	HepG2/C3	30 days	[23]
Acetaminophen, isoniazid, rifampicin	Drug-drug interaction, hepatoxicity	Lobule-like HepG2, HAEC	4 days	[136]
Diclofenac	Biotransformation	Multicellular platform: Hu8150 and HK8160	7 days	[30]
Phenacetin, diclofenac, lidocaine, ibuprofen, propranolol, prednisolone	Biotransformation variability	Human primary hepatocytes from donors	7 days	[31]
Bupropion/2-phenyl-2-(1-piperidinyl)propane), tolbutamide/sulphafenazole, omeprazole/ benzylnirvanol, testosterone/ketoconazole	Development of CYP450 inhibitors	HepaRG	24 hrs	[26]
Warfarina, dasatinib	Drug-drug interaction	HepaRG	24 hrs	[27]
Midazolam, phenacetin, acetaminophen	Biotransformation	Human primary hepatocytes	13 days	[35]
Tolbutamide, testosterone	Hepatic clearance by CYP3A1 and CYP2C11	Rat hepatocyte primary cell culture	15 days	[137]
Adaptaquin (HIF PHD inhibitors)	Hepatotoxicity	HepaRG	48 hrs	[138]
Adaptaquin and analogs	Biotransformation, hepatotoxicity	HepaRG	24 hrs	[36]
Rifampin, ketoconazole	Hepatotoxicity	Hepatic stellate cells isolated from rat	~14 days	[42]
Vitamin D	Biotransformation	HepG2 cells, RPTEC	~5 days	[139]
Vitamin E (-tocoferol)	Biosynthesis of metabolites to target 5-lipoxygenase	Human-liver-sinusoid, HepaRG cells, HUVEC, human monocyte (PBM)	~5 days	[40]
Ethanol	Detoxification and hepatotoxicity	HepG2	4 days	[24]

CYP450: cytochrome P450; HepG2/C3: human hepatocellular carcinoma/complement factor 3; HUVEC: human umbilical vein cell line; EA.hy926: endothelial cell; U937: human histiocytic lymphoma; HAEC: human aortic endothelial cell line; Hu8150: primary human hepatocytes; HK8160: human Kupffer cells; HepaRG: hepatic biprogenitor cell line; CYP3A1: cytochrome P450 3A1; CYP2C11: cytochrome P450 2C11; RPTEC: renal proximal tubule epithelial cells; PBM: peripheral blood mononuclear cells.

In order to monitor the physiology of the liver cells, some studies quantified the hepatic biomarker concentration (e.g., albumin, transferrin, alpha-1 antitrypsin, and ceruloplasmin) by the liver spheroids [10]. Also, immunophenotyping is frequently used to prove the identity or the structure of the hepatocyte, such as cytokeratin 18, MRP2 bile canalicular protein, and tight junction protein ZO-1. It is critical that these molecules maintain their expression over time [23, 24].

Prior to drug absorption within the body, metabolism of the xenobiotic agent occurs. This pathway transforms the drug into a hydrophilic molecule, which, in turn, helps during excretion. Depending on the drug, the biotransformation may occur in different organs, including the liver. There are two main phases for such biotransformation. Primarily, the molecule is modified by the addition of functional groups (hydroxy groups, epoxides, etc.). The enzymes from the family of the cytochrome 450 (CYP450) conduct these reaction processes. There are several isoforms of these molecules which may change between species. This change is essential, while there is no standard model that mimics all the isoforms. In humans, CYP3A4 catalyzes over 50% of the drugs and CYP2D6 over 20%. The second phase in the metabolic reaction process is to create a hydrophilic metabolite through the conjugation of charged groups.

The stability in the expression of CYP450 is a significant event in order to generate an efficient model. Such stability was studied by Ortega-Prieto et al. in 2018. The authors created a microbioreactor, with medium recirculation by a pneumatical micropump. The recirculation speed of the media allowed the nutrients and oxygen levels to remain stable. The primary hepatic spheroid attachment in the

microfluidic reactor was generated by a coated collagen polystyrene (PS) scaffold. The results show in primary human hepatocytes with micropump medium recirculation that the levels of CYP450 remained the same over forty days. This result represented 3-4-fold improvement compared to 2D platforms. Furthermore, a long-term hepatitis B model of infection was created by which the viral concentration over 12 days was monitored. An increase in the cytokines and immune receptors was observed when they were treated with interferon-alpha. The study was also able to predict human host responses against HBV. Moreover, with the addition of other, nonparenchymal hepatic cells, such as Kupffer cells, an efficient viral clearance was obtained. As a result, the device identified essential biomarkers at the early stages of infection [25].

The liver-on-a-chip devices also facilitate studying metabolic pathways in preclinical phases. Zakharyants et al. in 2016 and 2017 induced organoids using HepaRG cells and cultured them into a microbioreactor device with recirculating media in order to test the expression of CYP450. In the first study, the results showed the genetic expression of four isoforms of CYP450, including CYP2B6, CYP2C9, CYP2C19, and the most crucial one, CYP3A4. The authors tested several inhibitors for each isoform. The conclusion was that the 3D model recreated the regular expression of isoforms compared with static cultures. With these results, a second study was performed in which the authors tested the drug interaction of warfarin and dasatinib. Warfarin biotransformation was associated with CYP2C9 isoform, and dasatinib with CYP3A4. The study showed that the use of warfarin with compounds metabolized by the same isoform (CYP2C9) could lead to drug-drug interactions [26, 27].

Human primary hepatocytes are the cells frequently used for the analysis of drug toxicity. However, their limited *in vitro* proliferation capacity has prompted the search for alternative cells. Spheroids have been reported as a promising model to study *in vitro* hepatotoxicity, demonstrating better results than conventional 2D cell culture models. Furthermore, 3D spheroid cultures show appropriate sensitivity to analyze the biomarker's responses induced by hepatotoxic drugs. Foster et al. [28] evaluated the hepatotoxicity risk assessment of acetaminophen and fialuridine by monitoring the release of the hepatic biomarkers α-GST and miR-122. Both hepatotoxins produced dose- and time-dependent increases in miR-122 and α-GST release. These results confirm that the liver-on-a-chip model is sensitive for drug assessment [28].

During the *in vitro* culture of primary hepatocytes, many phenotype-specific functions are lost or significantly diminished. To maintain these functions, a fluidic 3D microreactor platform was introduced to preserve the metabolic activity of the human hepatocytes for more than two weeks. Long et al. [29] and Sarkar et al. [30] performed two different studies using liver-on-chip devices for preclinical studies. Both groups obtained the microdevice from CN Bio Innovations in which a pneumatic pump controlled the fluidic system and moved the media through the polyurethane membrane scaffold positioned between cells and pneumatic plates. Primary human hepatocytes (Hu8150) from healthy donors and Kupffer cells were cultured in this device. Long et al. (2016) tested the CYP450 activity under chronic inflammatory conditions and the effect of a biological drug named tocilizumab, which is a monoclonal antibody for rheumatoid arthritis. In this pathology, the inflammatory molecules decreased the CYP450 activity. The microdevice measured the drug activity and the CYP450 isoform recovery. Furthermore, the drug-drug interaction was analyzed with simvastatin [29]. Sarkar et al.'s work, on the other hand, is aimed at evaluating the biotransformation of diclofenac in the microdevice and compared the results with known *in vivo* metabolic profiles. The results showed similar metabolites for biotransformation in phases I and II, as reported within the human body. Moreover, the drug-induced toxicity measured by the protein markers, including albumin and lactate dehydrogenase (LDH), was found to be similar. By inducing inflammation, the authors created an immunocompetent model for the discovery of early biomarkers, proving the mimetic potential of 3D microfluidic devices [30].

The same bioreactor (CN Bio Innovations) also facilitated drug metabolite measurements for six different drugs. The objective of this study was to identify the variability of drug responses using four healthy hepatic cell donors. This variation refers to an individual average of intrinsic drug clearance. The device was suitable for analyzing the interdonor variability due to differential drug metabolites, LDH production for toxicity, hepatic gene expression levels, and hepatic albumin excretion [31]. Hepatic cells were the only cell types cultured in this bioreactor. This poses a shortcoming, as CYP450 isoform expression depends on the full cellular environment of the liver.

The traditional 2D human hepatocyte culture methods are reported to decrease, and eventually lose, the expression of the CYP450 isoforms [32]. In particular, the activity analysis of some isoforms of CYP450 reported in several studies has demonstrated a downregulation of CYP1A2, 2E1, and 3A4 within 14 and 28 days. These results suggest that microfluidic devices are more sensitive than the current 2D plate-based cultures [33]. A report from Proctor et al. [34] presents the testing of over 100 different drugs and their cytotoxicity within both 2D and 3D culture systems. The authors indicated that the 3D culture platforms allowed for easier manipulation and offered higher sensitivity than 2D cultures, while maintaining the specificity of *gold-standard* culture assays.

In microfluidic cultures, hepatocytes cultivated for 13 days have shown an increase of CYP2B6, CYP2C19, CYP2C8, CYP1A2, CYP2D6, and CYP3A4 mRNA and other molecules, including SULT1A1, UGT1A1, and HNF4a, during the kinetic analysis. This is in contrast with their Petri dish control cultures in which the increase in the number of molecules occurred only towards the end of the kinetic analysis [35, 36]. In monitoring these proteins, other studies have confirmed that a gradual, and significant, increase in CYP1A1, CYP1A2, CYP2E1, and CYP3A4 occurred using chip-based devices in comparison to 2D cultures [37].

Due to its well-known, high propensity induction of hepatotoxicity, acetaminophen is a drug that has been tested in several reports. Liver-on-a-chip devices have proven to be accurate in assessing the cytotoxic analysis and drug-drug

interaction of acetaminophen. Deng et al. [38] fabricated a 3D liver-sinusoid-on-a-chip (LSOC) by a lithographic technique using polydimethylsiloxane (PDMS) and polymethylmethacrylate (PMMA) with two polycarbonate (PC) porous membranes to mimic the microenvironment of the liver sinusoid (Figure 1). In this model, the authors introduced a multicellular culture using human hepatocellular carcinoma (HepG2) cells as a source of hepatocytes, human umbilical vein cells, human stellate cells, and human histiocytic lymphoma U937 cells to recreate the liver endothelium and stroma [38]. The drugs were perfused in the artificial blood, and cell viability was determined with methyl-thiazolyl-tetrazolium (MTT). The results showed that the hepatotoxicity of drug-drug interaction was 17.15% for acetaminophen-rifampicin, 14.88% for acetaminophen-omeprazole, and 19.74% for acetaminophen-ciprofloxacin. The results confirmed that this microfluidic liver model can be used to evaluate the hepatotoxicity of drug-drug interactions [38].

Some drugs may induce cell injury by inhibiting the mitochondrial enzyme function or even directly interrupting the respiratory complex. The tracking of oxygen consumption in this process could predict the toxic effect of these drugs. To analyze this type of metabolism, a microbioreactor with a removable inner microwell of PDMS bonded to glass coverslips was developed. The outer part of the device was fabricated with stainless steel and a top glass window. The device was equipped with a fusion touch syringe pump to perfuse the media. Each well was coated with collagen and cultured with HepG2/C3A and HeLa cells. Using a luminescence quenching assay, the authors quantified real-time oxygen, distribution of amiodarone and acetaminophen, and toxicity. When acetaminophen and amiodarone were introduced into the system, they showed the progressive inhibition of complex III of the mitochondrial electron transport chain and hepatotoxicity independent of CYP450 [39].

Pein et al. [40] fabricated a biochip with two polyethylene terephthalate (PET) porous membranes separated into upper and lower chambers and sealed with PS. The first and last microchannels contained human umbilical vein endothelial cells (HUVECs) and macrophages, and the central channel hosted the hepatic compartment with HepaRG hepatocytes and stellate cells. The device demonstrated vitamin E metabolites to act as inflammatory suppressors and elucidated the metabolic pathway. Moreover, the multicellular chip allowed for identifying the cellular features, such as chemotaxis, cytokine production, and cellular regulation, induced by the vitamin E metabolites [40].

The physiological elements measured in most of the studies that represent a healthy liver are albumin and urea production. If the concentration of either of these metabolites is impaired, it may result in hepatotoxicity. Mi et al. [41] developed a device consisting of a PDMS/glass chip with three chambers. The system consisted of an upper layer fabricated by lithography using PDMS and a lower layer of a glass slide (Figure 2(a)). The upper chamber contained the medium and the factors, while the middle and lower chambers were used for HepG2-laden collagen and HUVEC-laden collagen culture, respectively (Figures 2(b)–2(d)). The amounts of albumin and urea were evaluated over a period of 7 days after acetaminophen treatment. The results showed that albumin secretion and the urea concentration decreased with increasing acetaminophen concentration. The device achieved biomimetic functions and structure by maintaining bioactivity for seven days, while it has exhibited great potential for hepatotoxic drug screening [41].

Bhise et al. (2016) designed a platform that enables the bioprinting of hepatocyte spheroid-laden hydrogel constructs directly in the culture chamber of a bioreactor. The system consisted of three chambers divided by layers of PDMS and PMMA covered by a glass slide. Spheroids were then mixed with gelatin methacryloyl (GelMA) and printed in the middle chamber (Figures 3 and 4). The bioreactor can be disassembled to access the cells for biological assessment during the long-term culture period. The platform maintained the cultured spheroids viable and active for thirty days and represents an important step towards the fabrication of automated systems for high-throughput drug screening [23].

An important characteristic of the liver is its zonation, meaning that cells from different parts of the lobule are affected differently by structurally diverse and functionally different toxins. DILI triggered by various drug types that are metabolized in different zones of the liver is typically a cause for acute and chronic liver diseases. Weng et al. [42] fabricated a liver-on-a-chip consisting of a micropatterned collagen-coated PDMS membrane with diverter plates of polycarbonate (PC) to sandwich the membrane and a peristaltic pump for medium circulation (Figures 5(a)–5(f)). Stained primary liver cells (PLCs) were deposited on the membrane and incubated overnight (Figure 5(g)). Cells under controlled microenvironmental conditions were able to differentiate, and hepatic zonation and a dose-dependent effect of acetaminophen were observed. This device showed great potential for studying drug-induced liver injury in a more detailed manner [42].

Significant efforts have been made in developing microfluidic platforms for predicting human pharmacokinetics and pharmacodynamics using *in vitro* human models. 3D liver-on-chip models hold great potential for understanding the mechanisms of drug hepatotoxicity and for improving the *in vitro* ADME methods during drug development. Challenges such as reproducibility, 3D miniaturization of the proximal tubule, the use of appropriate materials for the device fabrication, and the stem cell differentiation are yet to be addressed for clinical applications. Cell-cell interaction and a dynamic microfluid flow have permitted mimicking the physiological environment and the maintenance of liver function. Therefore, facilitating a longer-term culture of hepatocytes which allows for the exploration of the modes of action and the biological responses to drugs and drug interactions is of great importance.

2.2. Kidney-on-Chip. The kidneys are involved in maintaining homeostasis in the several physiologic operations of the body, including the filtration and retention of essential compounds, blood pressure, and physiological pH regulation. The kidneys also mediate the excretion of waste materials, excess drugs, and their metabolites during drug metabolism. Due to these last functions, the analysis of the drug toxicity is

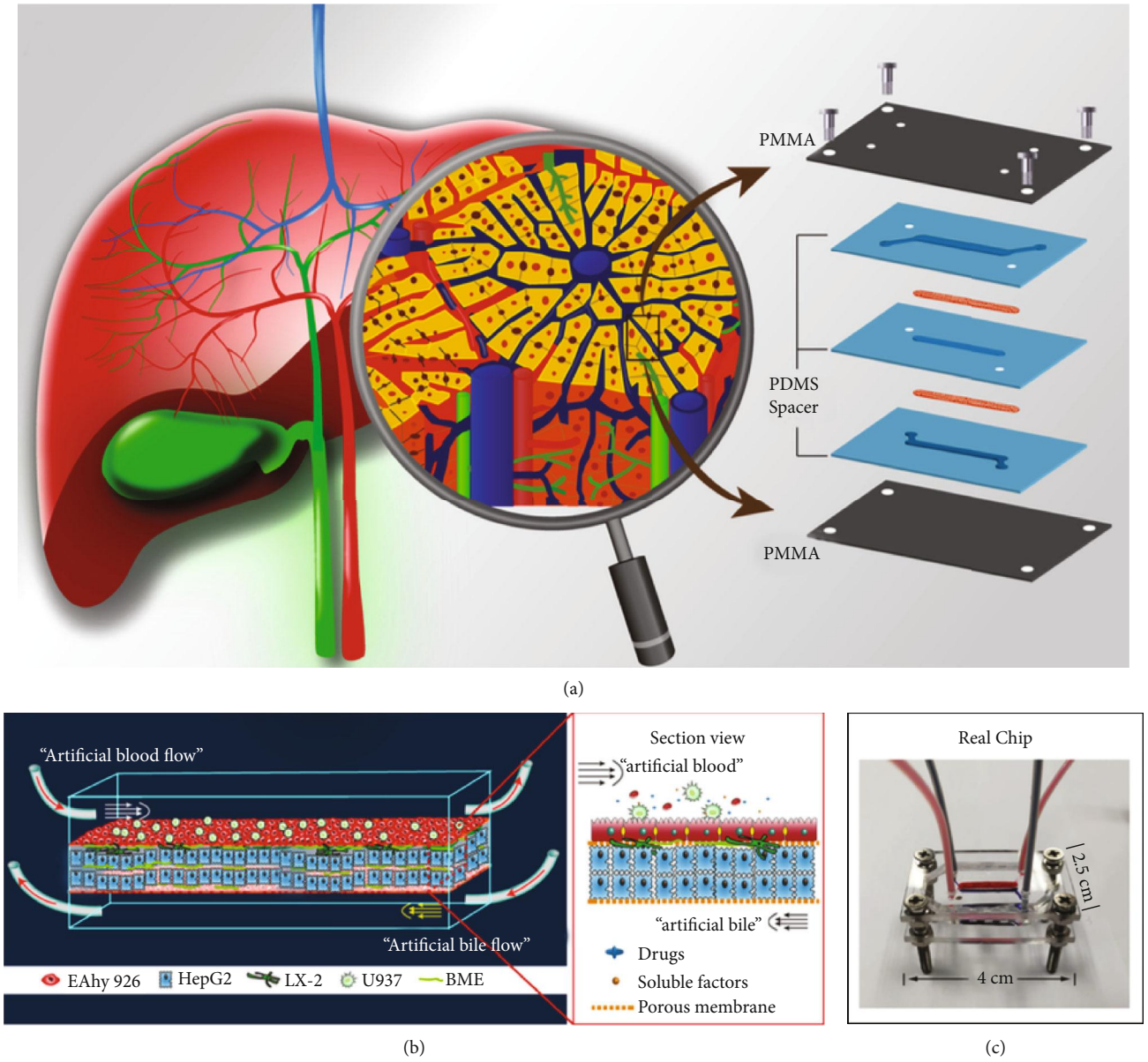

FIGURE 1: (a) Schematic of a liver sinusoid structure and the LSOC microdevice. Left: an illustration of the physiological structure of the liver sinusoid in the liver. Right: the design of the LSOC microdevice. (b) Schematic diagram of four cell lines seeded in the device. (c) Picture and size measurement of the chip. Reproduced (or adapted) with permission [38], ©2019, American Institute of Physics.

frequently performed within kidney model platforms [43]. The two factors that influence such excretion of waste compounds are the glomerular filtration rate (GFR) and the renal blood flow (RBF). While the primary factor delivers the drug to the kidney, the GFR eliminates the metabolites. The minimal functioning unit of a kidney is a nephron, consisting of the glomerulus, loop of Henle, and the proximal convoluted tubule. The glomerulus is where the major blood filtration process occurs. It consists of a network of capillaries through which circulating blood can be filtered in the urine, making it the most important part of the renal system. The tiniest construction element of this network is called a podocyte, a highly differentiated epithelial cell type that constitutes a major proportion of the kidney filtration barrier and regulates selective filtration. Renal function progressively reduces in the elderly, which may result in two pathologic entities: chronic kidney disease (CKD) (including glomerulonephritis, hypertensive nephrosclerosis, and diabetic nephropathy) and acute kidney disease (AKD) when blood clots or cholesterol deposits gather around the kidneys. Typically, drug excretion in these patients is impaired.

In vivo drug administration results in a complex process; the main focus of kidney-on-a-chip devices is to mimic the kidney physiology and function in order to determine the nephrotoxicity caused by the administration of different drugs [44]. In the design and development of a kidney-on-a-chip device, therefore, mimicking both factors (GFR and RBF) is of great importance. The complexity of the kidney anatomy makes it rather difficult to mimic the full organ on the chip (Figure 6). For that reason, the majority of the

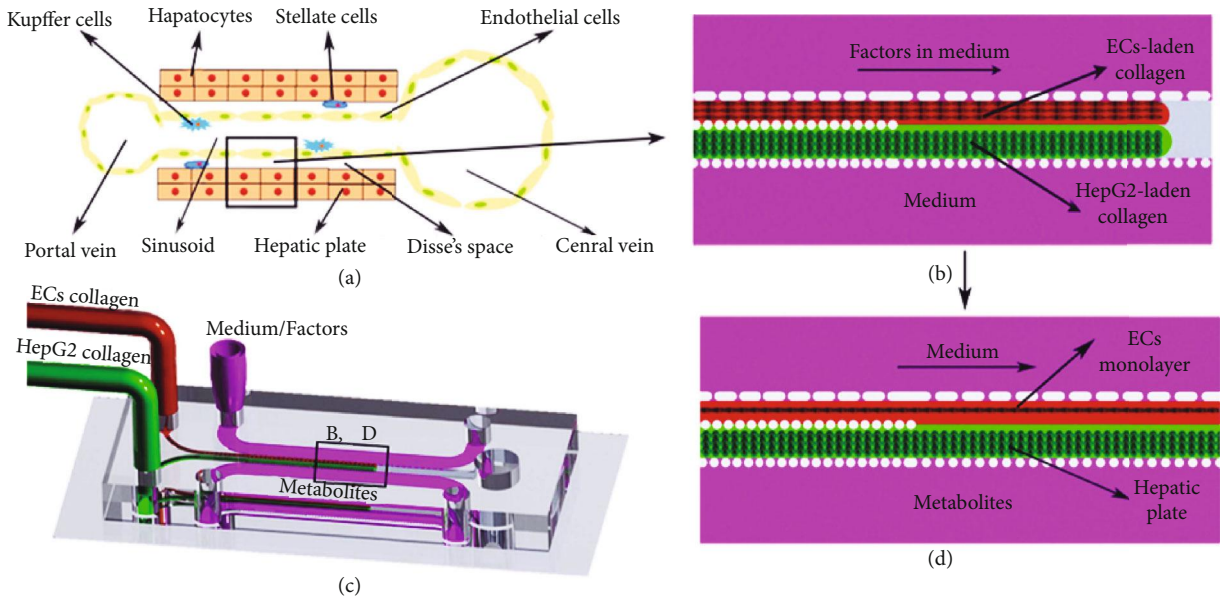

Figure 2: Formation of the biomimetic liver sinusoid on a chip. (a) Schematic diagram of a liver sinusoid. Hepatic plates and endothelial cell (EC) monolayers are the main part of this unit. (b) Injection of cell-laden collagen and medium with factors. (c) The 3D schematic diagram of collagen and medium injection process. (d) After the stimulation of factors for two days, an EC monolayer formed and medium with factors was changed to medium without factors, forming the liver sinusoid on a chip. Reproduced (or adapted) with permission [41], ©2018, IOP Science.

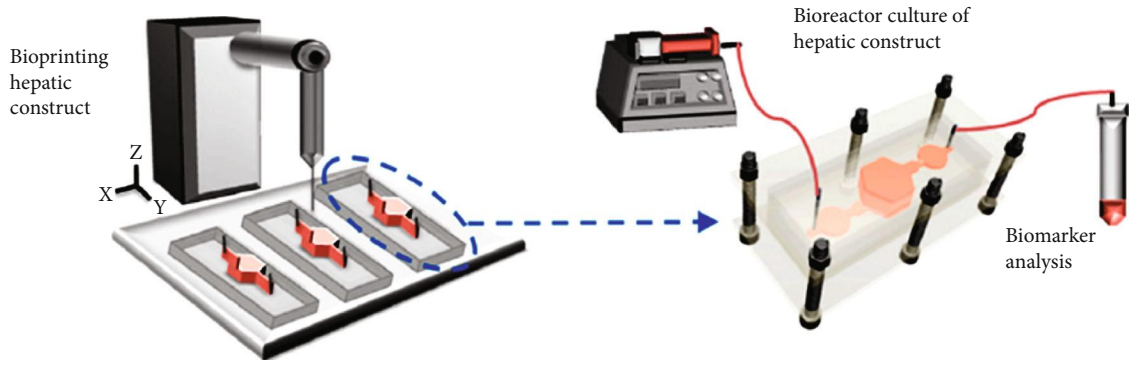

Figure 3: Schematic of the hepatic bioreactor culture platform integrated with a bioprinter and biomarker analysis module [23], ©2018, IOP Science.

studies focus on specific parts of the kidney, including the tubules or the glomerulus [45–47]. Some devices mimic solely a glomerulus-on-a-chip to measure nephrotoxicity or drug interactions, while others may mimic the renal tubular cells from a different part of the tubules in order to measure the toxicity damage or to simulate the urine flow rate.

The most common cell type used for the *in vitro* evaluation of kidney toxicity includes kidney proximal tubule epithelial cells (PTECs) [48, 49], immortalized kidney epithelial cells (HK-2) [50], dog kidney cells (MDCK), pig kidney cells (LLC-PK1) [51], and human proximal tubular epithelial cells (HPTECs) [52]. Traditional 2D culture systems or static organoid systems do not mimic the structural and functional characteristics of these cells [47, 49, 53–55]. Other studies are focused on mimicking nephrons in order to demonstrate a relationship between fluid flows and primary cell functionality [56]. With this overview, 3D models of kidney tissue that analyze human responses are essential for drug screening, disease modelling, and kidney organ engineering for tissue remodelling [56, 57]. Some of the latest examples of kidney-on-chip platforms for drug discovery, development, and analysis are thoroughly reviewed in this article (Table 2).

2.2.1. Analysis of Drugs in Kidney-on-Chip Devices. Traditional *in vitro* and *in vivo* studies using animal models are limited as there is a difference between the drug pharmacokinetics and pharmacodynamics in humans and in animals. An accurate system that identifies the nephrotoxicity of several compounds during the preclinical testing, therefore, can overcome the drawbacks of traditional models. Kidney-on-chip devices show excellent potentials in mimicking the structure and physiological environments of the organs while

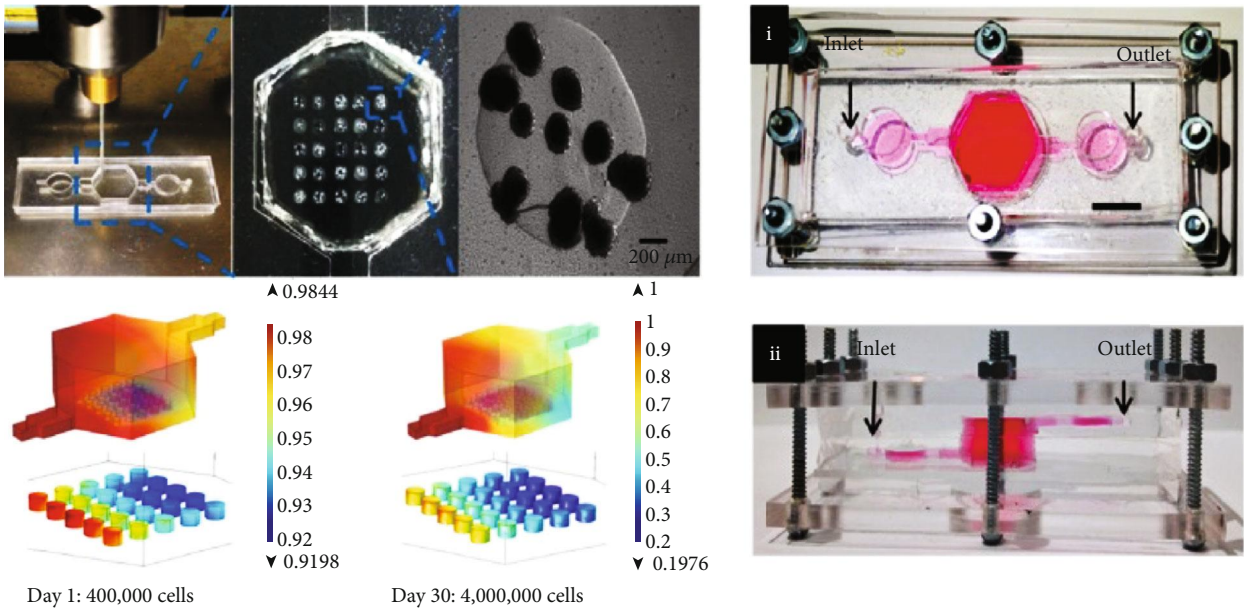

Figure 4: Bioprinting GelMA hydrogel-based hepatic construct within the bioreactor as a dot array. Top view (i) and side view (ii) of the assembled bioreactor with the inlet and outlet fluidic ports as indicated along with the oxygen concentration. Reproduced (or adapted) with permission [23], ©2018, IOP Science.

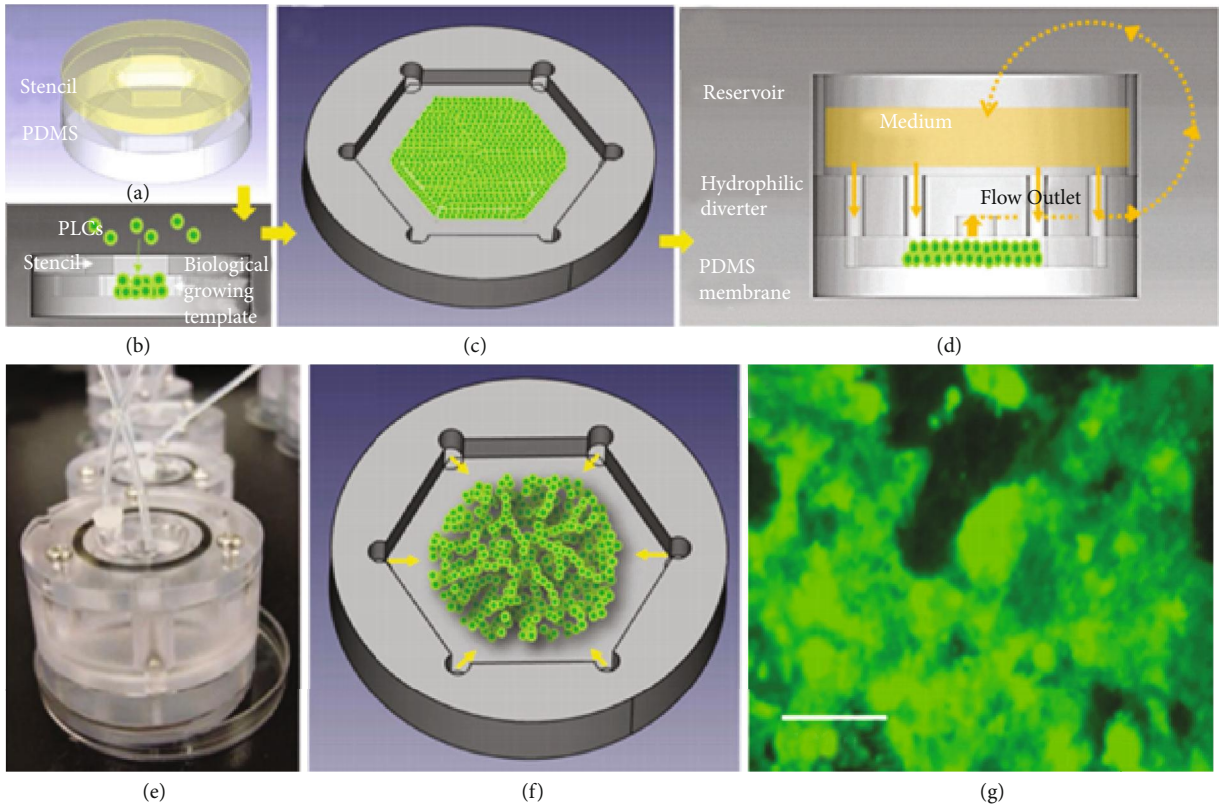

Figure 5: Design principles of a tissue incubator. Multilayered PLCs were deposited on PDMS membrane through a stencil (a) to create a biological growing template (b) and a hexagonal contour (c). After overnight culture, the stencil was removed, and a hydrophilic diverter was assembled with a reservoir to create micro-/macrocirculation (d). The hydrophilic diverter provides PLCs with vertical anchorage. (e) Photograph of the entire device. (f) Schematic diagram of the radial flow. (g) Liver-on-a-chip (LOC) shows the cell viability (green). Reproduced (or adapted) with permission [42], ©2017, Wiley Online Library.

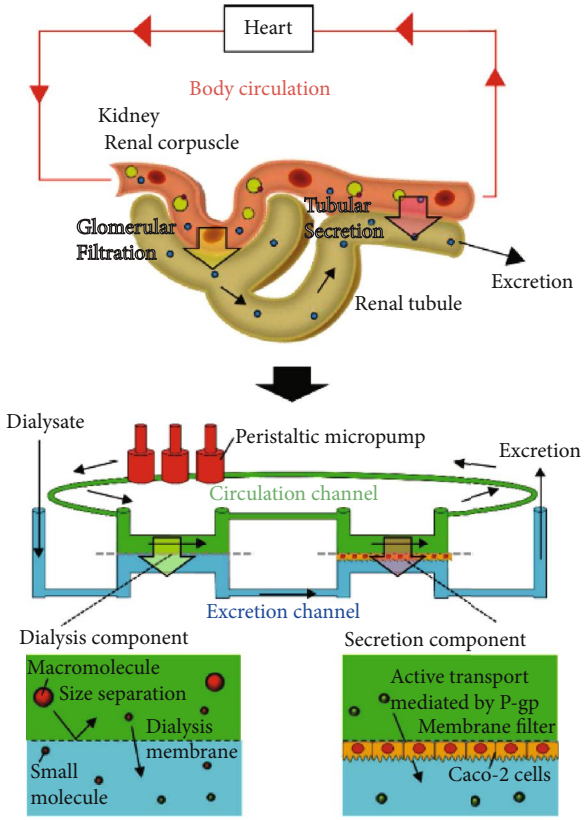

FIGURE 6: Renal excretion in the human body and the microfluidic kidney model which mimics the glomerular filtration and tubular secretion in the kidney. Reproduced (or adapted) with permission [45], ©2018, J-STAGE.

predicting drug effects, interactions, and toxicity. A microfluidic kidney-on-a chip device mimicked the differentiation of human-induced pluripotent stem cells (hiPSC) into mature podocytes that express markers for this phenotype. The device was fabricated through stereolithography using SU-8, silicon master mold, and PDMS. Four microchannels with two layers separated by a porous membrane created an ECM-cell interface to provide the appropriate culture media and to apply fluid shear stress (FSS). The array has proven to closely resemble the physiological behavior of *in vivo* environments. The authors have tested two different dosage assays under shear stress condition: (i) a daily gentamicin dose as a classic oral administration and (ii) a continuous infusion regimen. The cell mortality was 2% higher with the continuous regimen, which predicated that a normal regimen of 7-14 days would show a different pharmacokinetic profile. Also, the cell injury protein levels depended on the drug administration regimen. The study proved that one drug can lead to various outcomes and potentially damage kidney cells, depending on the way it is administered [54].

Primary cell lines cultured in the *in vitro* systems lack maintaining their physiological functions over an extended time. Induced pluripotent stem cells or immortalized cells have demonstrated to reproduce the proximal tubule characteristics. They are able to differentiate into podocytes and maintain the primary kidney cell functions for prolonged periods. A microfluidic device that uses podocytes cocultured with proximal tubule cells to mimic an accurate renal tubule has been proposed. Musah et al. [58] fabricated PDMS molds for developing microvascular channels and a porous membrane using stereolithography. The study differentiated hiPSC into podocytes for 35 days and improved the classical seeding. The upregulation of mature podocyte genes and downregulation of nephron progenitors confirmed a mature lineage, while the efficiency of differentiation was up to 90%. The podocytes were cultured on the top of the membrane and the glomerular endothelial cells on the opposite side of the membrane, separated by a glomerular basement membrane (GBM) to recapitulate the physiology and mechanical properties of the glomerular capillary. For five subsequent days, the cells were exposed to different concentrations of adriamycin (doxorubicin), a chemotherapeutic drug used to treat cancer. The results showed a dose-dependent toxicity through the quantification of albumin and inulin in the glomerular chip confirming a direct correlation of the drug-induced, dose-dependent cell damage. Moreover, cell destruction, higher urinary clearance, and albumin uptake were demonstrated within this platform [58].

The kidney proximal tubule plays a role in the absorption of nutrients, such as water and glucose, and secretes xenobiotics and protein-bound metabolites. Its cells, HPTECs, are frequently used to investigate the nephrotoxicity of several classes of drugs, including antibiotics and antiretrovirals [59]. Other studies evaluated a 3D tubular ECM scaffold to accurately reproduce the kidney's microenvironment and provide *in vivo*-like results [49, 60].

A study in 2016 described a 3D microphysiological system (MPS) consisting of a PDMS base with a collagen scaffold coated with an extracellular matrix (ECM) that resembled the human proximal tubule, which was used for growing PTECs for seven days. The authors analyzed the aquaporins and the sodium-glucose cotransporter-2 (SGLT2) inhibitors, a glucose uptake receptor, to prove the cell polarization in comparison to 2D models. The major contribution of this study was the assessment of metabolic competency in the case of ammonia biosynthesis and vitamin D biotransformation. The transportation of organic anionic solutes was sensitive to specific transport inhibitors, and the glucose reabsorption was 10-fold higher than that of previous reports and downregulated by the SLGT2 specific inhibition. This suggests that the device may be considered as a high-fidelity model that allows fundamental drug metabolism research [49].

In a recent study, the Nortis® device, with a chamber coated with type IV collagen, and an ECM to grow human primary PTECs, was explored. The device was applied to predict polymyxin (PMB) nephrotoxicity using injury biomarkers such as kidney injury molecule-1 (KIM-1), calbindin, clusterin, osteoactivin, VEGF, and α-GST. PTECs and immortalized cell lines were cultured and incubated in the chambers for 12 hours in the presence of the flow. Cell viability was determined by immunostaining. The authors concluded that the detection of biomarkers was fourfold higher than the controls after exposing PTECs to increasing concentrations of PMB and its analogs (NAB739 or NAB741) for 24 hours. This model has demonstrated a

Table 2: Summary of recent advancements of kidney-on-a-chip devices including the type of drug, the application, the applied cell, and the kinetics.

Drug type	Applications	Applied cell lines	Kinetics	Ref(s)
Gentamicin	Nephrotoxicity	MDCK	24 hrs	[54]
Vitamin D	Biotransformation	PTECs	>28 days	[49]
Polymyxin B	Nephrotoxicity	PTECs	14 days	[60]
Doxorubicin	Biodistribution	MDCK	—	[64]
	Nephrotoxicity, Nephrogenesis	NPC, EPCs	22 days	[61]
Cisplatin	Nephrotoxicity	Renal adenocarcinoma cell culture	24 hrs	[65]
Ciclosporin A	Nephrotoxicity, bioprinting	Convoluted renal proximal tubules	65 days	[47]
Adriamicin	Nephrotoxicity	hiPSC	>21 days	[58]

MDCK: Madin-Darby canine kidney; PTECS: proximal tubule epithelial cells; NPC: nephron progenitor cells; EPCs: endothelial progenitor cells; hiPSC: human-induced pluripotent stem cells.

capacity to detect drug toxicity within 24 hours of exposure [60].

Homan et al. (2016), on the other hand, developed a renal proximal tubule (PT) by combining bioprinting and organ-on-a-chip principles. The model consisted of a bioprinted silicon gasket with an open tubule to perfuse the cells (Figures 7(a)–7(d)). The ECM used in this study was composed of fibrinogen, gelatin, and two enzymes (thrombin and transglutaminase) that enabled the rapid solidification of the matrix around the 3D structures. Cell media and PTECs were perfused through the 3D convoluted tubular architecture on a chip through an external peristaltic pump (Figure 7(b), iv). By monitoring the variations of cell morphology, the nephrotoxicity of cyclosporine A (CysA) (typically used for transplant patients) was shown to be dose-dependent on CysA to induced damage. Moreover, the 3D PT and the perfused cells improved their albumin uptake and the albumin receptor, megalin. The platform tested over 65 days has proven to have a more extensive cell functionality than 2D cultures. The authors concluded that the model could be used for drug screening and disease modelling [47].

Homan et al. [61] later fabricated a millifluidic chip using silicone-based ink and gelatin for evaluating doxorubicin, a chemotherapeutic drug. H9 human embryonic stem cells (ESCs) were seeded into this device to develop organoids under controlled FSS. While the model was not used for any specific application, it has shown potential for studying kidney development, diseases, and regeneration [61].

Nephrotoxicity related to drugs has a significant patient morbidity and mortality rate, particularly on those exposed to a broad range of prescribed drugs, such as antibiotics, analgesics, and chemotherapeutic agents. The development of new approaches for the safety screening of drugs and other toxic compounds is therefore vital. Rayner et al. created a tunable human renal vascular-tubular platform (hRVTU) by a photolithography technique using PMMA layers separated by a collagen membrane. The authors developed a vascularized renal tubule using cells isolated from a single donor: HUVECs seeded into the top channel, human kidney epithelial cells (HKMECs) into the bottom channel, and fetal human kidney pericytes, into the collagen matrix [44, 45, 47, 49]. The platform has not been used for testing any drug; however, the model could hold great promise for studying kidney diseases and for drug development [62].

Kidney cells contain ion channels which control the ion concentration by absorption or secretion into the urine. To assess the functionality of ion channels in kidney-on-a-chip devices, Aschenbrenner et al. developed a low-cost device manufactured by 3D printing using acrylonitrile butadiene styrene (ABS) to measure the Ca^{++} flux. The device is composed of an inlet, a chamber, and an outlet, with a zigzag-shaped microfluidic channel. Transfected human embryonal kidney-derived (HEK293) cells with the capsaicin (a pungent alkaloid from chili peppers) receptor TRPV1 were seeded in the chamber and incubated overnight under standard conditions. Using cell morphology imaging during chemical stimulation with capsaicin, the fluorescence intensity showed a consistent increase with an increase in the intracellular calcium concentration. The authors concluded that the model was reliable for ion analysis [63].

It is, indeed, challenging to effectively reproduce the kidney's sophisticated microvessels and their physiology. A reported kidney-on-chip has modelled the microvessels for the evaluation of anticancer drugs. Bogorad et al. [64] employed a platform to study the pharmacokinetics and transport of doxorubicin in MDCK cells. The model contained perfusable microvessels to obtain fluorescence images to quantify drug transport at different time points. The developed microdevice recreated the structure and physiology of kidney cells. The results could be compared with previous reports describing renal cell receptor polarization explored through real-time imaging and quantitative analysis of doxorubicin permeability [64].

Other studies integrated sensors within the organ-on-a-chip devices for monitoring the drug-induced nephrotoxicity *in situ*. Additionally, the detection instruments such as smartphone-based fluorescence readers offer beneficial features in the monitoring of drugs. Cho et al. [65] incorporated a fluorescence nanoparticle immunocapture/immuneagglutination assay into a kidney-on-a-chip coupled to a smartphone-based microscope to evaluate the cytotoxicity of cisplatin on renal adenocarcinoma cells. The device consisted of three layers of PDMS with an inlet and outlet holes. The three layers were patterned onto glass, and the bottom substrate was etched in order to measure the analytes of interest. When the proximal tubular

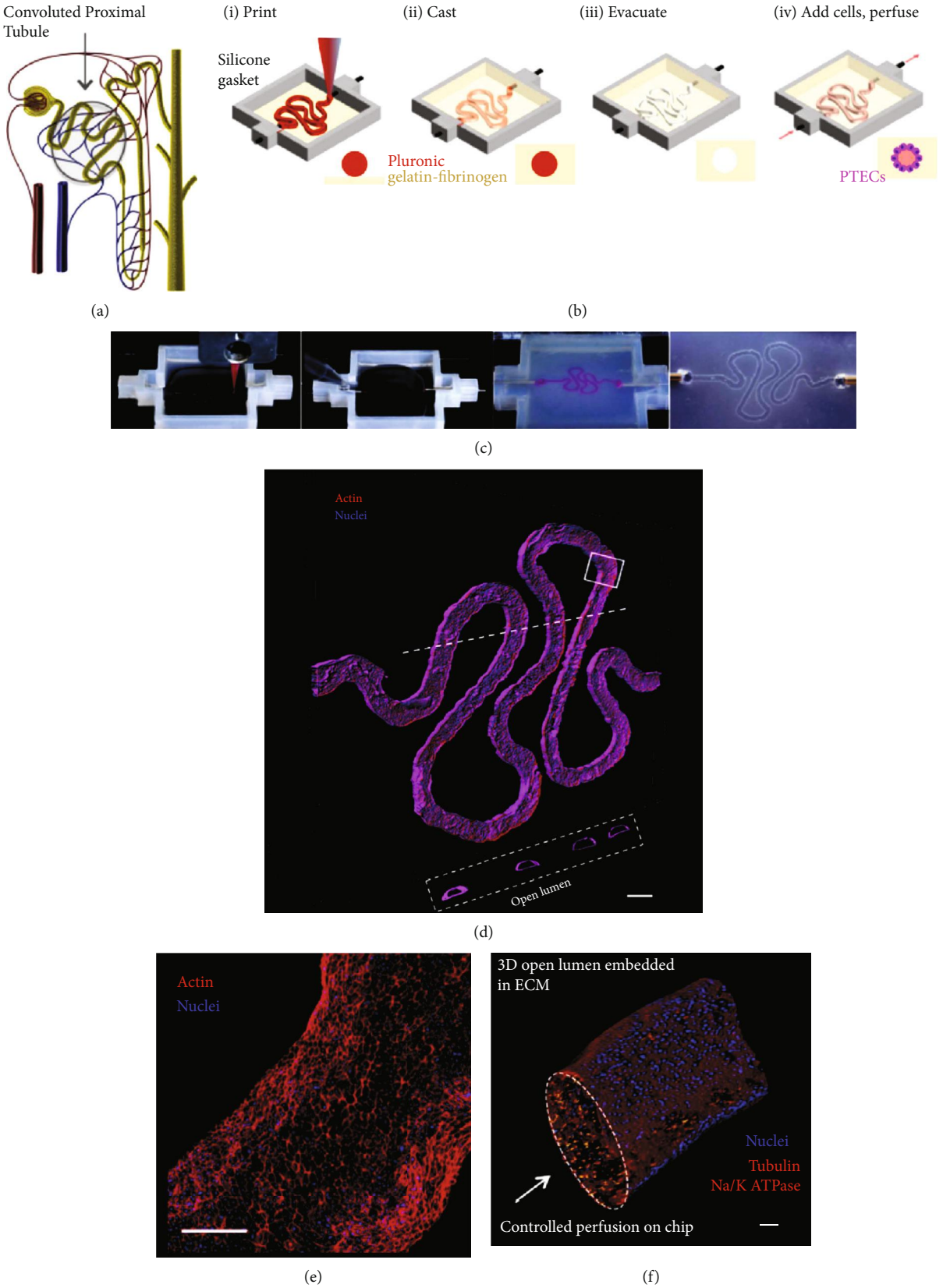

Figure 7: 3D convoluted renal proximal tubule on a chip. (a) Schematic of a nephron highlighting the convoluted proximal tubule; (b, c) corresponding schematics and images of different steps in the fabrication of 3D convoluted, perusable proximal tubules; (d–f) a 3D rendering of the printed convoluted proximal tubule acquired by confocal microscopy. Reproduced (or adapted) with permission [47], ©2016, Nature.

cells in the kidney are exposed to toxins, their brush border membrane released γ-glutamyl transpeptidase (GGT) into the lumen which was recognized by a sensor. The results established that with increasing cisplatin concentrations, the fluorescence intensity also increased. Furthermore, with the increase of cisplatin, γ-glutamyl transpeptidase antigens were released into the media; hence, cell viability decreases [65].

One of the major limitations for the development of kidney-on-chip devices is the lack of human podocytes, which are the main component of the glomerulus. With recent advances in the differentiation of podocytes from human pluripotent stem cells, and their coculture with renal parenchyma, this challenge is expected to be overcome. However, further research in this area is required. Moreover, development of more realistic 3D models that could integrate the glomerulus, the proximal tubular-like cells, and nephron-like cells is still on the horizon of research accomplishment. Such platforms would ideally mimic the human kidney and reproduce the biological processes of the kidney for the preclinical assessment of candidate drugs.

2.3. Lung-on-Chip. In mammals, the lungs are part of the lower respiratory system. Their composition includes airways, multiple branched blood vessels, and two main zones: the conducting zone, where the air enters, and the respiratory zone, where the exchange of oxygen and carbon dioxide occurs. The main parts are the bronchus, bronchiole, and alveoli, and each compartment has epithelial cells and a basement membrane. Within the alveoli, alveolar type I and type II cells exist. The alveolus is the smallest functional unit of the lung and provides a large surface area for gas exchange [66]. The biomimetics (and bioenergetics) of the lungs represent a unique challenge, as it includes several types of cells and mechanical forces since a periodic mechanical axis force is exerted with each respiratory cycle, and this dynamic mechanical force is difficult to recreate *in vitro* [67]. However, development of accurate lung tissue is critical to understanding the effects of drugs, toxins, and pathogens in such airways, as well as the understanding of infectious diseases which impact respiratory function.

Some models have used suspended gels to create the basal lung membrane. Humayun et al. [68] developed a microfluidic device using PMMA micromilling consisting of three chambers: (i) an upper microchamber for achieving an air-liquid interface and seeded with EC, (ii) a middle matrigel-collagen layer, and (iii) a lower chamber cultured with smooth muscle cells (SMC) (Figure 8). These chambers kept the cells functional and alive for 31 days, as measured by morphological markers, including ZO-1 tight junctions and F-actin [68]. Such cell stability allows further analysis of the lungs and impacts the measurement of a drug on lung functions.

Another device created by Stucki et al. [69] integrated respiration movements. The design has a bioartificial alveolar barrier, with a thin, porous, and flexible PDMS membrane. On this membrane, epithelial cells were cultured on the apical side and endothelial cells on the basal side. To generate a microdiaphragm, the membrane was stretched downwards into the pneumatic part and connected to pneumatic microchannels (Figure 9). The microdiaphragm applied a reproducible 3D cyclic strain to the cells to mimic the movements of the diaphragm (Figure 9). The study demonstrated that mechanical stress affected the permeability of the epithelial barrier [69]. Some of the latest examples of lung-on-chip platforms for drug discovery, development, and analysis are thoroughly reviewed in this article (Table 3).

2.3.1. Analysis of Drugs in Lung-on-Chip Devices. Air-borne toxins may affect the integrity of the epithelial barrier. During a study conducted by Liu et al. [70], they exposed lung cells to different levels of polluted air or cigarette smoke. Their device was fabricated by soft lithography with a middle PMMA layer having through-hole arrays. Each hole was pipetted agarose-gelatin and epithelial cells. In the upper chamber, these cells were always in contact with air or different air contaminants. Such accurate microdevices aided in the analysis of different lung injuries. In this study, the authors obtained a mimetic lung injury that induced an inflammatory response in the lung cells [70]. This device has the specific capabilities of the human lung to evaluate and predict drug toxicity *in vitro*.

A potential limitation of this device was that the applied cells used originated from adenocarcinoma human alveolar basal epithelial cells. Addressing the potential limitations of the model would require using primary human alveolar epithelial cells from a long-term culture.

Huh [71] created a microfluidic device that replicated the microarchitecture and dynamic microenvironment of the alveolar-capillary unit of the living human lung. The study introduced inflammatory insults, including proinflammatory cytokines and *E. coli* bacteria, into the upper alveolar compartment, to recapitulate the cellular immune response to microbial infection in human lung alveoli. This activated the endothelial cells on the opposite side of the membrane and resulted in the increased expression of adhesion molecules. This was followed by adhesion of human neutrophils circulating in the lower vascular channel to the endothelium and the subsequent transmigration across the tissue layers into the airspace [71]. This human breathing lung-on-a-chip, microengineered model has the potential to evaluate environmental toxins, such as silica nanoparticles.

The creation of devices that involve airways permits the analysis of lung inflammation and the testing of drugs. In the work of Benam et al. (2016), the microdevice consisted of two parallel PDMS channels divided by a porous PS membrane coated on both sides with type I collagen, on which epithelial (top air channel) or endothelial (bottom blood channel) cells were cultured to create a tissue-tissue interface. The study analyzed the structural features of the cell barriers with high mimetic results for 4-6 weeks. With this model, the authors induced an asthmatic phenotype and chronic obstructive pulmonary disease (COPD) and treated the cells with IL-13. Major molecular characteristics of asthma, including IL-8, RANTES, cellular damage, and goblet cells, were measured. The study reported a subsequent treatment of rheumatoid arthritis with tofacitinib to inhibit the signaling pathway of IL-13 or dexamethasone. The results were consistent with clinical findings, which indicated that the

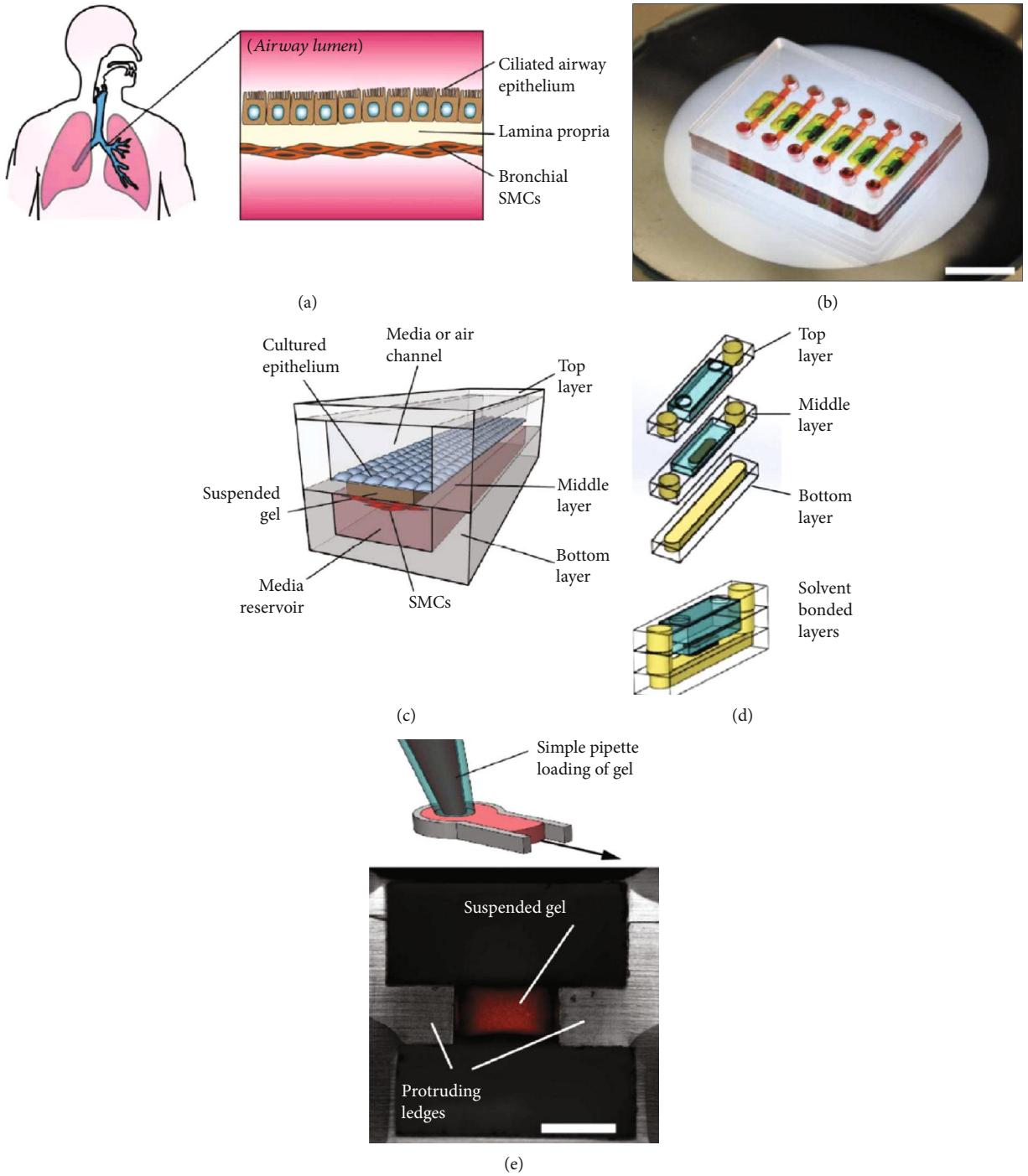

Figure 8: Lung airway-on-a-chip device design and fabrication. (a) Schematic of airway lumen tissue structure. (b) Photograph of an assembled lung airway microdevice (scale bar = 10 mm). (c) Lung airway microdevice schematic design. (d) Exploded view of the three PMMA layers. (e) The suspended hydrogel is introduced into the middle layer. Magnified image of the device cross-section (scale bar = 500 μm). Reproduced (or adapted) with permission [68], ©2018, Royal Society of Chemistry.

specific inhibitor, tofacitinib, restored normal cilia and reduced the cytokine production in comparison to corticosteroid administration, which was ineffective [67].

Pulmonary thrombosis affects 650,000–700,000 persons annually in the United States of America (USA), of which approximately 10% is due to an inopportune diagnosis. There is an absence of effective *in vitro* or animal models for studying this disease that could lead to the development of new treatments. A device composed of two PDMS microchannels, separated with a porous, thin, and flexible PDMS membrane, was fabricated. The membrane was coated with an ECM, which emulated the interaction between endothelial cells and the alveolus in the human lung (Figure 10). This model used whole human blood instead of a cell culture

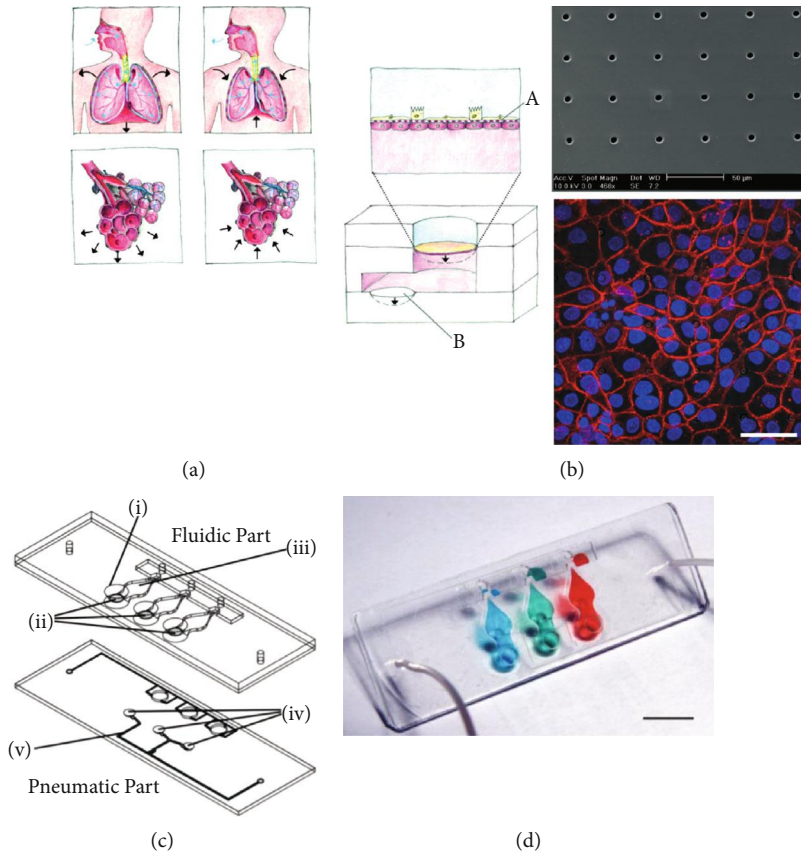

Figure 9: Design of the lung-on-a-chip. (a) In vivo, inspiration is controlled by the diaphragm. (b) In vitro, the 3D cyclic mechanical strain of the bioartificial alveolar membrane (A) induced by a microdiaphragm; (B) the bioartificial alveolar membrane is shown in the upper microscope picture. (c) The fluidic part consists of (i) alveolar cell culture wells, (ii) membranes, (iii) basolateral chambers, (iv) microdiaphragms, and (v) pneumatic microchannels. (d) Photograph of the lung-on-a-chip (scale bar, 10 mm). Reproduced (or adapted) with permission [69], ©2015, Royal Society of Chemistry.

Table 3: Summary of recent advancements in lung-on-a-chip systems including the type of drug, the application, the applied cell lines, and kinetics.

Drug type	Application	Applied cell lines	Kinetics	Ref(s)
Gefitinib	Antitumoral drug	A549, HFL1, and HUVEC	5 days	[73]
Parmodulin-2	Antithrombotic drug	hAEC and HUVEC	12 days	[72]
Tofacitinib	Anti-inflammatory drug	hAEC	5 weeks	[67]
ZnO and TiO_2 nanoparticles	Nanotoxicity	hAEC and HUVEC	3 days	[76]

A549 is an adenocarcinomic human alveolal basal epithelial cell. HFL1: human fetal lung fibroblasts; HUVECs: human umbilical cord cells; hAEC: primary human alveolar cells; ZnO: zinc oxide; TiO_2: titanium dioxide.

medium, leading to a device that could evaluate antithrombotic drugs *in vitro* [72]. In this work, the authors induced platelet activation and clot formation in the presence of fluid shear conditions by collagen exposure. As it occurs within *in vivo* systems, when the endothelium was stimulated by inflammatory cytokines, it promoted platelet recruitment and thrombus formation. A drug candidate, parmodulin-2 (PM2), was tested for the treatment of this injury. The drug possessed antithrombotic and anti-inflammatory properties as a result of the inactivation of protease-activated receptor-1, a peptide that mediates tissue inflammation and coagulation abnormalities. In this model, the drug indicated a potent protective and antithrombotic effect on human lung cells [72].

Gefitinib is an anticancer drug that inhibits the epidermal growth factor receptor tyrosine kinase (EGFR-TKIs) and which benefits non-small-cell lung cancer (NSCLC) patients. The drug is a tyrosine kinase inhibitor of the EGFR that regulates basic cellular functions, such as proliferation, migration, and differentiation, which play a role in the etiology of solid tumors. However, the initial drug resistance has become challenging. A research group introduced a lung tumor model with the cultured A549 lung cancer cell line and

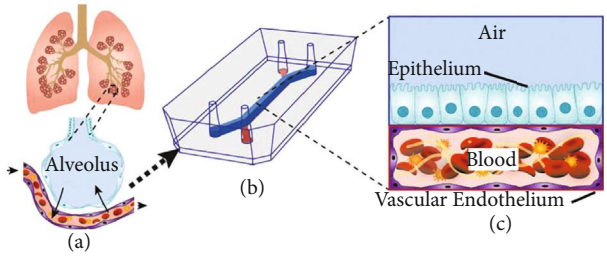

FIGURE 10: Microengineered model of human pulmonary thrombosis-on-chip. (a) A conceptual schematic of the human lung showing that the alveoli interact with the neighboring blood vessels during hemostasis or pulmonary dysfunction. (b) Engineering drawing of the microdevice. (c) Graphic illustration showing how the top compartment (1 mm wide and 1 mm tall) is cultured with human primary alveolar epithelial cells and the entire bottom chamber (1 mm wide and 250 mm tall) lined with human endothelial cells forming a lumen. Reproduced (or adapted) with permission [72], ©2017, American Society for Clinical Pharmacology and Therapeutics.

human fetal lung fibroblasts. In this study, the authors created a microfluidic device with a nanofiber membrane made from polylactic-co-glycolic acid (PLGA) and PDMS (Figures 11(a) and 11(b)). The electrospun PLGA membrane was designed to be biocompatible, porous, and permeable. The toxicity of gefitinib, an anticancer drug, was evaluated by testing the cell viability of the cocultured human non-small-cell lung cancer cells (A549), human fetal lung fibroblasts (HFL1), and HUVECs (Figures 11(c)–11(e)). A459 cells are typically sensitive to gefitinib; however, when cocultured with HFL1, it was found that these cells helped in the survival of the cancerous cells, despite the presence of the drug. When A549, HFL1, and HUVEC cells were cocultured, A549 stimulated the invasion of tumoral cells causing the death of HUVECs. This lung-on-a-chip device successfully simulated the tumor microenvironment and alveolar biochemical factors to evaluate the toxicity of a drug for personalized medicine [73].

Nanotechnology has been emerging as an important tool for many novel applications in the biomedical field. However, exposure to nanoparticles (NPs) has generated pulmonary diseases, such as asthma, pulmonary edema, emphysema, and lung cancer [74]. Titanium oxide (TiO_2) is considered safe; however, zinc oxide (ZnO) NPs induce toxicity to human lung cells by causing damage to the alveolar epithelial cells and human alveolar adenocarcinoma [75]. A recent study evaluated the toxicity of ZnO and TiO_2 in a lung-on-a-chip device, measuring reactive oxygen stress and apoptosis of the epithelial and endothelial cells. The device consisted of two parallel channels lined with human pulmonary alveolar cells and a lower chamber with human umbilical endothelial cells. In the middle channel, matrigel coverture mimicked a basal membrane. The NPs were delivered to the epithelial cells mimicking acute pulmonary nanoparticle exposure. Both nanoparticles showed dose-dependent toxicity on the two cell lines causing apoptosis. The ZnO particles showed higher membrane permeability due to cell destruction by oxygen species [75].

In line with these findings, another study introduced a mathematical model and practical device experiments predicting the nano- and microparticle delivery to the cell within microfluidic devices by closely mimicking the airways of the lungs [76]. ZnO and TiO_2 particles with diameters of $d \leq 700$ nm were spread in the air flow using different flow rates. The results confirmed that ZnO NPs were more toxic than TiO_2, showing higher reactive oxygen species and permeability. The system has accurately mimicked acute pulmonary nanoparticle exposure.

Despite numerous advancements in the development of lung-on-chip devices, there are still many challenges associated with the development of 3D *in vitro* lung models. Various designs and fabricated devices will further an understanding of organ physiology, drug toxicity, and drug interactions. Nevertheless, the lung-on-a-chip models need to use pluripotent stem cells, provide an appropriate biological environment to maintain the cell functions over extended periods of time, and incorporate ventilation mechanics into the miniaturized lung-on-chip platforms. These platforms could lead to the development of integrated systems to study the clinical course of lung diseases and to evaluate novel therapeutic strategies.

2.4. Gut-on-Chip. The first stage in the pharmacokinetics of a drug is the absorption of that drug. In that perspective, the route of administration of the drug is of great importance. Oral medications arrive at the gut that is covered by a membrane. The close interaction of the gut with ingested food, xenobiotics, and drugs induces the rupture and absorption of the consumed materials. The intestine contains villi and microvilli on the epithelial cells, which promote secretion, cellular adhesion, and absorption by increasing the surface area, among other factors [77]. The many functions of the gut, including peristaltic movements and intestinal microbiota which pertain, pose a great level of complexity, hence challenging their replication on static models. Single-dose and repeat-dose testing in toxicological studies is typically developed during the preclinical phases of drug development for identifying the effects of a drug on functions in the gut, including intestinal motility, nausea and emetic reflex, and absorption. *In vitro* cell culture techniques use a monolayer of human colon adenocarcinoma cells (Caco-2) and the human colorectal adenocarcinoma cell line (HT-29) to predict the rapid assessment of orally administered drugs. However, current *in vitro* models lack the careful mimicking of the tissue structure, the absence of microbiota [78], and the complexity of the gut functions, such as peristaltic movements and flow [79]. A considerable number of research studies have focused on the development of gut-on-a-chip devices and have attempted to closely model the characteristics of the intestine, including the microbiome [80]. Microfluidic organ-on-a-chip models of the human intestine are one of the most studied 3D models, as those platforms are very advanced in the integration of several cell lines, including Caco-2, HUVEC, myofibroblasts, primary intestinal epithelial cells, or immune cells. Such synergy allows researchers to evaluate drugs, diseases, microbiome interactions, colon cancer metastasis, and

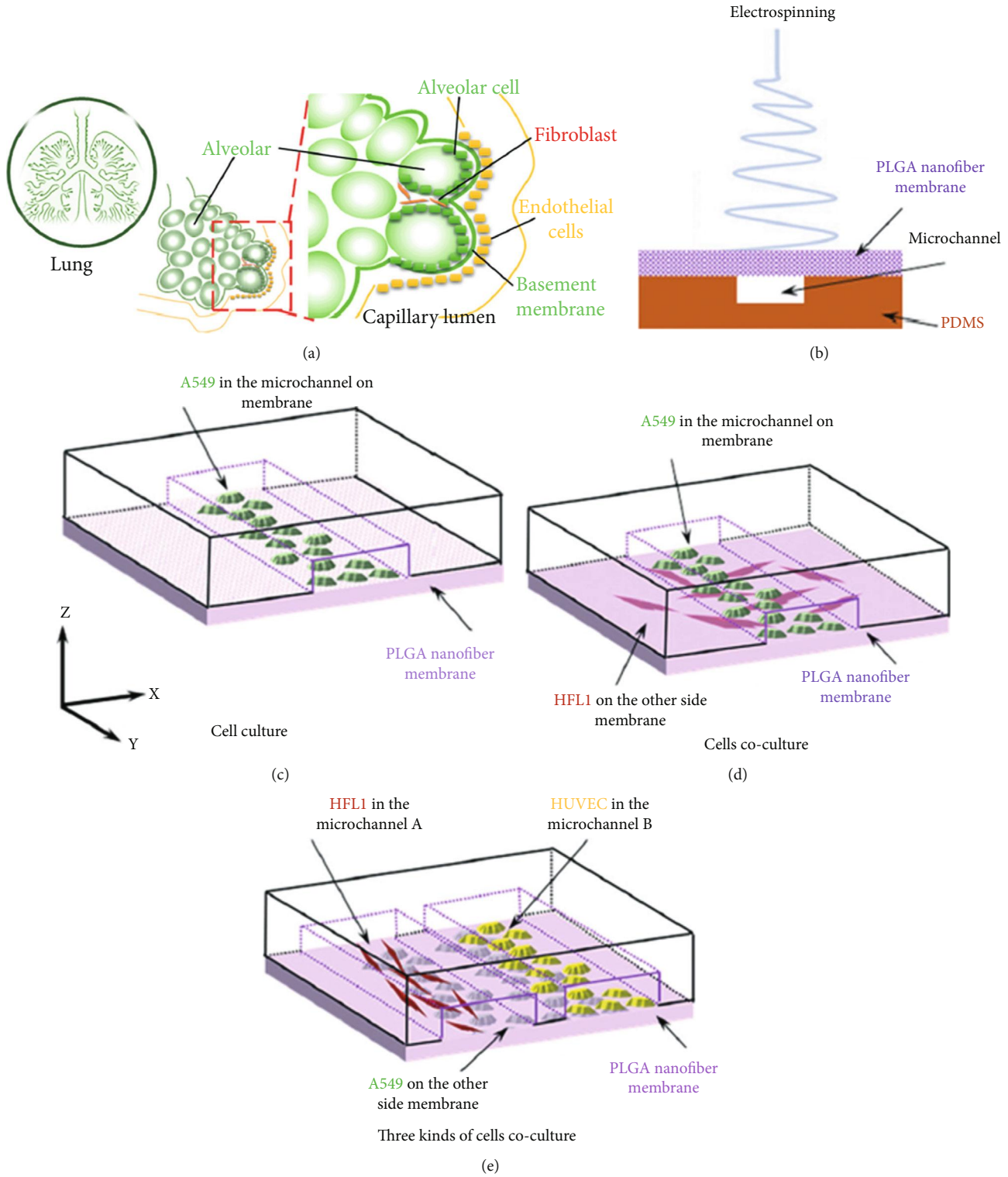

Figure 11: (a) Schematic diagram of the alveolar structure. (b) Schematic diagram of microfluidic chip with PLGA nanofiber membrane as substrate prepared by electrospinning. (c) Schematic diagram of culture of A549 cells on the chip. (d) Schematic diagram of the coculture of A549 cells and HFL1 cells. (e) Schematic diagram of the coculture of A549 cells, HFL1 cells, and HUVECs. Reproduced (or adapted) with permission [73], ©2018, Royal Society of Chemistry.

radiation effects in a single system. Some of the latest examples of gut-on-chip platforms for drug discovery, development, and analysis are thoroughly reviewed in this article (Table 4).

2.4.1. Analysis of Drugs in Gut-on-Chip Devices. Different devices with sophisticated microchannels and perfused chambers have been engineered where immune cells, gut

Table 4: Summary of recent advancements in gut-on-chip platforms including the type of drug, the applications, the applied cell lines, and the kinetics.

Drug type	Applications	Applied cell lines	Kinetics	Ref(s)
DMOG	Drug interaction Radiation-g	Caco-2 HUVEC	5 days	[84]
Isofosfamid, verapamil	Pharmacokinetics	Caco-2	11 days	[93]
Midazolam, indomethacin	Pharmacokinetics Toxicity	PiEC, human myofibroblast, Caco-2	21 days	[94]
Paracetamol	Toxicity	Caco-2, HepG2	14 days	[140]
Mariskat	Efficacy	Caco-2, hIEC	24 days	[141]
Rifampicin, ketoconazole	Pharmacokinetics	HiPCs	34 days	[142]

DMOG: dimethyloxaloyl; Caco-2: colon adenocarcinoma cells; HUVECs: human umbilical vein endothelial cells; PiEC: primary intestinal epithelial cells; HepG2: human hepatocellular carcinoma cells; hIEC: human intestinal epithelial cells; HiPCs: hormone independent prostate cells.

microbiome, and pathogens were cocultured, while fluids that deliver nutrients, drugs, and other compounds were flowing under controlled peristaltic-like motion. These devices mimic the human intestinal microenvironment and emulate many physiological and pathophysiological functions of the gut. They are used to study gastrointestinal infections, immune-microbiome inflammatory diseases (inflammatory bowel disease), ileus disease, celiac disease, colorectal cancer, etc., and to understand disease mechanisms. Some human enzymes, including CYP450, CYP2C9, CYP2D6, and CYP3A4, are the most important isoforms of P450 enzymes in phase 1 drug metabolism in humans [81]. The activity of such enzymes can be carefully studied within gut-on-chip devices. Furthermore, understanding the interactions between the gut cells, microbiota, and pathogens with drugs is crucial. Application of 3D microfluidic devices has opened windows of opportunity to predict the efficacy and safety of new and existing drugs. This technology has been used to develop human gut-on-a-chip models that emulate the human intestinal structure to culture human Caco-2 cells, commensal and pathogenic microorganisms, and immune cells inside its cyclic mechanical forces thereby emulating an *in vivo* intestine [82].

A microfluidic gut-on-a-chip model was developed to analyze and provide new insights on the pathophysiology of inflammatory gut diseases, including bowel disease and ileus, and to determine the bacterial overgrowth. The authors fabricated the device from flexible PDMS with three microchannels, where the central channel has an ECM-coated porous membrane that was seeded with the cells. Caco-2 cells were cultured under peristaltic movements and were exposed to the flow of the culture medium through the upper and lower microchannels to promote the formation of villi structures. The platform was intended for the growth of the gut microbiome and for drug assessment. Moreover, the platform was used to evaluate the effects of probiotics and antibiotics, confirming that peristaltic forces play an important role in the gut biome preventing overpopulation [79, 83]. In the gene analysis, it was observed that cells cultured with the microfluidic devices change the expression of 22,097 genes compared to static cultures. Moreover, the addition of probiotic bacteria for 72 h in the gut-on-chip exhibited a different profile compared to chips without bacteria. When the enteroinvasive *E. coli* bacteria were introduced to the system, the microbiota also protected the height of the villi and decreased the lesion area [83].

To address the mimetic capacity of microfluidic devices in gut cells, most of the available studies have demonstrated the natural structure of the intestine layers (Figure 12(a)). One such study is that of Jalili-Firoozinezhad et al. [84] in which the villus intestinal epithelium polarization with ZO-1 tight junctions and an apical brush border were created within a gut-on-chip device. The authors also mimicked the production of mucus and alkaline phosphatase or sucrase-isomaltase within the platform. The effect of γ-radiation on villus morphology, cytotoxicity, apoptosis, and ROS was studied in this platform. The study confirmed that cells exposed to γ-irradiation induce changes in intracellular ROS and cause disruption of epithelial and endothelial integrity. Moreover, dimethyloxalylglycine (DMOG) used as pretreatment shielded the gut cells and diminished the harmful effects of radiation (Figures 12(b) and 12(c)) [84].

Shim et al. (2017) fabricated a generic gut-on-chip device consisting of three layers of PDMS with a membrane incorporating a collagen scaffold to mimic the intestinal villi, providing a reservoir for cell culture and fluid shear to improve cell differentiation and the physiological functions of the gut. The first layer was equipped with reservoirs for storing media, the second layer with fluidic channels made from a wafer mold to replicate the villi, and the third layer with a hole at the center. The microfluidic chip resembled the human intestine, with villi-shape structures. Caco-2 cells were seeded, stained with phalloidin and DAPI, and cultured under gravity flow for 14 days. Cells from this line were used due to the physical and physiological resemblance they share with gut cells [77]. Cell morphology examination showed that the cells were able to reproduce the villi structure and the fluidic shear in the 3D chip. The authors concluded that the villi had an important reduction in height, maybe due to contraction of the Caco-2 cells, degradation by protease proteins, and also due to the fluidic shear. However, exposing cells to the perfusion culture improved their metabolic activity, confirming that the gut-on-a-chip device could work as a platform for assessment of drug absorption and metabolism [77].

A more sophisticated model that mimicked the human intestine was developed by Villenave et al. [85]. The multilayer platform was composed of two microchannels

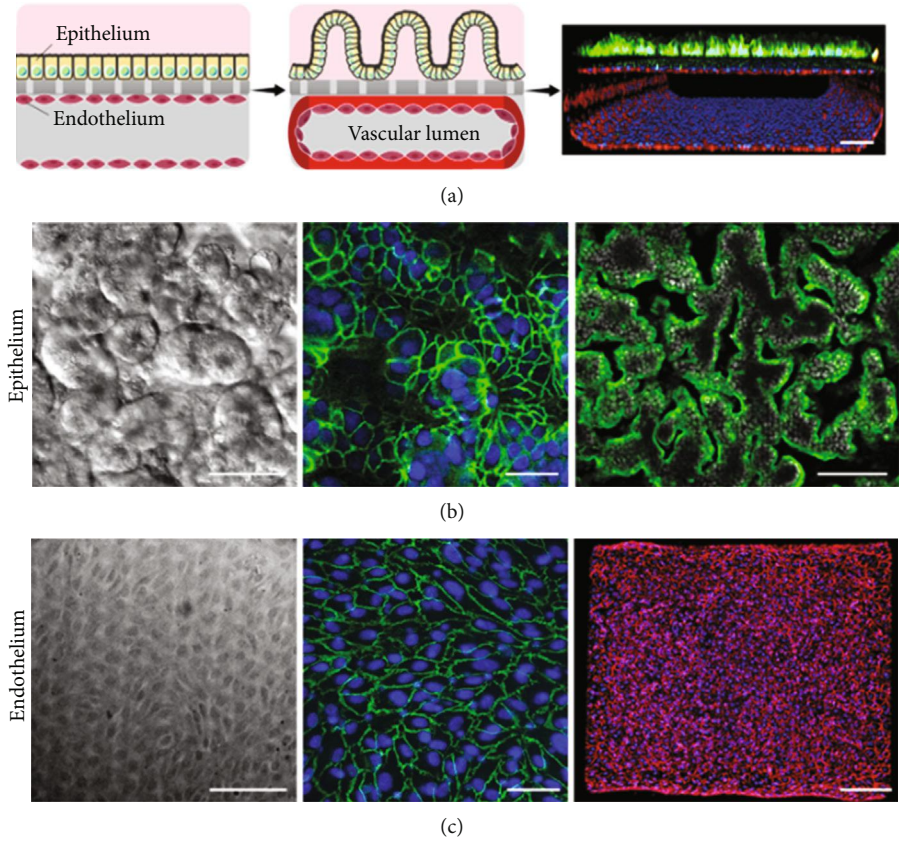

FIGURE 12: (a) Schematic showing the human intestinal epithelium and endothelium when initially plated on opposite sides of the matrix-coated porous membrane within the two-channel microfluidic device. (b) Microscopic views showing the villus morphology of the human intestinal epithelium and the immunofluorescence staining of the junction protein. (c) Microscopic views showing the planar morphology of the human endothelium and views of the immunofluorescence staining of the associated proteins. Reproduced (or adapted) with permission [84], ©2018, Nature.

separated by a porous membrane and was fabricated through lithography using a previously reported method [79, 82]. Outside the channels were two vacuum chambers that were used to simulate intestinal forces and movements within the device (Figures 13(a) and 13(b)). The membrane was cultured/coated with human Caco-2 intestinal epithelial cells for six days (Figure 13(c)). In this study, coxsackievirus B1 (CVB1) was used to infect the gut cells and subsequently to evaluate the reaction. Once the intestine cells had grown on the porous membrane, the virus was activated, and the response of the infection was measured through luminescence assays and real-time polymerase chain reaction (RT-qPCR). Results from the luminescent assay and the morphological analysis indicated that the device could be used successfully to monitor the behavior of the infection. It was also concluded that peristalsis facilitates infection downstream due to the flow and that the response varies in time according to the route of the infection and depending on the flow direction [85].

A substantial number of studies report that Caco-2 and HT-29 cell lines isolated from tumor sites can anchor several gene mutations with each passage, which might not accurately represent the human intestine. Therefore, other cell types could be cultured within gut-on-chip devices, including organoids. In particular, human intestinal organoids (HIOs) derived from either human biopsy or iPSC were repeatedly reported in the literature [86]. Kasendra et al. [87] developed a human small intestine-on-chip containing primary intestinal epithelium cells isolated from biopsy-derived human organoids, which resembled the intestinal epithelium and showed efficient monolayer formation when gut microvascular endothelial cells were seeded within the lower chamber. The device was fabricated from PDMS with a porous ECM-coated PDMS membrane, as described previously (Figure 14(a)) [79, 82, 83]. The formation of villi-like structures could be improved by using chemical gradients of growth factors, such as Wnt-3A, responding, and noggin, though the exact mechanism of the formation of villi-like structures remains unclear [87].

Using flow cytometry, Workman et al. [88] have shown that HIOs obtained from iPS cocultured with mesenchymal cells can be incorporated into a gut-on-chip platform. The device was fabricated using PDMS with a microchannel architecture, and the membrane was produced on a silicon mold. The organoids were stained and seeded under flow conditions for ten days, and the cells were polarized and used to assess the effect of interferon- (IFN-) γ. The chips were analyzed microscopically, and villi-like projections were observed, demonstrating that they belong to the gut lineage cells [88].

Recent studies describe how drug metabolism could also occur in the intestine during absorption induced by the gut

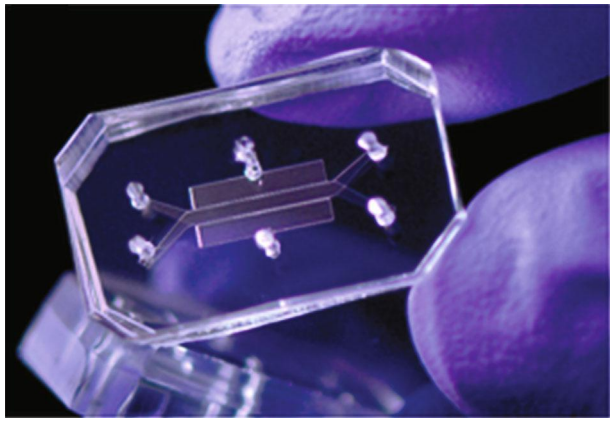

(a)

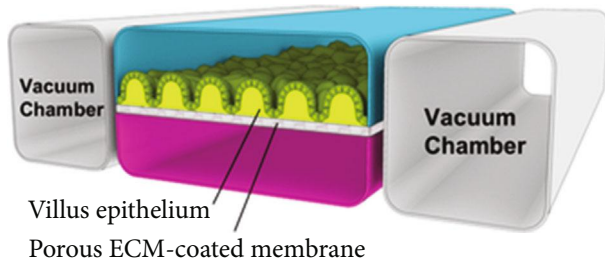

(b)

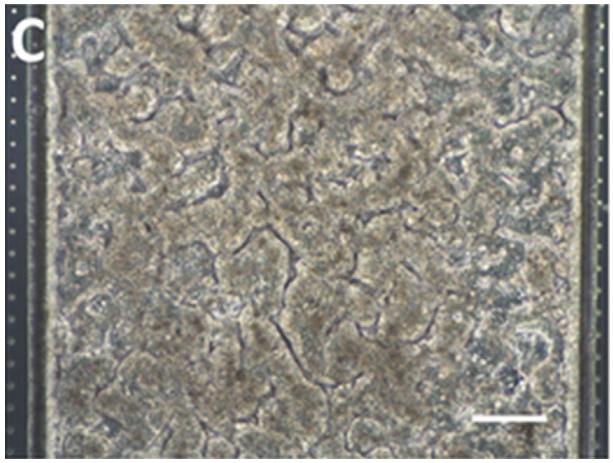

(c)

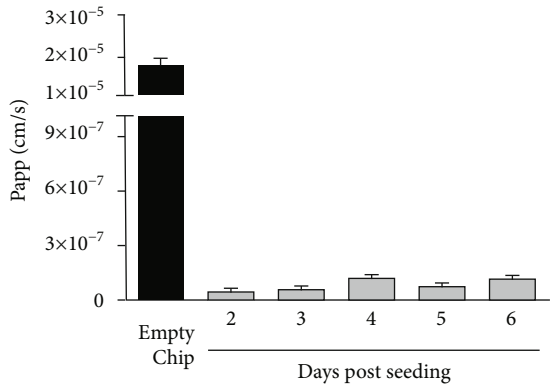

(d)

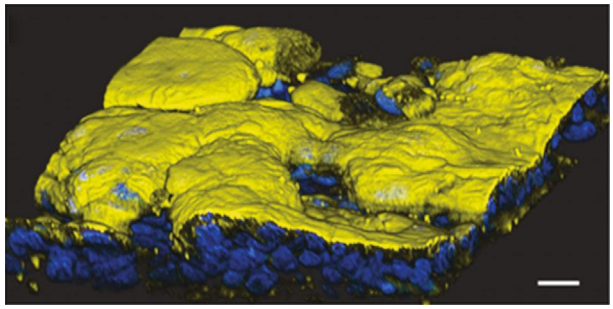

(e)

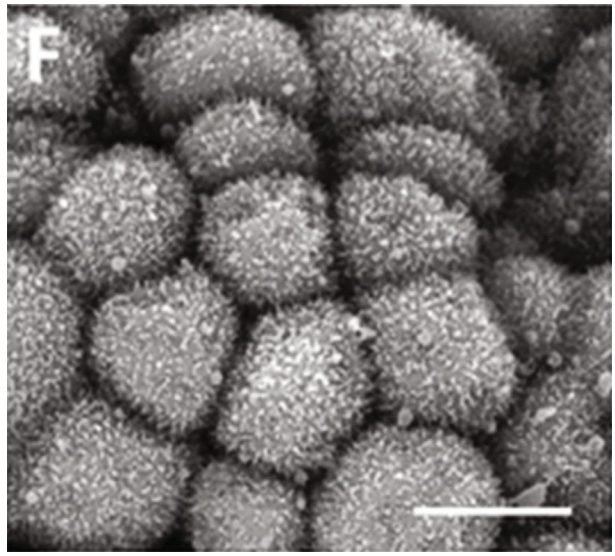

(f)

Figure 13: Gut-on-a-chip microfluidic device. (a) Photograph and (b) schematic of the device. (c) Micrograph of human Caco-2 intestinal epithelial cells cultured in the device. (d) Apparent permeability (Papp) of the epithelium assessed by adding fluorescent inulin-FITC. (e) Confocal immunofluorescence micrograph of human villus intestinal epithelium formed inside the gut-on-a-chip and stained for villin (yellow). (f) SEM micrographs of the apical surface of the villus epithelium. Reproduced (or adapted) with permission [85], ©2017, Public Library of Science.

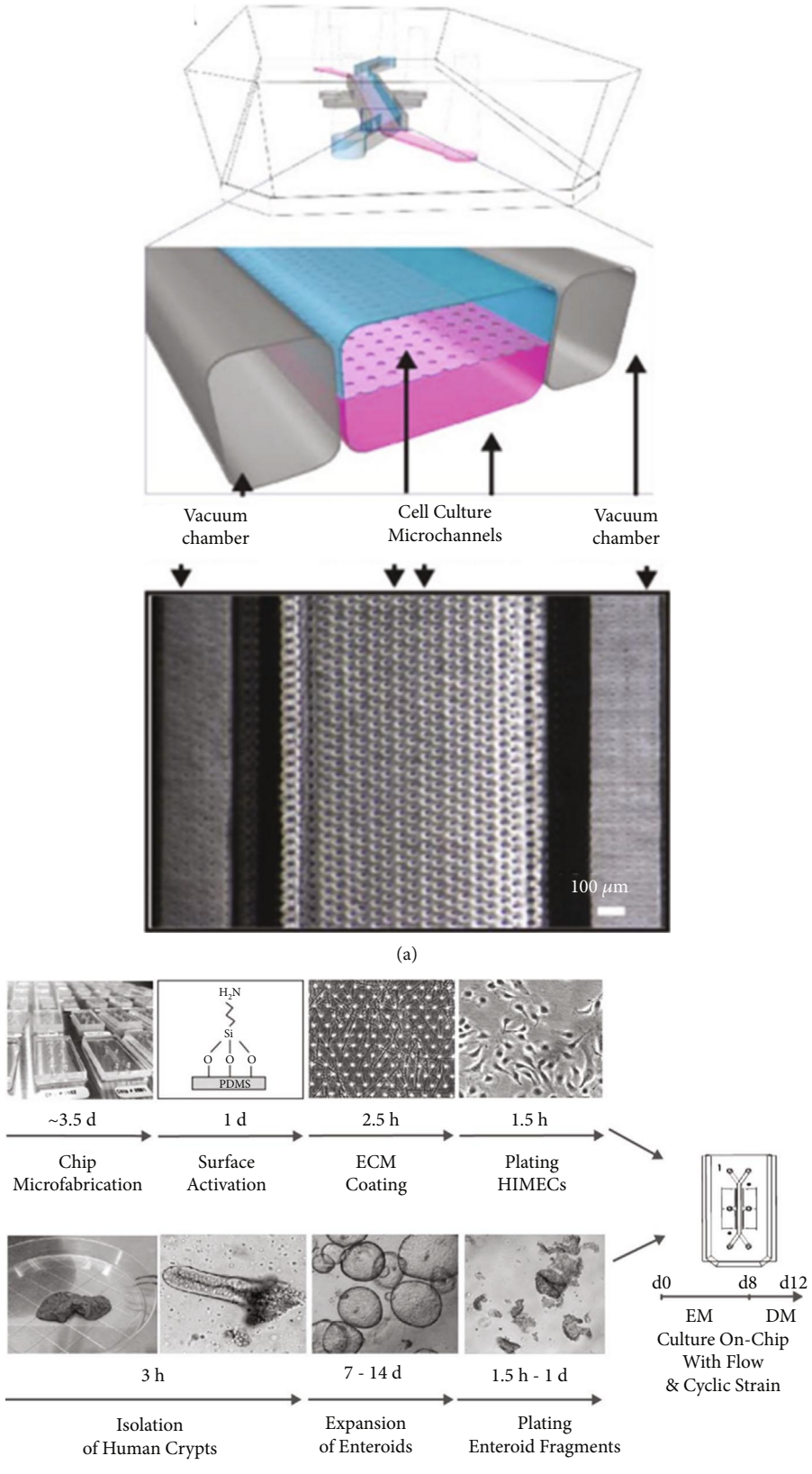

Figure 14: Fabrication of the primary human intestine chip. (a) A schematic microdevice showing the upper epithelium (blue), the lower microvascular cells (pink), and the porous membrane in-between. The different microfluidic channels and some components are shown. (b) Schematic representation of the procedure involved in the establishment of microfluidic cocultures (epithelium and endothelium). Reproduced (or adapted) with permission [87], ©2018, Nature.

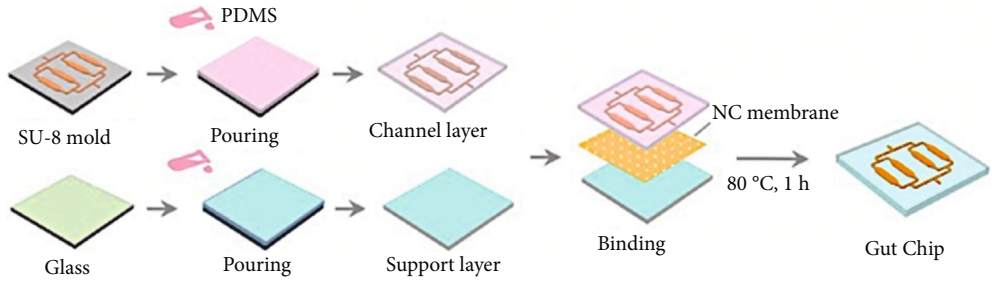

Figure 15: Fabrication process of the biomimetic human gut-on-a-chip. The channel layer and the support layer were made of PDMS, and the middle layer was fabricated of nitrocellulose. Reproduced (or adapted) with permission [93], ©2018, Wiley Online Library.

microbiome [89–92]. Guo et al. reported a device that consisted of three layers: a channel layer, a central porous layer of collagen I and nitrocellulose (NC), and a support layer derived from PDMS (Figure 15). Using Caco-2 cells in the microfluidic model, the authors analyzed the CYP3A4 and CYP2C9 enzymes and their expression levels. Both proteins showed an increase in the expression level within the 3D *in vitro* system after five days in comparison to the static cultures. SEM images confirmed that the membrane offered functionality for cell growth, and a high protein-binding capability, which improved cell adhesion. Also, the study confirmed that the model promotes the expression of the CYP3A4 and CYP2C9 in Caco-2 cells influenced by the porous NC membrane [93]. To verify their functionality, they evaluated the metabolism of verapamil and ifosfamide. The principal metabolite of verapamil produced by CYP3A4/CYP3A5 is *N*-norverapamil, and the CYP3A4/CYP2B6 metabolite derived from ifosfamide is 2-DCE-IFM. Within the device, the detection of both metabolites occurred on day 5, showing a higher cell efficiency compared with the monolayer culture.

Another study used the same cytochromes as Guo and coworkers to verify the expression and functionality of the CYP45 isoforms on the transformation of midazolam, rifampicin, ketoconazole, and indomethacin within a 3D *in vitro* platform. The multicellular 3D primary human intestinal tissue model consisted of a layer of cultured cells, such as human primary cells, polarized gut epithelium, and adult human intestinal myofibroblasts. The study confirmed the toxicity and inflammation responses of the epithelial cells due to the presence of indomethacin. Furthermore, an upregulation of inflammatory genes and epithelial cell death, as a result of the toxic effect of the tumor necrosis factor alpha (TNF-α) and LDH, was recorded within this 3D platform [94].

Some other promising models measure the efficiency of the gut barrier to perform drug transport studies and other xenobiotic agents in real time using Caco-2 cells and electrodes for transepithelial electrical resistance [95]. In one of these studies, a device consisting of eight microchambers was designed with a commercial Teflon membrane coated with thiolene to ensure effective bonding between the chip layers. Caco-2 cells were seeded under medium flow for 9-10 days. A cell viability test was performed after staining the cells for one day. The results confirmed that the device could be used as a functional drug transport model [95]. This miniaturized intestine-on-chip was found to be a promising platform for the detection of duodenum cell injuries and infections, among others.

The close mimicking of the gut's microenvironment is crucial for studying the metabolism of drugs. The addition of microbiota to the devices provides new perspectives and physiological models for a wide range of diseases. An abundance of Firmicutes and Bacteroidetes phyla are responsible for several gut functions, including absorption, metabolism, and excretion. Classical models including explants or transwells are not suitable for drug development due to their limited culture lifespan. Higher accuracy in the recreation of the microenvironment of the gut within the device may be critical to the discovery and metabolic assessment of drugs or nutraceuticals.

2.5. Heart-on-Chip. The cardiovascular system is a complex model of muscle tissue, blood vessels, and blood constituents. Cardiac muscle tissue is composed of organized cardiomyocytes (CMs) that contain a single nucleus in the center of the cell and connected to one another by intercalated discs that contain the gap junctions and the desmosomes that are important for cardiac muscle contraction. Cardiovascular diseases (CVDs) are among the most significant leading cause of premature death in developed countries. Several drugs cause cardiac toxicity, which manifests as proarrthymia in patients with or without clinical symptoms and leading to hemodynamic deterioration, syncope, or death [96]. Because of drug-related cardiac complications, the assessment of cardiovascular safety during drug development is of paramount importance. Therefore, there is a high demand for new drugs to prevent or treat CVDs. Nevertheless, the drug development for CVDs is hindered by the lack of adequate models to correctly mimic the cardiac muscle. Additionally, many drugs for the treatment of other organs or diseases have side effects or adverse reactions on cardiac tissue, which is a primary risk to consider during diverse drug development. For example, fenfluramine, developed to treat obesity, seldane for treating allergies, and rofecoxib, to be used as analgesic, have adverse effects on the cardiovascular system [97].

Recent advances in microfluidics and stem cell research provide an opportunity to recreate the cellular microenvironment to allow stem cell differentiation and an evaluation of their behavior. One of the most significant challenges in this area of research is to have a scaffold with a particular

Table 5: Summary of recent advancements in cardiotoxicity modelling and testing including the type of drug, the application, the applied cell lines, and the kinetics.

Drug type	Application	Applied cell lines	Kinetics	Ref(s)
DXR	Toxicity	HUVECs and hiPSC-CMs	33 days	[56]
	Pharmacokinetics and toxicity	hCMs and HepG2	24 hours	[100]
Isoprenaline	Toxicity	CMs and hiPSC-derived CMs	6 days	[101]
TiO_2 and Ag nanoparticles	Cardiotoxicity	CMs and NRVMs	35 hrs	[103]

DXR: doxorubicin; HUVECs: human umbilical vein endothelial cells; hiPSC: human-induced pluripotent stem cells; CMs: cardiomyocytes; hCMs: human primary cardiomyocytes; HepG2: human hepatocellular carcinoma; NRVMs: neonatal rat ventricular myocytes; TiO_2: titanium dioxide; Ag: silver.

architecture that mimics the cardiac tissue reproducing the hierarchical structure of the native myocardium with all its functions, including mechanical contractions, molecular transport, electrical activity, and specific responses to drug stimulation [98]. Heart-on-chip devices should reproduce the cellular organization level in a living heart through a very well-assembled and aligned tissue structure [99]. Additionally, there is a need for the integration of blood vessels to produce cardiovascular organoids [56]. Heart-on-chips based on the use of cardiac organoids can mimic the heart's main functions, including the synchronous contraction, the transport of nutrients and oxygen, and the removal of waste products, making them useful devices for testing potential therapeutic agents [56]. Some of the latest examples of heart-on-chip platforms for drug discovery, development, and analysis are thoroughly reviewed in this article (Table 5).

2.5.1. Analysis of Drugs in Heart-on-Chip Devices. Cardiac toxicity is responsible for nearly half of new drug recalls. The recent development of heart-on-chip platforms to evaluate drug toxicity has provided the potential to replicate a human-like response to compounds known to affect the heart's physiology. Zhang et al. fabricated a 3D endothelialized microfibrous scaffold using a bioprinter, a bioink, and cells (Figure 16). GelMA, a mixture of alginate, gelatin, and a photoinitiator, was used as bioink. HUVECs were resuspended in the ink, bioprinted through continuous deposition, and cultured for 15 days, resembling a blood vessel. After 33 days, cardiomyocytes and hiPSC-cardiomyocytes, with their respective medium, were seeded and incubated over each scaffold and exposed to doxorubicin, an anticancer drug. With a microfluidic perfusion bioreactor, the endothelialized-myocardium-on-chip model was used as a platform for cardiovascular drug screening. The toxic effects of doxorubicin on cardiomyocytes and endothelial cells were associated with the drug dose. It was concluded that the combination of bioprinting, microfluidics, and stem cells in this platform was useful for developing next-generation human organ models for personalized drug screening to mitigate drug-induced cardiovascular toxicity [56]. The development of these bioprinted 3D scaffolds, where cell lineages can interact together to recapitulate the organ physiology, could subsequently be used for *in vitro* drug testing and for mechanistic biological studies.

An integrated heart/cancer-on-chip (iHCC) to reproduce the side effects of anticancer drugs was created using a few main components: a PDMS perfusion layer and a control layer and a peristaltic pump. These components of the platform were fundamental, as the flow was created in the closed-circuit loop providing circulation within the culture chambers (Figure 17). The chip was developed using soft lithography and was used for the culture of human primary cardiomyocytes (hCMs) and HepG2 and for their subsequent treatment with doxorubicin for 24 hours. Based on the findings of this study, the platform offered the possibility of culturing different cells and recapitulated physiological and pathological conditions for the evaluation of drug toxicity [100].

In another study, Marsano et al. developed a beating heart-on-chip that can generate functional 3D microcardiac tissues. The device was equipped with two compartmentalized PDMS microchambers separated by a PDMS membrane. The top compartment was subdivided into a central channel and two side channels. Cardiomyocytes and human iPSC-derived cardiomyocytes were suspended into a matrix of fibrin gel in the central channel, while the culture medium was replenished through the side channels and generated a 3D cell construct. By pressurizing the bottom compartment, the PDMS membrane deformed, thereby compressing the 3D cell construct (Figure 18). A cyclic pressure signal mimicked systolic and diastolic phases. This study demonstrated a method to generate mature and functional 3D cardiac microconstructs. Cyclic mechanical stimulation was found to improve the maturation of the microengineered cardiac tissues (μECTs) [101]. This microfluidic platform could be used to evaluate the cardiac microphysiological system by assessing the effects of drugs on cardiac cells.

Nowadays, the use of engineered nanomaterials (ENM) is in constant rise, potentially posing unknown health responses when inhaled. Therefore, developing prevention strategies and treatments against these nanoscaled materials is an important research area in the event that they are harmful to the human body. TiO_2 NPs are widely used in sunscreens, cosmetics, paints, tiles, etc. TiO_2 NPs may result in ROS production, causing oxidative stress, inflammation, and the risk of cancer [102]. The study of the biosafety of nanoparticles and the toxic effects of TiO_2 requires a device that can provide an environment and conditions which mimic that of real tissues. In the case of the heart, it requires an ECM, along with a movement-contraction mechanism. A muscle-inspired aligned nanofiber was produced by electrospinning using a mixture of polycaprolactone (PCL) and polydopamine (PDA) [103]. The device consisted of four layers: (i) a gelatin layer over a PDMS base which was used as support for the scaffold and the cardiomyocytes, (ii) a PDMS layer, (iii) a thin

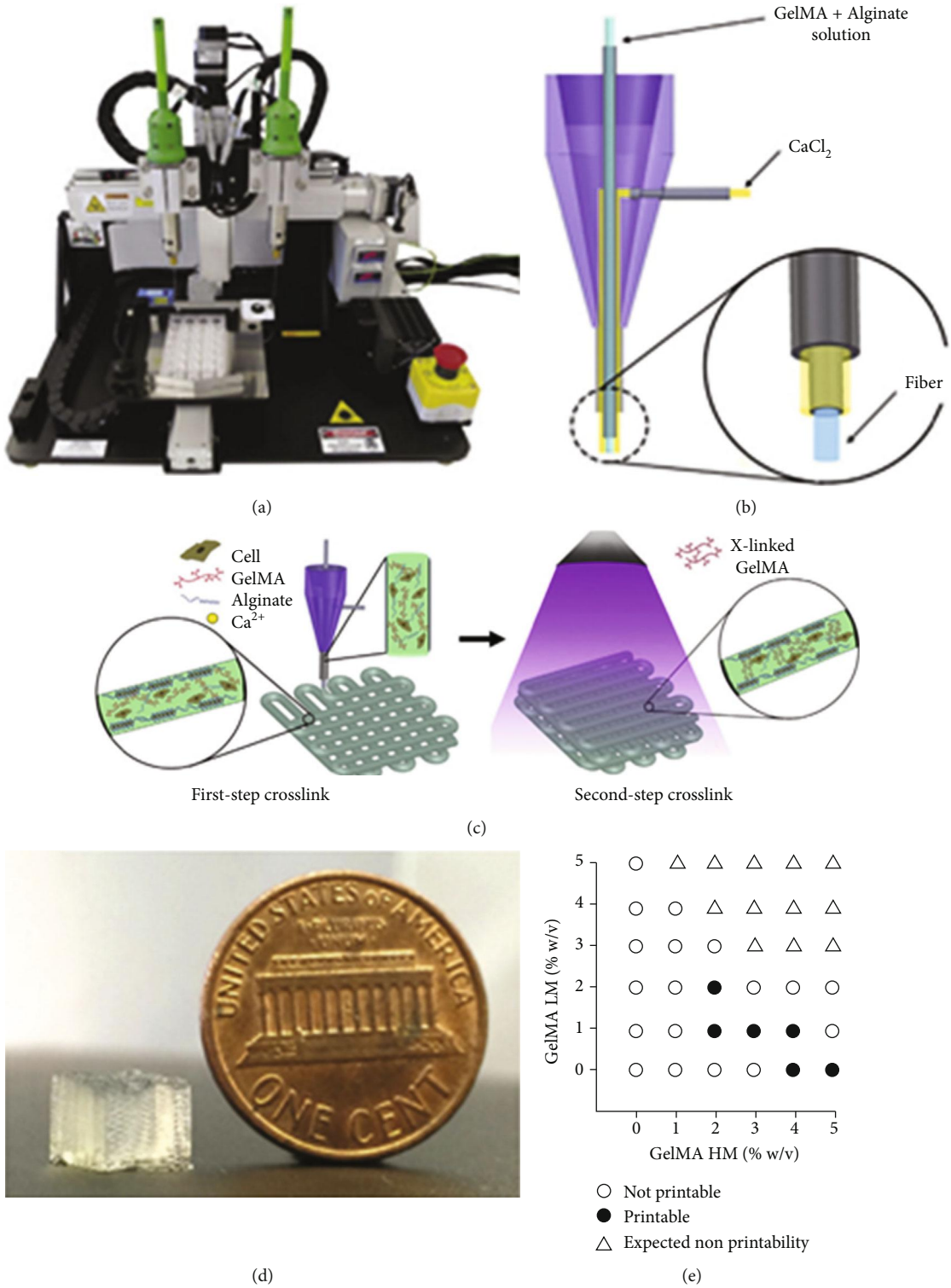

FIGURE 16: (a) Organovo Novogen MMX bioprinter. (b) Schematic of the coaxial needle where the bioink is delivered from the core, and the ionic crosslinking $CaCl_2$ solution is sheathed on the side. (c) Schematic diagrams showing the two-step crosslinking process, with $CaCl_2$ followed by UV illumination. (d) Photograph of a bioprinted cubic microfibrous scaffold. (e) Bioink optimization where conditions of printability and nonprintability for different concentrations of GelMA-HM and GelMA-LM were analyzed. Reproduced (or adapted) with permission [56], ©2016, Elsevier.

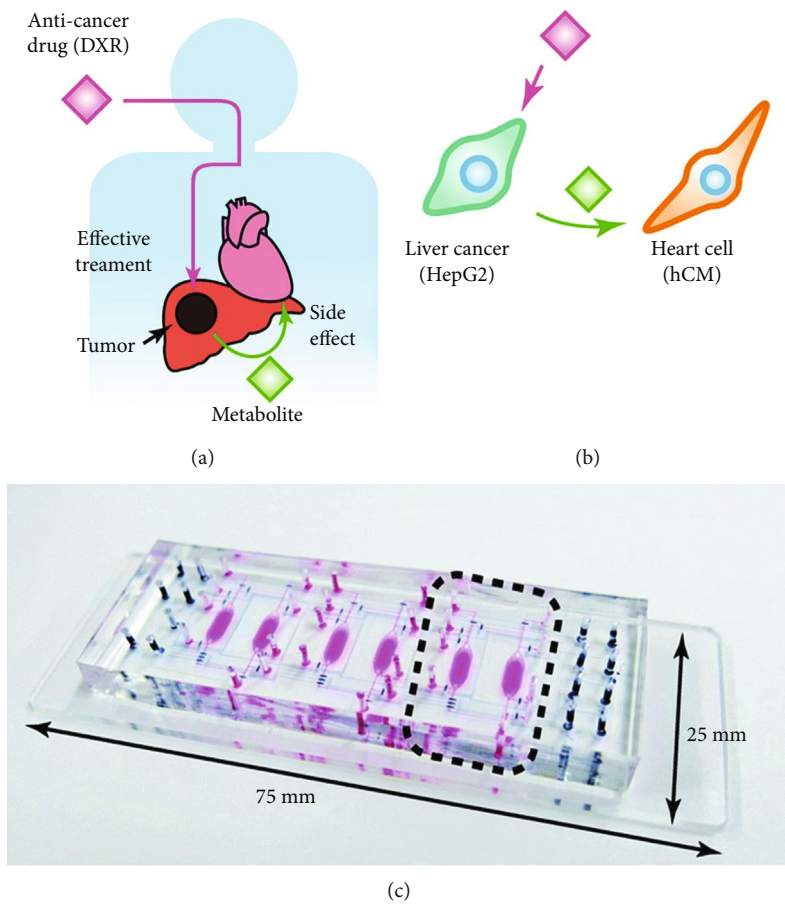

Figure 17: Integrated heart/cancer on a chip, (a, b) Communication between liver cancer cells and healthy heart cells through exchange of metabolites and the side effects of an anticancer drug. (c) Photograph of an actual iHCC fabricated on a glass slide. Reproduced (or adapted) with permission [100], ©2017, Royal Society of Chemistry.

sensor film (responsible for the contractions), and (iv) a lower PDMS layer. Neonatal rat ventricular myocytes (NRVMs), grown on the scaffold, were developed into a mature and functional tissue. TiO_2 NPs and silver (Ag) were added directly to the scaffold. The collected data established that high doses of TiO_2 NPs (100 μg/mL) affected the contractile function and damaged the tissue structure after 48 hours of exposure [103].

The structural colors of living flora and fauna have inspired researchers to develop hydrogels, nanoshells, filaments, and several bioinspired materials [104–107]. To mimic the color shift mechanism of chameleons, Fu et al. (2018) created a heart-on-chip system using such bioinspired materials. The hydrogel scaffolds were fabricated using colloidal crystal templates prepared with silicon dioxide (SiO_2) nanoparticles assembled on glass slides. GelMA was subsequently infiltrated into the templates, polymerized with UV light, and etched with hydrofluoric acid. Silicon patterned wafers were used to obtain colored hydrogels that were disinfected with UV light before seeding with cardiomyocytes isolated from rat pups. The biohybrid colored hydrogel contained perfused microfluidic chambers to provide the medium and the drug solution to the living cells (Figure 19). The platform was used to evaluate isoproterenol, a drug used for mild or transient episodes of bradycardia and heart block. The authors featured this system in a study of the microphysiological monitoring of biological systems and for drug screening [99].

The complexity of the anatomical and physiological structure of the heart muscle has been a major driving parameter for the fabrication of new devices that track cardiac impulses, analyze mechanical properties, and mimic some of the main atrophic characteristics. Development of a system that optimizes 3D cell seeding, while maintaining the electrophysiologic characteristics and mimicking the blood flux, represents an excellent opportunity to understand the pathogenesis of certain chemotherapeutic treatments. The adverse effects of chemotherapeutic drugs are not well-studied due to the time-lapse of *in vitro* assays and insufficient knowledge regarding the continuous monitoring of such drugs.

2.6. Skin-on-Chip. Skin is the largest organ of the body and is comprised of epidermis, dermis, and hypodermis layers, which are mainly comprised of keratinocytes, fibroblasts, and adipocytes, respectively. The epidermis is in charge of preventing the entry of exogenous materials and pathogens, while the dermis protects internal organs and regulates water evaporation. The human skin serves as a physiological barrier to safeguard the internal organs. Since the skin is an outer barrier, it is constantly exposed to many chemical substances and

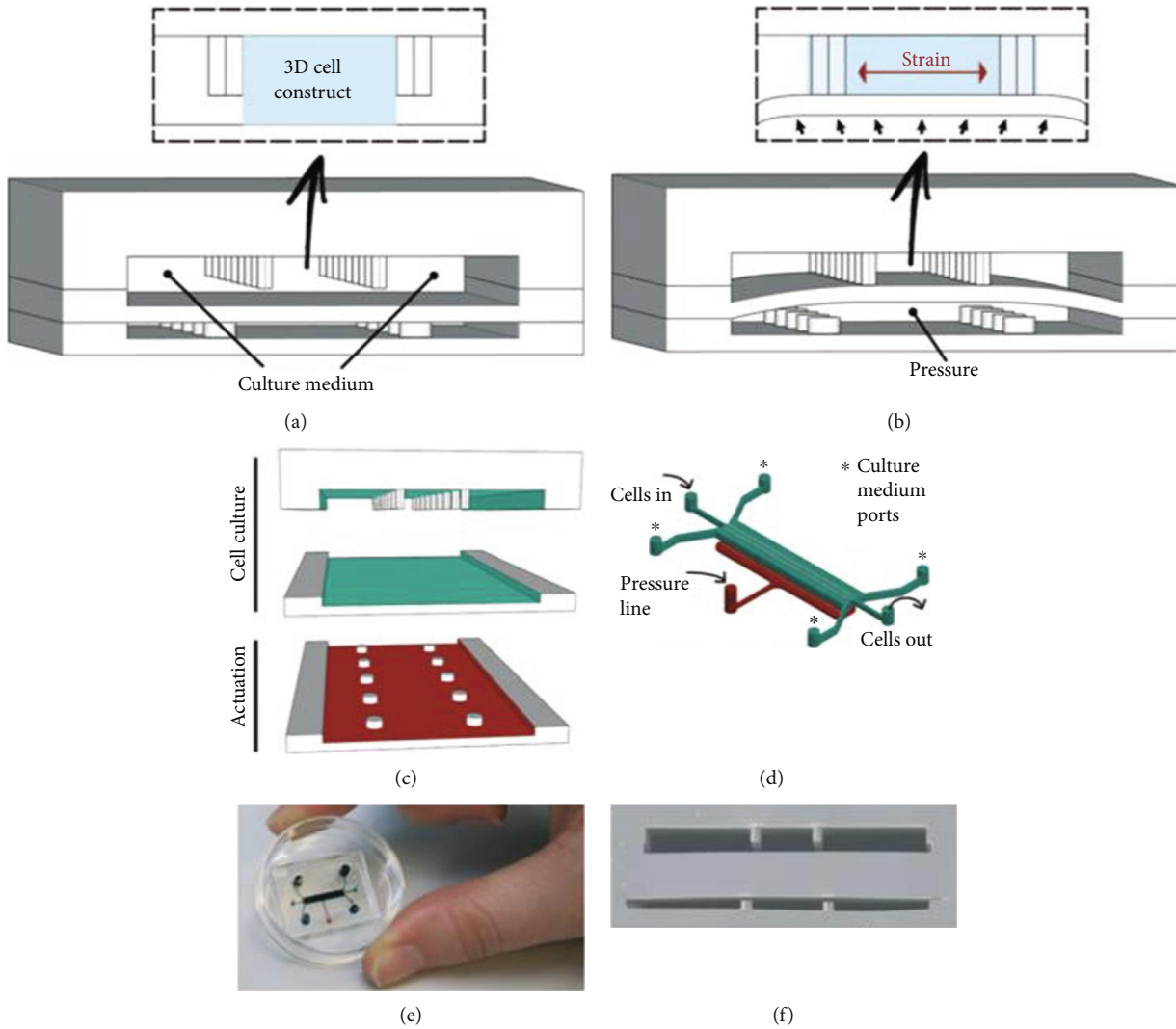

Figure 18: Design of the 3D heart-on-a-chip microdevice. (a) The device uses two compartmentalized PDMS chambers. (b) By pressurizing the bottom compartment, the compression transduces into a uniaxial strain applied to the 3D cell construct. (c) Inside view of the PDMS chambers. (d) 3D sketch of both compartments. (e) Picture of an actual 3D heart-on-chip device. (f) Scanning electron microscopy image of a cross-section of the device (scale bar, 500 μm). Reproduced (or adapted) with permission [101], ©2016, Royal Society of Chemistry.

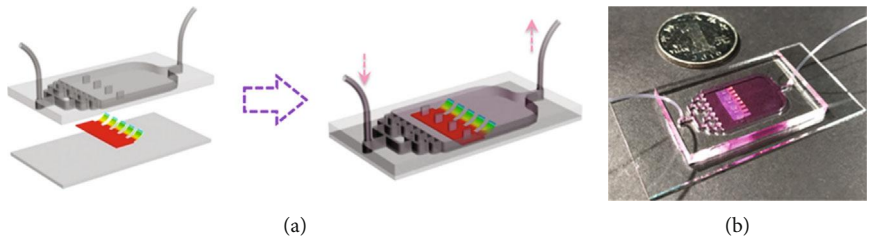

Figure 19: The applications of the biohybrid structural color hydrogels in a heart-on-a-chip system. (a) Schematic of the construction of the heart-on-a-chip by integrating the biohybrid structural color hydrogel into a bifurcated microfluidic system. (b) Image of the biohybrid structural color hydrogel integrated heart-on-a-chip. Reproduced (or adapted) with permission [99], ©2018, American Association for the Advancement of Science.

biological agents, including cosmetics, skin detergents, UV light, pathogenic microorganisms, and environmental pollutants [108]. Animal models have been extensively used to evaluate cosmetics and diverse drugs. Nevertheless, the ethical considerations, high costs, time-consuming processes, the limited ability to represent the real human physiology and metabolism, and the impossibility of performing quantitative studies remain as main drawbacks for drug testing and disease

modelling. To overcome these limitations, the development of 3D microfluidic platforms, where cells are cultured in an ECM as better simulators of skin functions, is gaining attention [109].

During drug testing in this organ, the complexity of the diffusion at the several layers of skin represents a significant disadvantage in animal or 2D models. Percutaneous-dermal absorption requires three steps: penetration of the compound to a skin layer, permeation through the layers, and resorption into blood circulation. The chemical interaction with the hydrophilic nature of the skin must be tested in an accurate 3D model that leads to the analysis of drug interactions. One of the standard tests for skin permeation of drugs or transdermal delivery systems is the diffusion cell apparatus, also known as the Franz diffusion cell [110, 111]. In this overview, the latest skin-on-chip technologies are summarized, including those that improved on the Franz diffusion cell analysis. Some of the latest examples of skin-on-chip platforms for drug discovery, development, and analysis are thoroughly reviewed in this article (Table 6).

2.6.1. Analysis of Drugs in Skin-on-Chip Devices. Recent advances in microfluidic cell culture systems enable the construction of *in vitro* human skin models that can be used to evaluate the toxicity of drugs and other compounds [112]. Current skin models have been developed to evaluate the efficacy of drugs and the effect of UV radiation and of aging by using keratinocytes, fibroblasts, melanocytes, and stem cells to better reproduce the physiology of the skin. Wufuer et al. (2016) developed a skin-on-chip device to mimic the structures and functional responses of human skin [108]. The model comprised of three PDMS and two porous membrane layers to coculture human epidermal keratinocytes (HaCaT), human skin fibroblasts (HS27), and HUVECs mimicking the epidermis, dermis, and the endothelium layers. Skin inflammation and edema were induced by perfusing TNF-α through the dermal layer (Figure 20). The model analyzed the expression levels of proinflammatory cytokines and the efficacy of dexamethasone, a drug used for treating inflammation and edema, in order to demonstrate the functionality of the system. The results showed that IL-1β, IL-6, and IL-8 levels increased with 25 ng/mL and 50 ng/mL of dexamethasone but decreased with 100 ng/mL of dexamethasone, confirming the dose-dependent effectiveness of the anti-inflammatory drug.

Mori et al. [113] fabricated a 3D skin-on-a-chip microdevice with perfusable vascular channels coated with endothelial cells that comprised a skin equivalent fixed to a culture device connected to an external pump and tubes. The skin equivalent contained normal human dermal fibroblasts (NHDFs), normal human epidermal keratinocytes (NHEKs), and HUVECs. The authors evaluated the percutaneous absorption of the model drugs, caffeine and isosorbide dinitrate (ISDN), through the skin equivalent layer during the perfusion of Dulbecco's modified Eagle's medium (DMEM) in the vascular channels. Its feasibility was demonstrated by measuring the permeation of the applied drugs through the vascular channels. Both drugs reached the vascular channels after ~5 min of drug application and took ~30 min to reach the skin equivalent. These results confirmed that the model can be used for the development of skin treatments and cosmetics.

Lee et al. (2017) described the construction of a 3D multicellular microfluidic chip for an *in vitro* skin model. The device consisted of two layers of PDMS. The bottom layer consists of microfluidic channels for vascular cells, and the top layer contained a skin cell culture chamber. The chip, controlled by gravitational effects, was placed on a platform tilted at a certain angle to induce a specific flow. The results suggested that the presence of flow plays a crucial role in maintaining the viability of cells. The 3D skin chip with vascular structures can be a valuable *in vitro* model for reproducing the interactions between the different components of the skin tissue. It operates in a more physiologically realistic manner in demonstrating the consumption of oxygen and homogenous diffusion of glucose, which enables the system for assessing the reaction of the skin to cosmetic products and drugs [109].

A recent innovative study tested the efficacy of penicillin and neutrophil migration in human tissue infected with *Staphylococcus aureus*. This device has three compartments: a column, a blood channel, and a migration zone. The fabrication was done by soft photolithography on PDMS cured overnight and bonded to the glass-bottomed well plates. The skin tissue was taken from a human skin microbiopsy and autologous blood (Figures 21(a) and 21(b)). The infection model involved a pretreatment of the biopsy with the bacteria which was subsequently injected into the device. The authors initially measured neutrophil migration on the middle section of the chip, interpreted as activation of the cells in the presence of the pathogen. The very interesting result revealed that the time of migration correlates with a pattern of infection. Additionally, the study provided the efficacy test of the penicillin, showing bacterial clearance and indirect attenuation of neutrophil migration over time [114].

The Franz diffusion cell approach is the most common methodology to evaluate drug permeation *in vitro*; however, the test suffers from poor reproducibility [115]. To overcome that limitation, Lukács et al. [116] designed and fabricated a skin-on-chip device by using PMMA and polylactic acid (PLA) through 3D printing to evaluate caffeine penetration. The microfluidic diffusion chamber contained two skin holders with layers for a skin sample or membrane (Figures 22(a) and 22(b)). The authors simultaneously ran the *in vivo* experiments using the Franz diffusion system, in order to compare the results of caffeine absorption. The data showed that both tests provided similar C_{max} values, while more advanced systems are needed to assess and evaluate drug formulations [116].

In a similar study, Alberti et al. [117] tested the diffusion of caffeine, salicylic acid, and testosterone on human primary fibroblasts and keratinocytes in a microfluidic skin permeation platform validated by the Franz diffusion cell. The system was composed of a multichambered microfluidic chip fabricated by the thermal bonding of three thermoplastic layers and six polytetrafluoroethylene (PTFE) membrane disks or human skin punches and twelve silicone membrane connectors. This innovative design permitted the accumulation of perfused media in a 96-well plate. The permeability coefficient (Kp) of caffeine was $0.83^{\circ}\mathrm{cm\,h^{-1}}$ and $0.94^{\circ}\mathrm{cm\,h^{-1}}$ for the skin platform and Franz cells, respectively. The Kp value for salicylic acid

Table 6: Summary of recent advancements in skin-on-chip and drug testing including the type of drug, the application, the applied cell lines, and the kinetics.

Drug type	Application	Applied cell lines	Kinetics	Ref(s)
Dexamenthasone	Efficacy	HaCaT, HUVEC, HS27	3 days	[108]
	Efficacy	GM-3348, HUVEC, human macrophages (primary cell culture)	Over 48 hrs	[123]
Caffeine ISDN	Absorption	HUVEC, NHDFs, NHEKs	10 days	[113]
Penicillin	Efficacy	Human skin biopsy, peripheral human blood	>24 hrs	[114]
Caffeine	Diffusion	Rat skin cells	—	[116]
Caffeine Salicylic acid Testosterone	Diffusion	N/TERT-1, human primary fibroblast	—	[117]
TNPs	Toxicity	HaCaT	48-72 hrs	[121]

HaCaT: human epidermal keratinocytes; HUVECs: human umbilical vein endothelial cells; HS27 and GM-3348: human fibroblast; ISDN: isosorbide dinitrate; NHDFs: normal human dermal fibroblasts; NHEKs: normal human epidermal keratinocytes; N/TERT-1: keratinocytes; TNPs: titanium dioxide nanoparticles.

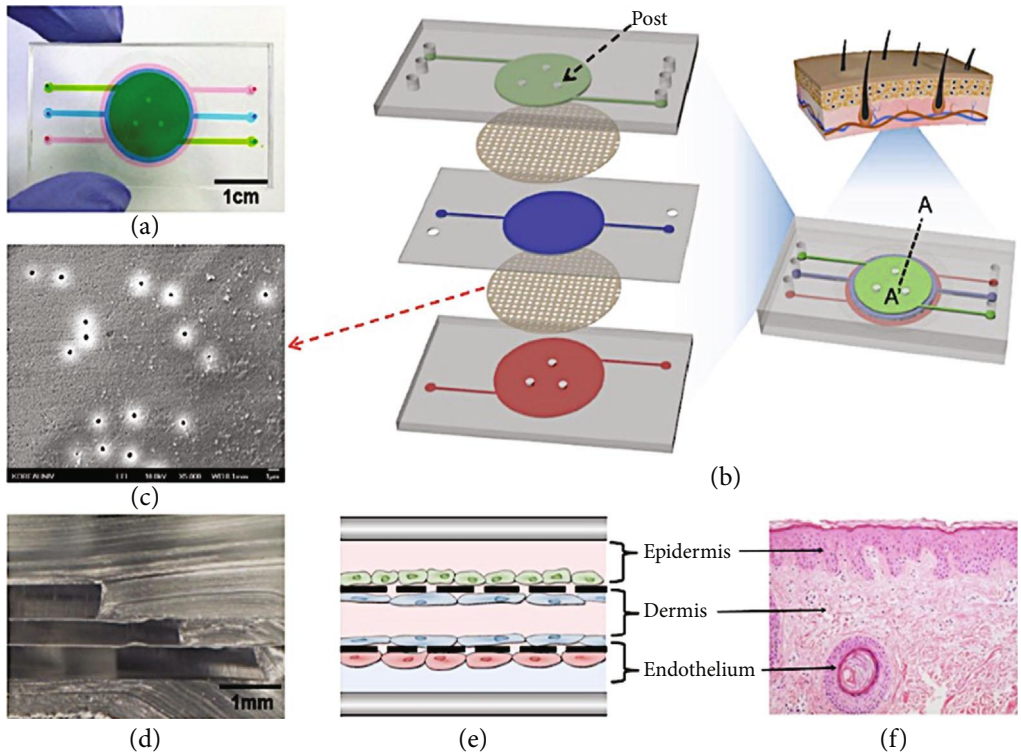

Figure 20: Description of the microfluidic device. (a) Image of a skin-on-a-chip device filled with fluid in three different colors. (b) 3D scheme of the skin-on-a-chip system comprising three PDMS layers and two PET porous membranes (footprint: 48 mm × 26 mm; height: 7 mm). (c) SEM image of PET porous membranes (pore size: 0.4 μm) obtained from Transwell. (d) Cross-sectional image of A–A′. (e) Schematic of the skin-on-a-chip system, including three separate channels with four vertically stacked cell layers. (f) Representative histological skin section stained with hematoxylin and eosin to indicate the cellular organization of skin. Reproduced (or adapted) with permission [108], ©2016, Nature.

was 11°cm h^{-1} and 10°cm h^{-1} and for testosterone 8.2°cm h^{-1} and 9.2°cm h^{-1}, confirming that the permeation test of the microfluidic system was highly accurate and similar to the Franz model [117].

Ramadan et al. [118] further corroborated these findings using an air-liquid interface and transepithelial electrical resistance (TEER) probes to evaluate the effects of lipopolysaccharides and UV irradiation on the cell growth and tight junction formation allowing a more realistic *in vivo* culture environment. The findings of this study indicated that dynamic perfusion allowed for an increase of cell viability for up to 17 days [118].

More recently, Alexander et al. [119] fabricated a skin-on-chip integrated with a sensor to evaluate the TEER and the extracellular acidification rate (EAR) integrating an automated air-liquid interface. The biochip device was comprised

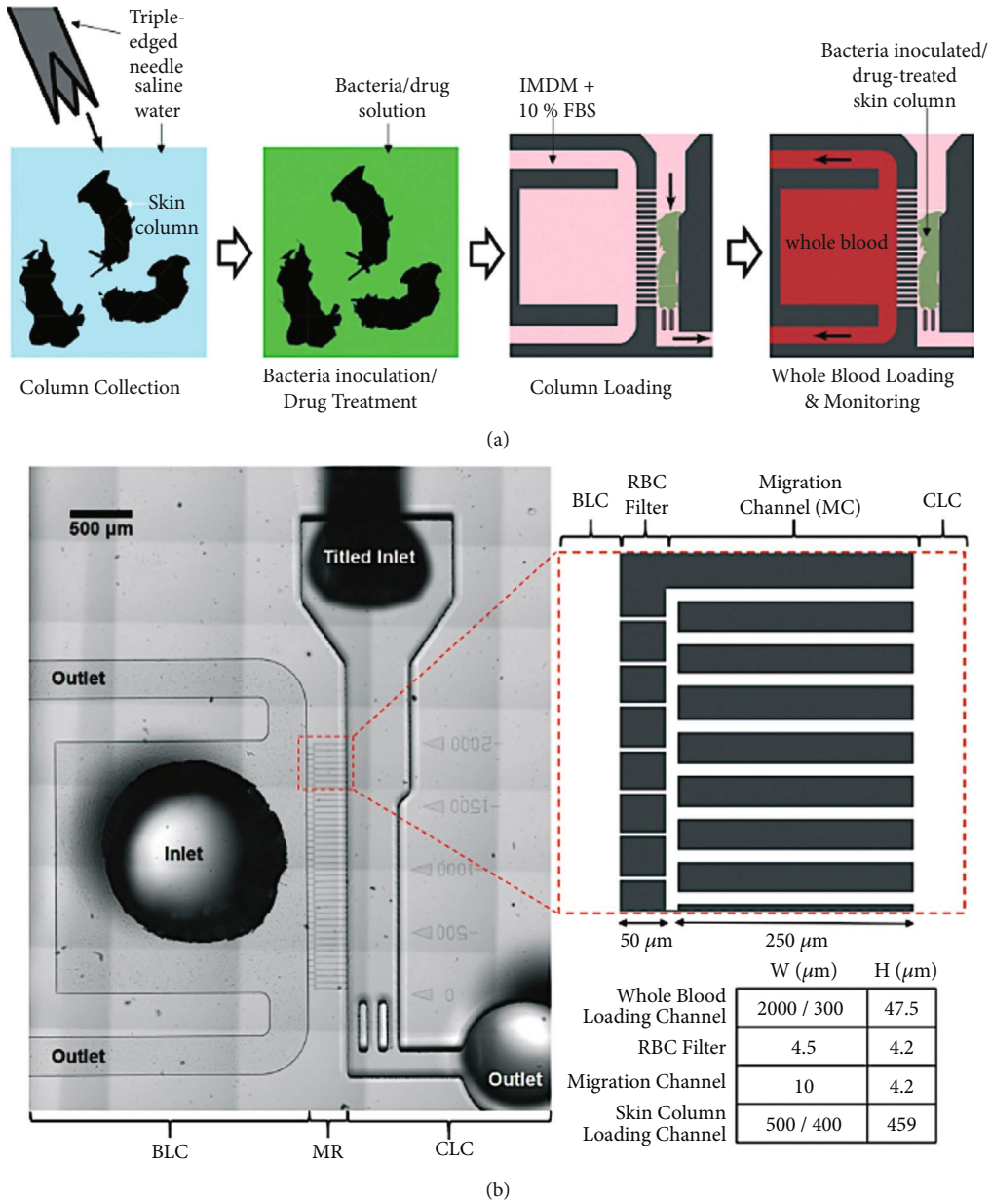

FIGURE 21: *Ex vivo* skin-on-a-chip assay for the diagnosis of skin and soft tissue infections. (a) Schematics of the human skin and blood sample loading. (b) Microfluidic design of *ex vivo* skin-on-a-chip. Left shows the bright field image of *ex vivo* skin-on-a-chip. Top-right represents the design of the migration channel (MC). Bottom-right shows the dimension of ex vivo skin-on-a-chip components: whole blood loading channel (BLC), red blood cell (RBC) filter, MC, and skin column loading channel (CLC). Reproduced (or adapted) with permission [114], ©2018, Royal Society of Chemistry.

of membranes that were inserted into the culture chamber where murine fibroblast cells and medium were perfused through an inlet opening into the chamber formed below the membrane. Pores at the bottom of the membrane allowed for the passive diffusion of fresh nutrients to the basal layer of cells and of the waste products from the cells. Nutrient-depleted medium was then pumped out of the chamber through an outlet (Figures 23(a) and 23(b)). The device used TEER sensors to continuously monitor the cells noninvasively. This study was a proof-of-concept that demonstrated the capability of the custom-made device to maintain stable culture conditions to be used as a screening platform for the evaluation of drug candidates and to understand their mode of action [119].

The skin experiences constant physical stimuli including stretching. Exposure to excessive physical stimuli stresses the skin and can accelerate aging. In the study of Lim et al., the effect of physical stress was studied to generate knowledge on skin aging using a skin equivalent model of aged wrinkled skin-on-a-chip (WSOC). To create this platform, two PDMS layers were constructed through soft lithography. The first structure contained chambers and a magnet placed on an aluminum mold with a hole for the magnet placement. The second mold was responsible for communicating channels

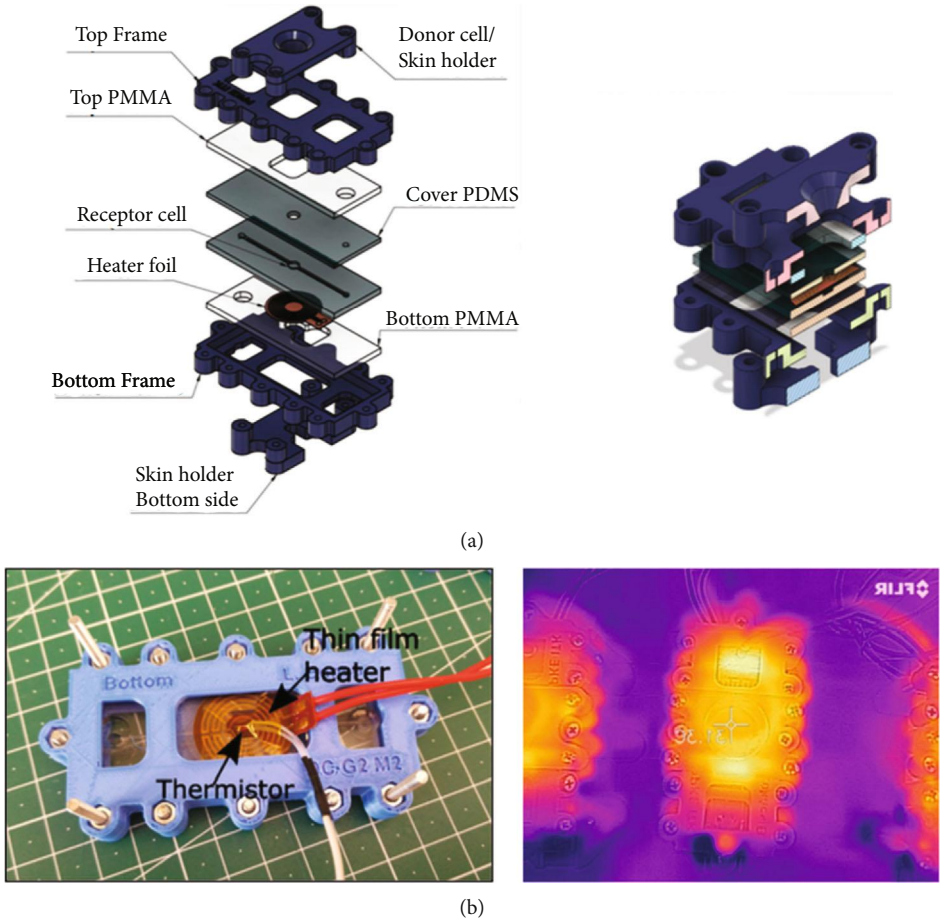

FIGURE 22: : Schematic view of the microfluidic diffusion chamber. (a) Layer by layer view. (b) The bottom side of the chip and temperature control measurement. Reproduced (or adapted) with permission [116], ©2018, MDPI.

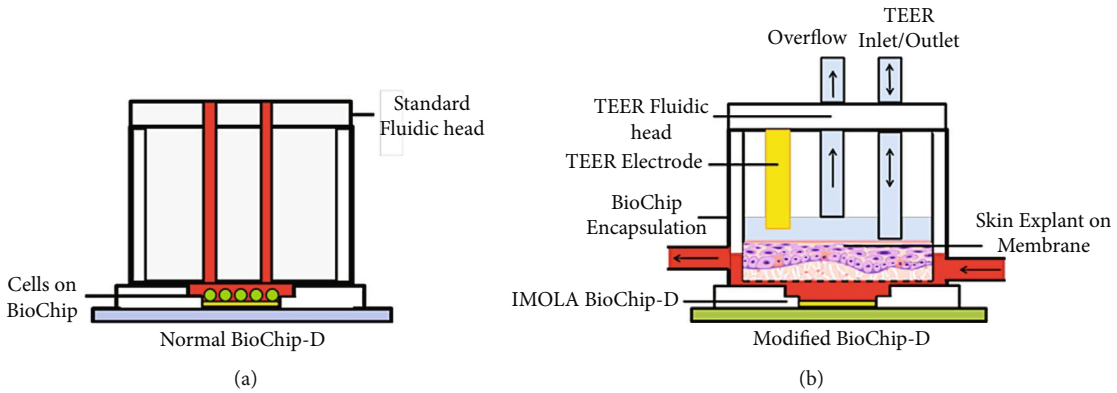

FIGURE 23: Schematic diagrams: (a) standard biochip with fluidic head and (b) modified biochip. Reproduced (or adapted) with permission [119], ©2018, MDPI.

between chambers. The device provided a platform to study the effects of antiwrinkle drugs used in cosmetic applications. The model allowed human fibroblasts and keratinocytes to be perfused with other elements to form 3D skin equivalents that were then stretched for 12 h per day at either 0.01 or 0.05 Hz for up to seven days to form WSOC. After seven days of constant stress, the results demonstrated an increase in collagen and fibronectin within the ECM expressed by fibroblasts. Fibroblasts are known to be responsible for the formation of resilient and elastic skin. Keratinocytes, which are responsible for the production of keratin, were notably decreased when compared with the control, unstretched skin tissue. The experiment showed positive results for the replication of an *in vitro* skin aging model. Moreover, the

platform could be applied for antiwrinkle cosmetics and medicines [112].

Many commercial sunblock products use organic or inorganic UV filters to block harmful UV rays. TiO_2 and ZnO are commonly used as UV blockers in sunscreens, but despite the protection they provide against cutaneous phototoxicity, these chemicals can cause oxidative stress-mediated toxicity in cells by absorbing UV radiation after direct exposure to UV sunblockers [120]. McCormick et al. [121] developed a skin model to evaluate the toxicity of titanium dioxide nanoparticles (TNPs) and the effect of UV irradiation. The chip was made from PDMS, while quartz plates and 96-well plates were used to expose the HaCaT to UV and TNPs as shown in Figures 24(a)–24(d). The study demonstrated that TNPs absorbed a wide range of UV-A and UV-B wavelengths protecting the cells when exposed to UV irradiation. The live/dead staining cell test showed an IC_{50} (50% viability) value of 35.6 mJ/cm^2 when they were exposed to UV without TNPs [121]. Overall, these results provide valuable information for the study of nanoparticle toxicity and drug testing.

The versatility of the microfluidic systems gives flexibility to the function of such devices. In that perspective, Hakimi et al. [122] fabricated a handheld skin printer with several microfluidic compartments and a cartridge that contains bioinks and a cross-linker for wound healing application (Figures 25(a)–25(c)). The cartridge was 3D printed using a resin, integrated Luer lock connectors, and wells (Figure 25). The bioinks were prepared with different formulations based on fibrinogen, hyaluronic acid, alginate, collagen type I, and keratinocytes allowing the deposition of sheets that were cross-linked at the site of deposition. The position of the cartridge allowed the coordination of the flow rates when it was delivered to the skin. *In vivo* assays, performed in animal models, demonstrated that cells added to the bioink and *in situ* delivered enhanced granulation tissue formation and increased wound healing. This portable device can also be used to deliver compounds and/or drugs for *in situ* wound healing [122].

Similarly, in a recent study, Biglari et al. [123] developed a skin wound-on-chip model to assess the anti-inflammatory effect of macrophages and dexamethasone on wound healing during inflammation induced with TNF-α. The device, fabricated with PDMS, consisted of three channels: two lateral channels for human dermal fibroblast (GM-3348) and human macrophages from primary cell culture and an inner channel for endothelial cells (HUVEC). Macrophages were also cocultured with HUVECs and fibroblasts to simulate an inflammatory condition. In addition, dexamethasone was used to test the efficacy on reducing the TNF-α-induced inflammation on damaged fibroblasts. The authors found that the macrophages produced cytokines that induced fibroblast differentiation to myofibroblasts during the wound healing process, while dexamethasone increased vascularization. The wound-on-chip model may help to gain insight into the mode of action of a drug in wound healing and the potential for a preclinical test for new drugs and cosmetics [123].

Skin-on-a-chip devices are perhaps the most advanced systems in the category of organ-on-chip. They represent successful platforms for wound regeneration, drug testing, and toxic agent testing, including UV light, allergens, and cosmetics. Skin-on-a-chip platforms can replicate injuries or induced-disease environments through the incorporation of several cell lines. The addition of biosensors can measure compounds in real-time during examinations of drug penetration or drug toxicity. Despite tremendous efforts, certain challenges with respect to the cell microenvironment and full cellular compatibility assays are yet to be addressed. The majority of studies use primary cell cultures, cell lines (human and animal-derived), differentiated induced pluripotent stem cells (iPSCs), or a combination of them, within the same device. Mimicking the real microenvironment is necessary to control these variables and their compatibility with a validation system. Another challenge is the long-lasting cultures that may require cell heterogenicity and delivery of nutrients. Most devices could maintain a viable skin system over 30 days. However, for studying extended treatment efficacy, drug permeability, and toxicity over time, a longer culture period is needed. Another limitation of the current 3D *in vitro* skin models is that they do not recapture the human skin architecture and physiology. In particular, an ideal model must be comprised of epidermis and dermis layers and the presence of vascular structures for the diffusion of nutrients and signaling molecules. Furthermore, the present devices lack the long-term survival of competent full-thickness skin. We believe that a 3D skin chip with vascular structures can be a valuable *in vitro* model for reproducing the interactions between different components of the skin tissue and thus function as a more physiologically realistic platform for testing skin reactions to cosmetic products and drugs.

2.7. Brain-on-Chip. The brain is the most sophisticated component of the central nervous system (CNS). It is comprised of about 86 billion neurons, the electrically excitable cells that receive signals from the body's sensory organs and then output information to the organs, communicating in trillions of synaptic connections. Apart from the neurons, the CNS is comprised of numerous other cells, including astrocytes, oligodendrocytes, and microglia that fulfil a crucial role for many functions of the body. Unlike other cells, neurons do not divide, and neither do they die off to be replaced by new ones. Research regarding brain development is still limited, as the main models that have been used are animal models. Such models have limitations, including high cost, time-consuming and labor-intensive procedures, and experimental variations [124]. To overcome those limitations, systems capable of imitating the *in vivo* neuronal plasticity must be developed [125]. As an alternative, biomedical research has attempted to mimic this complex human organ using traditional 2D cultures. Expectedly, such platforms are far from realistically representing the physiology of the brain, especially the neuronal plasticity, and the effective blood-brain barrier (BBB), a selective diffusion barrier that protects the brain from the effects of numerous drugs [126]. This barrier involves a vascular endothelial layer that interacts with astrocytes and neurons and plays a vital role in evaluating drug delivery and drug toxicity. Thus, this barrier has been used

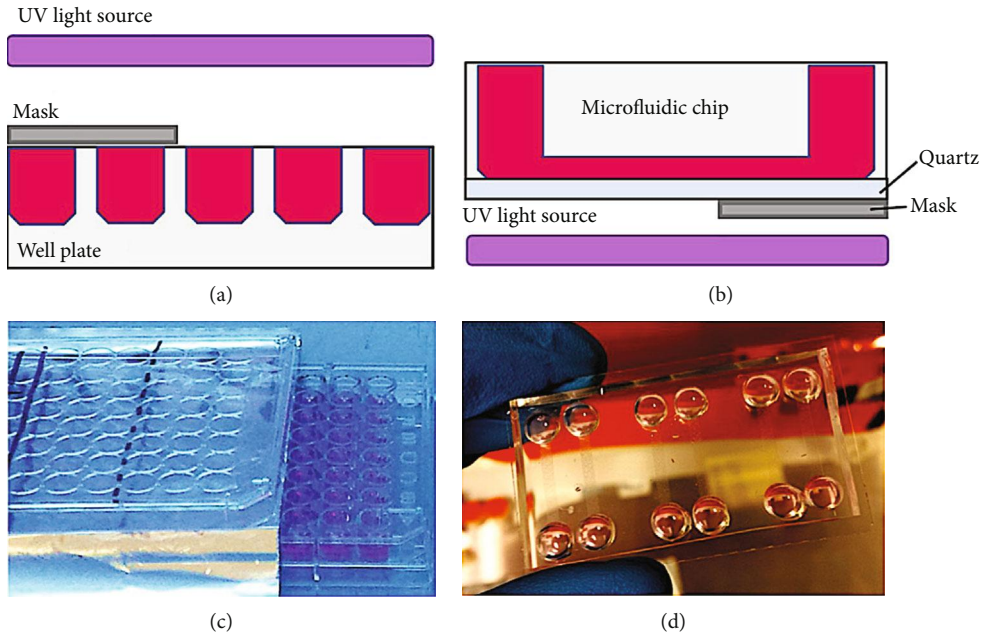

Figure 24: Diagram of different UV exposure methods, with (a) top-down UV from the biosafety cabinet on a 96-well plate and (b) bottom-up UV from the light table on a microfluidic chip. Photographs of (c) well plate and (d) microfluidic device. Reproduced (or adapted) with permission [121], ©2019, American Institute of Physics.

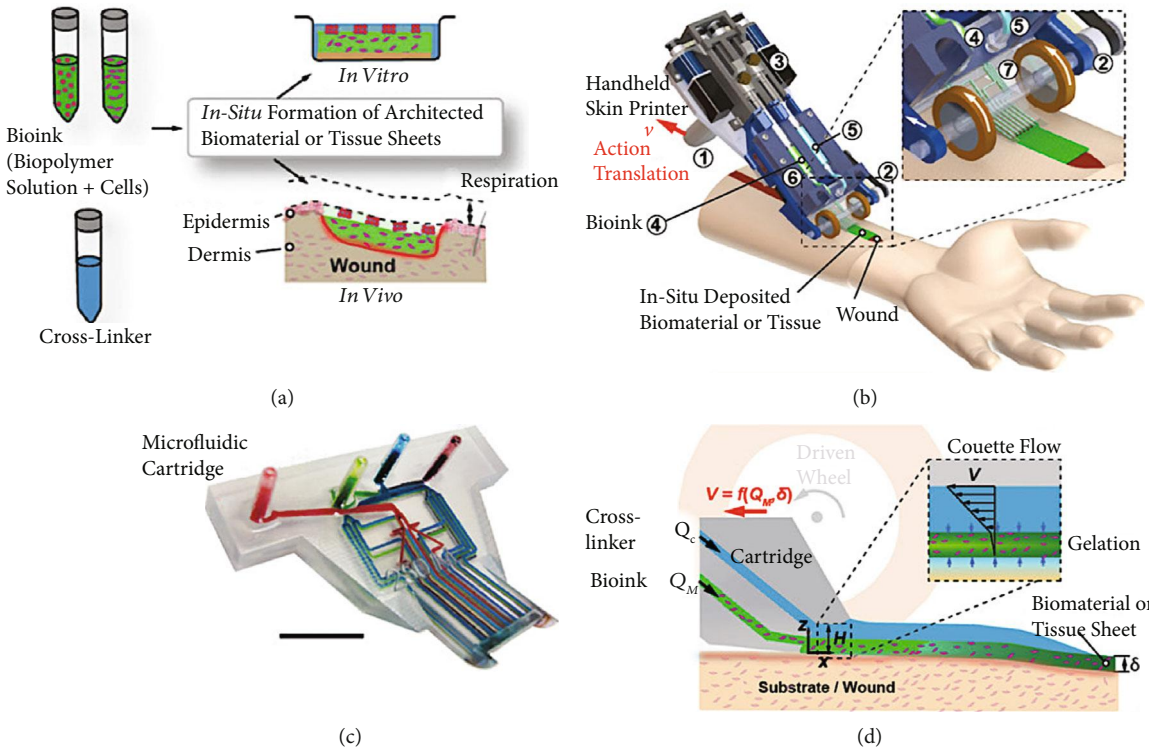

Figure 25: Handheld skin printer: (a) schematic diagram illustrating working principle of handheld bioprinter. (b) Rendered image of handheld bioprinter. (c) Photograph of 3D printed microfluidic cartridge. Scale bar 10 mm. (d) Schematic sideview image showing sheet formation between moving microfluidic cartridge and deposition surface or wound. Inset indicates fluid velocity profiles in bioink (green) and cross-linker layers (blue). Reproduced (or adapted) with permission [122], ©2018, Royal Society of Chemistry.

Table 7: Summary of recent advancements in *in vitro* models in brain toxicity testing including the type of drug, the application, the applied cell lines, and the kinetics.

Drug type	Application	Applied cell lines	Kinetics	Ref(s)
Amyloid-β	Toxicity (disease mimic)	Neural progenitor suspension (cortical rat cells)	Over 10 days	[125]
CXCL12, SLIT2-N	Chemotactic effect	Progenitor hNT2, primary hNPC, hBMECs	8 weeks	[143]
Antihuman transferrin receptor (MEM-189), MoAb	Transcytosis	TY10, hBPCT, hAst		[131]
Dextran	Permeability	Astrocytes (pup), primary cortical cells (rat), HUVEC	Over 7 days	[130]
		hCMEC/D3	Over 4 days	[144]

CXCL12, SLIT2-N: chemokines; hNT2: human teratocarcinoma cells; hNPC: human fetal neural progenitor cells; hBMECs, TY10: human brain microvascular endothelial cells; MoAb: monoclonal antibody; hBPCT: human brain pericyte; hAst: human astrocytes; HUVECs: human umbilical vein endothelial cells; hCMEC/D3: human cerebral microvascular endothelial cell line; TEER: transendothelial electrical resistance.

to study the mechanisms of degenerative diseases, including Alzheimer's disease (AD), Parkinson's disease (PD), and amyotrophic sclerosis (AS). Recently, 3D models based on microfluidics have become widely applied to study brain functions and neurotoxicity for the purpose of drug discovery. Such devices facilitate cell-cell interactions by resembling fundamental dynamic conditions of the native brain environment. Some of the latest examples of brain-on-chip platforms for drug discovery, development, and analysis are thoroughly reviewed in this article (Table 7).

2.7.1. Analysis of Drugs in Brain-on-Chip Devices. Brain-on-chip technology is aimed at modelling brain tissue in order to test and predict the effects of certain drugs, to establish new treatments to reverse or prevent neurodegenerative diseases (such as AD and PD), and to screen candidate therapeutic drugs for toxicity. AD is the most common type of dementia and affects tens of millions of people worldwide [127]. The monomeric amyloid-β is a peptide associated with a variety of biological brain functions; however, its soluble oligomers accumulate and form senile plaques that are implicated in the pathogenesis of AD. Research has featured the effects of amyloid-β peptides on the neuronal body of the brain. Park et al. (2015) developed a microfluidic chip that was based on 3D neurospheroids that could closely mimic the *in vivo* brain microenvironment by providing a constant flow of fluid. The PDMS chip contained a concave microwell array for the formation of homogeneous neurospheroids having a uniform size with 3D cytoarchitecture. The osmotic micropump system was connected to an outlet to provide a continuous flow of medium at the interstitial flow level [125]. When the flow on the spheroids was reduced, the size differentiation was inversely accelerated. Traditional mature molecules like beta-III tubulin showed an increase when the active interstitial flow was induced. By providing a 3D cytoarchitecture and interstitial flow, the chip mimicked the microenvironment of a normal brain and those of AD patients, facilitating the investigation of amyloid-β effects on 3D neural tissue. Furthermore, modelling the blood-brain barrier was necessary, as it is a critical structure between the central nervous system and the rest of the body. The authors tested the toxicity of amyloid-β protein on neurospheroids under dynamic or static conditions for 7 days. By using this platform, it was confirmed that neurospheroids cultured under dynamic conditions showed a larger size than those cultured under static conditions, while the amyloid-β reduced cell viability under static conditions. Moreover, the fluidic model also demonstrated that the treatment with amyloid-β decreased the synapsing levels, and it permeated deeper than static assays, which enhanced the biomimetic disease modelling [125].

As was mentioned, the BBB is a selective diffusion barrier within the brain. It is comprised of several cell types that together with tight junctions can protect the brain from the passage of drugs or other compounds directly into the brain [128]. Advances in microfluidic and nanofabrication have contributed to the development of *in vitro* BBB-on-chip platforms that are unique tools for studying the physiology of the brain, neurodegenerative diseases, neurotoxic compounds, and drug discovery. Brown et al. [129] designed a microfluidic device introduced as a neurovascular unit (NVU) comprised of both a vascular chamber and a brain chamber separated by a porous PDMS membrane, allowing cell-to-cell communication between endothelial cells, astrocytes, and pericytes. The NVU had four crucial design features that helped mimic the BBB: (i) adjustable flow on both sides of the barrier, (ii) low media-to-cell volume, (iii) scaffolding to orient and support multiple cell types, and (iv) easy adjustment of the device orientation. The upper layer was used for perfusion, loading, and sampling for the brain compartment with pericytes, neurons, astrocytes, and ED ECM (collagen 1) [129]. The shear stress increased the expression of tight junction molecules and successful dextran permeability through the mimetic BBB. A limitation of this model was the use of PDMS that impedes cell adhesion due to its hydrophobicity. While the device was not used to test any drug, it was demonstrated to have potential to be used for drug discovery due to its close resemblance to the structure of the BBB.

In a 3D neurovascular device, Adriani et al. [130] explored further the mimicking of the BBB. The barrier was made from PDMS by soft lithography and bonded to glass coverslips. The device was composed of four channels connected to cell culture media and a hydrogel scaffold arranged with nine trapezoidal structures. Three different cell types were seeded within the device, namely, astrocytes, primary cortical cells, and HUVEC cells. This simultaneous cell culture allowed a permeability assessment of the *in vitro* BBB. Dextran label particles were introduced to the system to

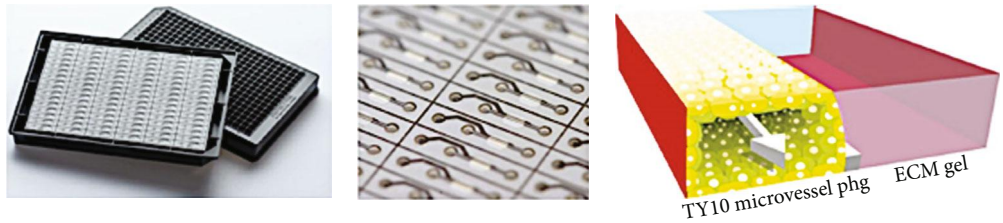

(a) (b) (c)

Figure 26: OrganoPlate device platform. (a) Schematic of the two-lane OrganoPlate. (b) Zoom-in of the bottom of the two-lane OrganoPlate. (c) 3D schematic of the chip. Reproduced (or adapted) with permission [131], ©2018, Springer.

assess the permeability of the endothelial barrier. The structure, natural function, and maturation of each cell type were measured with specific cell markers. The permeability of dextran in cocultures was higher than the respective monolayers. Nevertheless, the device suffered from certain limitations due to the HUVEC differential species of the cells forming leakier barriers that do not mimic the BBB [130].

Another *in vitro* BBB model was developed in a high-throughput membrane-free microfluidic platform. Due to the intrinsic hydrophobicity of PDMS that impedes cell adhesion and can cause nonspecific absorption of proteins and hydrophobic analytes, Wevers et al. [131] chose a commercial microfluidic platform (Figure 26(a)) that employs optical quality glass and polymers that are biocompatible and low compound-absorbing. In this platform, a two-channel OrganoPlate was used for seeding human brain pericytes (hBPCT), human brain microvascular endothelial cells (TY10), and human astrocyte (hAst) cell lines for the evaluation of antibody BBB-shuttle models. In this assay, the transcytosis across the BBB was assessed by the introduction of an antihuman transferrin receptor (MEM-189 mIgG1). The platform allowed for the patterning of ECM gel (Figure 26(c)) through surface tension. A blood vessel was grown adjacent to that gel, and a channel was used to insert the astrocytes and pericytes (Figure 26(b)). The system was free of artificial membranes and accommodated fluid flow through the blood vessels, while allowing fluid phase sampling of molecules that penetrated the endothelial and matrix layers. The tests were performed through the antibody transcytosis assay and Meso scale discovery (MSD). The results showed that the passaging of antibody MEM-189 through the BBB model was approximately twofold higher than the control antibody, indicating that the model can serve as a strong method to study the passage of large molecules and the antibody penetration of brain endothelial cells [131].

Organophosphates (OPs) are one of the principal constituents of insecticides, pesticides, and biological weapons (nerve agents). OP-based compound exposure may occur through direct contact, inhalation, or ingestion. OPs can cause varying levels of toxicity, whose symptoms include diarrhea, nausea, vomiting, sweating, muscle tremors, confusion, drowsiness, seizures, and brain damage [132]. The BBB restricts delivery and permeability of many pharmaceuticals and blood-borne compounds to the central nervous system. However, some OPs can penetrate through the BBB, inhibiting acetylcholinesterase activity, and therefore causing neurotoxicity. Emerging BBB-on-chip models represent a promising alternative to evaluate neurotoxic compounds. Recently, Koo et al. [133] reported a bioprinted 3D platform to study the toxicity of OPs. A microfluidic chip (OrganoPlate) was used to coculture immortalized murine brain endothelial cells, immortalized murine brain neuroblastoma, murine astrocytes, and murine microglia cells (Figures 27(a)–27(c)) to evaluate the *in vitro* neurotoxicity of four OPs: dimethyl methylphosphonate (DMMP), diethyl methylphosphate (DEMP), diethyl cyanophosphonate (DECP), and diethyl chlorophosphate (DCP). The acetylcholinesterase assay showed that DMMP and DEMP can penetrate through the BBB and inhibit acetylcholinesterase activity only at higher concentrations, while DECP and DCP showed strong toxicity even at lower concentrations, inhibiting both acetylcholinesterase and cell viability. These results are similar to the results from *in vivo* counterpart assays [133].

In another report, Shah et al. used a 3D brain-on-a-chip system to evaluate the effect of nitrophenyl isopropyl methylphosphonate (NIMP), commonly called Sarin gas. A commercial MEA device (a tool used for neuronal network studies) with integrated microscopes was used to evaluate the protective effect of pyridostigmine bromide (PB). PB is a drug capable of restoring the enzymatic activity of acetylcholinesterase, when the neurons are exposed to OPs. It was used during the Gulf War as a pretreatment from the harmful effects of nerve agents. Human iPSC-derived neurons and astrocytes pretreated with PB were cultured on the chip and monitored for 35 days. The results showed a higher toxic effect on the cells exposed to NIMP and the cells pretreated with PB, than those cells exposed only to DMSO. Therefore, it is likely that PB does not have the ability penetrate the BBB [134].

In brain cancer, the cells grow to form a mass of tissue that interferes with brain functions. One of the most common types of brain cancer is a glioblastoma. The *in vitro* cancer-on-chip models have been used to study the biological processes of the disease and to evaluate the efficacy of drug therapies. Fan et al. [135] developed a device to study a very aggressive cancer type known as glioblastoma multiform (GlBM). The chip was made of 3-(trimethoxysilyl)propyl methacrylate (TMSPMA) and poly(ethylene glycol)diacrylate (PEGDA) hydrogels fabricated by soft lithography. The GlBM cells (U87) were cultured in the PEGDA hydrogel which formed 3D spheroids within seven days. The effectiveness of two anticancer drugs, pitavastatin and irinotecan, was studied, together with the drug response over the surface of

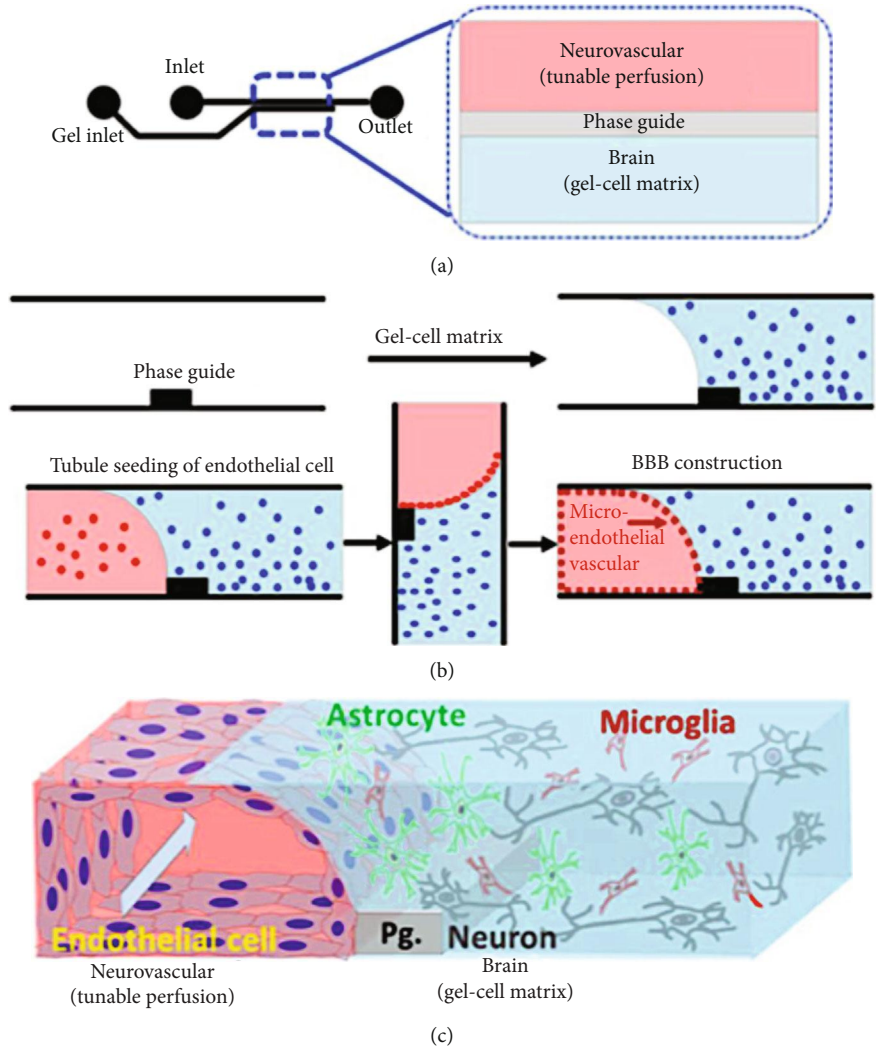

Figure 27: 3D brain construction for high content OP toxicity screening; (a) structure and format application of in vitro culture ware, (b) experimental procedure for constructing 3D neurovascular/brain compartment, and (c) scheme of 3D tetraculture for brain on chip. Reproduced (or adapted) with permission [133], ©2018, Nature.

the spheroids. The results showed that the drugs were diffused through the porous hydrogel matrix into the microwells. Also, it was confirmed that the combination of the two drugs was more effective in reducing the size of the GlBM spheroids, compared with either drug in isolation [135]. All these features provide a key ability to studying drug delivery, as well as determining the pharmacokinetics and pharmacodynamics of new drugs and therapies in the brain.

The high interaction of the cells in the brain requires a considerable research effort to recreate the heterogenicity of cellular communications in microfluidic devices. However, the advances are significant to study the brain barrier drug permeability *in situ* and provide real-time measurement of compounds through the addition of biosensors. This achievement was representative of the enormous need for an accurate brain-on-chip system. Fabrication methods in the future must improve the ability to integrate a better microenvironment for the scaffold-neuronal cells in this complex organ. Furthermore, brain functions are strongly related to, and coordinated by, the entire body; hence, a realistic brain physiology could only be studied in the context of other organs, including the endocrine and circulatory systems.

3. Conclusions and Perspectives

This comprehensive review provides a thorough analysis of the latest advancements in the area of organ-on-chip devices aimed at drug discovery, development, and/or assessment. The latest strategies and achievements reported in the literature highlighting key-playing organs including the liver, kidney, lung, gut, heart, skin, and brain were examined. In addition, the fabrication strategies and the specific application of each device, as well as advantages and disadvantages of each system, were reviewed. Despite the immense advances in the area, there remain a number of significant challenges yet to be addressed with respect to the organ-on-chip devices. Standardization and optimization of the manufacturing methods rely highly on the characteristics of the respective organ, including the anatomical structure, cell interaction, morphology, and basal molecular expression, as

well as the design of the devices, mathematical fluidic modelling, and biocompatibility of the materials used in fabrication, among others.

Another challenge is to facilitate cell heterogenicity. Most studies use immortalized cell lines, primary cell culture, and cell explants, as well as animal or human cells. This may lead to noncomparable results with questionable reproducibility and accuracy that might, in turn, be incompatible with the actual organ. The selection of cells is crucial and should be decided depending on the aim of each developed model. Moreover, high cell viability and long-lasting cell cultures are vital to further explore the potential of these devices. While the majority of the studies have not achieved culture periods longer than 30 days, it is evident that microfluidic systems with continuous flux and automatized circulation could significantly enhance the periodicity of cell viability and culture. Furthermore, frequent supplementation of each specific cell media and mimicked physiological fluid or blood substitute could play a major role in the metabolic functions of the organs. Another important aspect in the fabrication and function of organ-on-chip devices is the validation process. Most studies to date lack the validation step and a close or contemporaneous comparison with the actual organ. A multidisciplinary research approach could dramatically impact all of the involved elements in such devices and would present a major step forward in carefully mimicking human organs. The success of organ-on-chip devices in drug development, drug metabolism, toxicity, safety, and efficacy assays in preclinical trials depends on overcoming each of the mentioned experimental challenges.

Abbreviations

2-DCE-IFM: 2-Deschloroethyl-ifosfamide metabolite
MTT: 3-(4,5-Dimethylthiazol-2-yl)-2,5-diphenyltetrazolium bromide
TMSPMA: 3-(Trimethoxysilyl)propyl methacrylate
DAPI: 4,6-Diamidino-2-phenylindole
ABS: Acrylonitrile butadiene styrene
AKD: Acute kidney disease
A549: Adenocarcinomic human alveolar basal epithelial cells
α-GST: Alpha glutathione *S*-transferase
AD: Alzheimer's disease
ATCC: American Type Culture Collection
AS: Amyotrophic sclerosis
MEM-189 mIgG1: Antihuman transferrin receptor
BLC: Blood loading channel
BBB: Blood-brain barrier
Ca^{++}: Calcium cation
$CaCl_2$: Calcium chloride
CMs: Cardiomyocytes
CVDs: Cardiovascular diseases
CNS: Central nervous system
CKD: Chronic kidney disease
COPD: Chronic obstructive pulmonary disease
Caco-2: Colon adenocarcinoma cells
CLC: Column loading channel
CVB1: Coxsackievirus B1
CysA: Cyclosporin A
CYP450: Cytochrome P450
CYP2D6: Cytochrome P450 family 2, subfamily D, polypeptide 6
CYP2E1: Cytochrome P450 family 2, subfamily E, polypeptide 1
CYP3A4: Cytochrome P450 family 3, subfamily A, polypeptide 4
CYP2B6: Cytochrome P450 family 2, subfamily B, polypeptide 6
CYP2C9: Cytochrome P450 family 2, subfamily C, polypeptide 9
DCP: Diethyl chlorophosphate
DECP: Diethyl cyanophosphonate
DEMP: Diethyl methylphosphate
DMMP: Dimethyl methylphosphonate
DMSO: Dimethyl sulfoxide
DMOG: Dimethyloxalylglycine
DXR: Doxorubicin
DILI: Drug-induced liver injury
DMEM: Dulbecco's modified Eagle's medium
ESCs: Embryonic stem cells
EA.hy926: Endothelial cells
ENM: Engineered nanomaterials
EGFR-TKIs: Epidermal growth factor receptor tyrosine kinase
ECs: Epithelial cells
SU-8: Epoxy-based negative photoresist
EAR: Extracellular acidification rate
ECM: Extracellular matrix
F-actin: Filamentous-actin (protein)
FSS: Fluidic shear stress
FITC: Fluorescent isothiocyanate
FEP: Fluorinated ethylene-propylene
GelMA: Gelatin methacryloyl
GelMA-HM: Gelatin methacryloyl-high degree
GelMA-LM: Gelatin methacryloyl-low degree
GlBM: Glioblastoma multiform
GBM: Glomerular basement membrane
GFR: Glomerular filtration rate
HepaRG: Hepatic biprogenitor cell line
HBV: Hepatitis B virus
HNF4a: Hepatocyte nuclear factor 4 alpha
HiPCs: Hormone independent prostate cells
HAEC: Human aortic endothelial cell line
hAst: Human astrocytes
TY10: Human brain microvascular endothelial cell
hBMECs: Human brain microvascular endothelial cells
hBPCT: Human brain pericytes
hCMEC/D3: Human cerebral microvascular endothelial cell line
HT-29: Human colorectal adenocarcinoma cell line
HEK293: Human embryonal kidney-derived
HaCaT: Human epidermal keratinocytes
HFL1: Human fetal lung fibroblasts
hNPC: Human fetal neural progenitor cells

GM-3348: Human fibroblast
HS27: Human fibroblasts
LX-2: Human hepatic stellate cell
HepG2: Human hepatocellular carcinoma
HepG2/C3: Human hepatocellular carcinoma/complement factor 3
U937: Human histiocytic lymphoma cell line
hiPSC: Human-induced pluripotent stem cells
hIEC: Human intestinal epithelial cells
HIOs: Human intestinal organoids
HK-2: Human kidney epithelial cells
HKMECs: Human kidney microvascular endothelial cells
HK8160: Human Kupffer cells
hCMs: Human primary cardiomyocytes
HPTECs: Human proximal tubular epithelial cells
hRVTU: Human renal vascular-tubular platform
hNT2: Human teratocarcinoma cells
HUVECs: Human umbilical vein endothelial cells
HIF PHDs: Hypoxia inducible factor prolyl hydroxylase
iPSCs: Induced pluripotent stem cells
iHCC: Integrated heart/cancer on a chip
IFN: Interferon
IFN-α: Interferon-alpha
IL-13: Interleukin-13
IL-8: Interleukin-8
ISDN: Isosorbide dinitrate
N/TERT-1: Keratinocytes
KIM-1: Kidney injury molecule-1
LDH: Lactate dehydrogenase
LSEC: Liver sinusoidal endothelial cell
LOC: Liver-on-a-chip
LSOC: Liver-sinusoid-on-a-chip
MDCK: Madin-Darby canine kidney
MSD: Meso scale discovery
mRNA: Messenger ribonucleic acid
miR-122: Micro-RNA-122
μECTs: Microengineered cardiac tissues
MEA: Microelectrode array
MPS: Microphysiological system
MC: Migration channel
MoAb: Monoclonal antibody
MRP2: Multidrug resistance protein 2
NPs: Nanoparticles
NRVMs: Neonatal rat ventricular myocytes
NPC: Nephron progenitor cells
NVU: Neurovascular unit
Nrf2: NF-E2-related transcription factor
NC: Nitrocellulose
NIMP: Nitrophenyl isopropyl methylphosphonate
NAFLD: Nonalcoholic fatty liver disease
NPCs: Nonparenchymal cells
NSCLC: Non-small-cell lung cancer
NHEKs: Normal epidermal keratinocytes
NHDFs: Normal human dermal fibroblasts
OPs: Organophosphates
PD: Parkinson's disease
PM2: Parmodulin-2
PBM: Peripheral blood mononuclear cells
LLC-PK1: Pig kidney cells
PEGDA: Poly(ethylene glycol) diacrylate
PLGA: Poly(lactide-co-glycolide)
PMMA: Poly(methylmethacrylate)
PCL: Polycaprolactone
PC: Polycarbonate
PDA: Polydiacetylene
PDMS: Polydimethylsiloxane
PET: Polyethylene terephthalate
PLA: Polylactic acid
PMB: Polymyxin B
PS: Polystyrene
PTFE: Polytetrafluoroethylene
hAEC: Primary human alveolar cells
Hu8150: Primary human hepatocytes
PiEC: Primary intestinal epithelial cells
PLCs: Primary liver cells
Wnt-3A: Protein
p53: Protein 53
UGT1A1: Protein coding gene
PT: Proximal tubule
PTECs: Proximal tubule epithelial cells
PB: Pyridostigmine bromide
ROS: Reactive oxygen species
RT-qPCR: Real-time polymerase chain reaction
RBC: Red blood cells
RANTES: Regulated on activation, normal T cell expressed and secreted
RBF: Renal blood flow
RPTEC: Renal proximal tubule epithelial cells
RES: Reticuloendothelial system
SEM: Scanning electron microscopy
SiO2: Silicon dioxide
Ag: Silver
SMC: Smooth muscle cells
SGLT2: Sodium-glucose cotransporter-2
SULT1A1: Sulfotransferase 1A1
3D: Three-dimensional
TiO2: Titanium dioxide
TNPs: Titanium dioxide nanoparticles
TEER: Transepithelial electrical resistance
TRPV1: Transient receptor potential V1
TEM: Transmission electron microscopy
TNF-α: Tumor necrosis factor alpha
2D: Two-dimensional
UV: Ultraviolet
VEGF: Vascular endothelial growth factor
WSOC: Wrinkled skin-on-a-chip
ZnO: Zinc oxide
ZO-1: Zonula occludens-1
GGT: γ-Glutamyl transpeptidase.

Conflicts of Interest

The authors declare no conflict of interest.

Authors' Contributions

Aida Rodriguez-Garcia and Jacqueline Oliva-Ramirez have contributed equally to this work.

Acknowledgments

The authors would like to acknowledge the financial and technical support of Writing Lab, TecLabs, and Tecnológico de Monterrey for the production of this work. The graphical abstract was created by BioRender software through a licensed subscription.

Supplementary Materials

The supplementary file includes graphical abstract of the manuscript. *(Supplementary Materials)*

References

[1] B. Zhang, A. Korolj, B. F. L. Lai, and M. Radisic, "Advances in organ-on-a-chip engineering," *Nature Reviews Materials*, vol. 3, no. 8, pp. 257–278, 2018.

[2] J. Park, I. Wetzel, I. Marriott et al., "A 3D human triculture system modeling neurodegeneration and neuroinflammation in Alzheimer's disease," *Nature Neuroscience*, vol. 21, no. 7, pp. 941–951, 2018.

[3] M. E. Katt, A. L. Placone, A. D. Wong, Z. S. Xu, and P. C. Searson, "In vitro tumor models: advantages, disadvantages, variables, and selecting the right platform," *Frontiers in Bioengineering and Biotechnology*, vol. 4, 2016.

[4] I. W. Mak, N. Evaniew, and M. Ghert, "Lost in translation: animal models and clinical trials in cancer treatment," *American Journal of Translational Research*, vol. 6, no. 2, pp. 114–118, 2014.

[5] Q. Wu, J. Liu, X. Wang et al., "Organ-on-a-chip: recent breakthroughs and future prospects," *Biomedical Engineering Online*, vol. 19, no. 1, p. 9, 2020.

[6] Y. S. Zhang, K. Yue, J. Aleman et al., "3D bioprinting for tissue and organ fabrication," *Annals of Biomedical Engineering*, vol. 45, no. 1, pp. 148–163, 2017.

[7] S.-S. Yoo, "3D-printed biological organs: medical potential and patenting opportunity," *Expert Opinion on Therapeutic Patents*, vol. 25, no. 5, pp. 507–511, 2015.

[8] W. Peng, P. Datta, B. Ayan, V. Ozbolat, D. Sosnoski, and I. T. Ozbolat, "3D bioprinting for drug discovery and development in pharmaceutics," *Acta Biomaterialia*, vol. 57, pp. 26–46, 2017.

[9] S. H. Lee and J. H. Sung, "Organ-on-a-chip technology for reproducing multiorgan physiology," *Advanced Healthcare Materials*, vol. 7, no. 2, article 1700419, 2018.

[10] R. K. Kankala, S.-B. Wang, and A.-Z. Chen, "Microengineered organ-on-a-chip platforms towards personalized medicine," *Current Pharmaceutical Design*, vol. 24, no. 45, pp. 5354–5366, 2018.

[11] H. Kimura, Y. Sakai, and T. Fujii, "Organ/body-on-a-chip based on microfluidic technology for drug discovery," *Drug Metabolism and Pharmacokinetics*, vol. 33, no. 1, pp. 43–48, 2018.

[12] S. E. Park, A. Georgescu, and D. Huh, "Organoids-on-a-chip," *Science*, vol. 364, no. 6444, pp. 960–965, 2019.

[13] G. Tuschl, B. Lauer, and S. O. Mueller, "Primary hepatocytes as a model to analyze species-specific toxicity and drug metabolism," *Expert Opinion on Drug Metabolism & Toxicology*, vol. 4, no. 7, pp. 855–870, 2008.

[14] W. B. Jakoby and I. H. Pastan, *Methods in Enzymology: Cell Culture*, Academic Press, New York, NY, USA, 1979.

[15] T. Mseka, J. R. Bamburg, and L. P. Cramer, "ADF/cofilin family proteins control formation of oriented actin-filament bundles in the cell body to trigger fibroblast polarization," *Journal of Cell Science*, vol. 120, no. 24, pp. 4332–4344, 2007.

[16] J. Rodés, J. P. Benhamou, A. Blei et al., *Textbook of Hepatology: From Basic Science to Clinical Practice*, Wiley-Blackwell Publishing, 3rd edition, 2008, https://www.wiley.com/en-us/Textbook+of+Hepatology&;3A+From+Basic+Science+to+Clinical+Practice&2C+3rd+Edition-p-9781405181518.

[17] L. DeLeve, "Hepatic microvasculature in liver injury," *Seminars in Liver Disease*, vol. 27, no. 4, pp. 390–400, 2007.

[18] T. Adachi, H. Nakagawa, I. Chung et al., "Nrf2-dependent and -independent induction of ABC transporters ABCC1, ABCC2, and ABCG2 in HepG2 cells under oxidative stress," *Journal of Experimental Therapeutics and Oncology*, vol. 6, no. 4, pp. 335–348, 2007.

[19] K. P. Kanebratt and T. B. Andersson, "Evaluation of HepaRG cells as an in vitro model for human drug metabolism studies," *Drug Metabolism and Disposition*, vol. 36, no. 7, pp. 1444–1452, 2008.

[20] S. J. Lee, Y. J. Lee, and K. K. Park, "The pathogenesis of drug-induced liver injury," *Expert Review of Gastroenterology and Hepatology*, vol. 10, no. 10, pp. 1175–1185, 2016.

[21] A. Choe, S. K. Ha, I. Choi, N. Choi, and J. H. Sung, "Microfluidic gut-liver chip for reproducing the first pass metabolism," *Biomedical Microdevices*, vol. 19, no. 1, 2017.

[22] Y. Wang, W. Su, L. Wang et al., "Paper supported long-term 3D liver co-culture model for the assessment of hepatotoxic drugs," *Toxicology Research*, vol. 7, no. 1, pp. 13–21, 2018.

[23] N. S. Bhise, V. Manoharan, S. Massa et al., "A liver-on-a-chip platform with bioprinted hepatic spheroids," *Biofabrication*, vol. 8, no. 1, article 014101, 2016.

[24] B. Corrado, V. Gregorio, G. Imparato, C. Attanasio, F. Urciuolo, and P. A. Netti, "A three-dimensional microfluidized liver system to assess hepatic drug metabolism and hepatotoxicity," *Biotechnology and Bioengineering*, vol. 116, no. 5, pp. 1152–1163, 2019.

[25] A. M. Ortega-Prieto, J. K. Skelton, S. N. Wai et al., "3D microfluidic liver cultures as a physiological preclinical tool for hepatitis B virus infection," *Nature Communications*, vol. 9, no. 1, 2018.

[26] A. A. Zakhariants, O. A. Burmistrova, M. Y. Shkurnikov, A. A. Poloznikov, and D. A. Sakharov, "Development of a specific substrate—inhibitor panel (liver-on-a-chip) for evaluation of cytochrome P450 activity," *Bulletin of Experimental Biology and Medicine*, vol. 162, no. 1, pp. 170–174, 2016.

[27] A. A. Zakharyants, O. A. Burmistrova, and A. A. Poloznikov, "The use of human liver cell model and cytochrome P450 substrate—inhibitor panel for studies of dasatinib and warfarin interactions," *Bulletin of Experimental Biology and Medicine*, vol. 162, no. 4, pp. 515–519, 2017.

[28] A. J. Foster, B. Chouhan, S. L. Regan et al., "Integrated in vitro models for hepatic safety and metabolism: evaluation of a human liver-chip and liver spheroid," *Archives of Toxicology*, vol. 93, no. 4, pp. 1021–1037, 2019.

[29] T. J. Long, P. A. Cosgrove, R. T. Dunn II et al., "Modeling therapeutic antibody-small molecule drug-drug interactions using a three-dimensional perfusable human liver coculture platform," *Drug Metabolism and Disposition*, vol. 44, no. 12, pp. 1940–1948, 2016.

[30] U. Sarkar, K. C. Ravindra, E. Large et al., "Integrated assessment of diclofenac biotransformation, pharmacokinetics, and omics-based toxicity in a three-dimensional human liver-immunocompetent coculture system," *Drug Metabolism and Disposition*, vol. 45, no. 7, pp. 855–866, 2017.

[31] N. Tsamandouras, T. Kostrzewski, C. L. Stokes, L. G. Griffith, D. J. Hughes, and M. Cirit, "Quantitative assessment of population variability in hepatic drug metabolism using a perfused three-dimensional human liver microphysiological system," *Journal of Pharmacology and Experimental Therapeutics*, vol. 360, no. 1, pp. 95–105, 2017.

[32] C. Rowe, M. Shaeri, E. Large et al., "Perfused human hepatocyte microtissues identify reactive metabolite-forming and mitochondria-perturbing hepatotoxins," *Toxicology In Vitro*, vol. 46, pp. 29–38, 2018.

[33] B. Delalat, C. Cozzi, S. Rasi Ghaemi et al., "Microengineered bioartificial liver chip for drug toxicity screening," *Advanced Functional Materials*, vol. 28, no. 28, article 1801825, 2018.

[34] W. R. Proctor, A. J. Foster, J. Vogt et al., "Utility of spherical human liver microtissues for prediction of clinical drug-induced liver injury," *Archives of Toxicology*, vol. 91, no. 8, pp. 2849–2863, 2017.

[35] R. Jellali, T. Bricks, S. Jacques et al., "Long-term human primary hepatocyte cultures in a microfluidic liver biochip show maintenance of mRNA levels and higher drug metabolism compared with Petri cultures," *Biopharmaceutics & Drug Disposition*, vol. 37, no. 5, pp. 264–275, 2016.

[36] A. A. Poloznikov, S. V. Nikulin, A. A. Zakhariants et al., ""Branched tail" oxyquinoline inhibitors of HIF prolyl hydroxylase: early evaluation of toxicity and metabolism using liver-on-a-chip," *Drug Metabolism Letters*, vol. 13, no. 1, pp. 45–52, 2019.

[37] J. Theobald, A. Ghanem, P. Wallisch et al., "Liver-kidney-on-chip to study toxicity of drug metabolites," *ACS Biomaterials Science & Engineering*, vol. 4, no. 1, pp. 78–89, 2017.

[38] J. Deng, X. Zhang, Z. Chen et al., "A cell lines derived microfluidic liver model for investigation of hepatotoxicity induced by drug-drug interaction," *Biomicrofluidics*, vol. 13, no. 2, article 024101, 2019.

[39] S. Prill, D. Bavli, G. Levy et al., "Real-time monitoring of oxygen uptake in hepatic bioreactor shows CYP450-independent mitochondrial toxicity of acetaminophen and amiodarone," *Archives of Toxicology*, vol. 90, no. 5, pp. 1181–1191, 2016.

[40] H. Pein, A. Ville, S. Pace et al., "Endogenous metabolites of vitamin E limit inflammation by targeting 5-lipoxygenase," *Nature Communications*, vol. 9, no. 1, p. 3834, 2018.

[41] S. Mi, X. Yi, Z. du, Y. Xu, and W. Sun, "Construction of a liver sinusoid based on the laminar flow on chip and self-assembly of endothelial cells," *Biofabrication*, vol. 10, no. 2, article 025010, 2018.

[42] Y.-S. Weng, S. F. Chang, M. C. Shih, S. H. Tseng, and C. H. Lai, "Scaffold-free liver-on-a-chip with multiscale organotypic cultures," *Advanced Materials*, vol. 29, no. 36, p. 1701545, 2017.

[43] S. K. Nigam, W. Wu, K. T. Bush, M. P. Hoenig, R. C. Blantz, and V. Bhatnagar, "Handling of drugs, metabolites, and uremic toxins by kidney proximal tubule drug transporters," *Clinical Journal of the American Society of Nephrology*, vol. 10, no. 11, pp. 2039–2049, 2015.

[44] R. Huang, W. Zheng, W. Liu, W. Zhang, Y. Long, and X. Jiang, "Investigation of tumor cell behaviors on a vascular microenvironment- mimicking microfluidic chip," *Scientific Reports*, vol. 5, no. 1, article 17768, 2015.

[45] Y. Sakuta, I. Takehara, K.-i. Tsunoda, and K. Sato, "Development of a microfluidic system comprising dialysis and secretion components for a bioassay of renal clearance," *Analytical Sciences*, vol. 34, no. 9, pp. 1073–1078, 2018.

[46] E. J. Weber, A. Chapron, B. D. Chapron et al., "Development of a microphysiological model of human kidney proximal tubule function," *Kidney International*, vol. 90, no. 3, pp. 627–637, 2016.

[47] K. A. Homan, D. B. Kolesky, M. A. Skylar-Scott et al., "Bioprinting of 3D convoluted renal proximal tubules on perfusable chips," *Scientific Reports*, vol. 6, no. 1, article 34845, 2016.

[48] T. T. G. Nieskens and A.-K. Sjögren, "Emerging in vitro systems to screen and predict drug-induced kidney toxicity," *Seminars in Nephrology*, vol. 39, no. 2, pp. 215–226, 2019.

[49] M. Adler, S. Ramm, M. Hafner et al., "A quantitative approach to screen for nephrotoxic compounds in vitro," *Journal of the American Society of Nephrology*, vol. 27, no. 4, pp. 1015–1028, 2016.

[50] M. J. Ryan, G. Johnson, J. Kirk, S. M. Fuerstenberg, R. A. Zager, and B. Torok-Storb, "HK-2: an immortalized proximal tubule epithelial cell line from normal adult human kidney," *Kidney International*, vol. 45, no. 1, pp. 48–57, 1994.

[51] G. Gstraunthaler, W. Pfaller, and P. Kotanko, "Biochemical characterization of renal epithelial cell cultures (LLC-PK1 and MDCK)," *American Journal of Physiology-Renal Physiology*, vol. 248, no. 4, pp. F536–F544, 1985.

[52] M. A. Perazella, "Renal vulnerability to drug toxicity," *Clinical Journal of the American Society of Nephrology*, vol. 4, no. 7, pp. 1275–1283, 2009.

[53] J. Sateesh, K. Guha, A. Dutta, P. Sengupta, and K. Srinivasa Rao, "Design and analysis of microfluidic kidney-on-chip model: fluid shear stress based study with temperature effect," *Microsystem Technologies*, vol. 25, no. 7, pp. 2553–2560, 2019.

[54] S. Kim, S. C. LesherPerez, B. . C. Kim et al., "Pharmacokinetic profile that reduces nephrotoxicity of gentamicin in a perfused kidney-on-a-chip," *Biofabrication*, vol. 8, no. 1, article 015021, 2016.

[55] S. Musah, N. Dimitrakakis, D. M. Camacho, G. M. Church, and D. E. Ingber, "Directed differentiation of human induced pluripotent stem cells into mature kidney podocytes and establishment of a glomerulus chip," *Nature Protocols*, vol. 13, no. 7, pp. 1662–1685, 2018.

[56] Y. S. Zhang, A. Arneri, S. Bersini et al., "Bioprinting 3D microfibrous scaffolds for engineering endothelialized myocardium and heart-on-a-chip," *Biomaterials*, vol. 110, pp. 45–59, 2016.

[57] L. Yang, S. V. Shridhar, M. Gerwitz, and P. Soman, "Anin vitrovascular chip using 3D printing-enabled hydrogel casting," *Biofabrication*, vol. 8, no. 3, article 035015, 2016.

[58] S. Musah, A. Mammoto, T. C. Ferrante et al., "Mature induced-pluripotent-stem-cell-derived human podocytes reconstitute kidney glomerular-capillary-wall function on a chip," *Nature Biomedical Engineering*, vol. 1, no. 5, p. 0069, 2017.

[59] L. H. Lash, "Role of bioactivation reactions in chemically induced nephrotoxicity," in *Drug Metabolism Handbook*, pp. 761–781, Wiley Online Library, 2008.

[60] E. J. Weber, K. A. Lidberg, L. Wang et al., "Human kidney on a chip assessment of polymyxin antibiotic nephrotoxicity," *JCI Insight*, vol. 3, no. 24, 2018.

[61] K. A. Homan, N. Gupta, K. T. Kroll et al., "Flow-enhanced vascularization and maturation of kidney organoids in vitro," *Nature Methods*, vol. 16, no. 3, pp. 255–262, 2019.

[62] S. G. Rayner, K. T. Phong, J. Xue et al., "Reconstructing the human renal vascular–tubular unit in vitro," *Advanced Healthcare Materials*, vol. 7, no. 23, article 1801120, 2018.

[63] D. Aschenbrenner, O. Friedrich, and D. F. Gilbert, "3D printed lab-on-a-chip platform for chemical stimulation and parallel analysis of ion channel function," *Micromachines*, vol. 10, no. 8, p. 548, 2019.

[64] M. I. Bogorad and P. C. Searson, "Real-time imaging and quantitative analysis of doxorubicin transport in a perfusable microvessel platform," *Integrative Biology*, vol. 8, no. 9, pp. 976–984, 2016.

[65] S. Cho, A. Islas-Robles, A. M. Nicolini, T. J. Monks, and J. Y. Yoon, "In situ, dual-mode monitoring of organ-on-a-chip with smartphone-based fluorescence microscope," *Biosensors and Bioelectronics*, vol. 86, pp. 697–705, 2016.

[66] J. A. Zepp and E. E. Morrisey, "Cellular crosstalk in the development and regeneration of the respiratory system," *Nature Reviews Molecular Cell Biology*, vol. 20, no. 9, pp. 551–566, 2019.

[67] K. H. Benam, R. Villenave, C. Lucchesi et al., "Small airway-on-a-chip enables analysis of human lung inflammation and drug responses in vitro," *Nature Methods*, vol. 13, no. 2, pp. 151–157, 2016.

[68] M. Humayun, C.-W. Chow, and E. W. K. Young, "Microfluidic lung airway-on-a-chip with arrayable suspended gels for studying epithelial and smooth muscle cell interactions," *Lab on a Chip*, vol. 18, no. 9, pp. 1298–1309, 2018.

[69] A. O. Stucki, J. D. Stucki, S. R. R. Hall et al., "A lung-on-a-chip array with an integrated bio-inspired respiration mechanism," *Lab on a Chip*, vol. 15, no. 5, pp. 1302–1310, 2015.

[70] X.-J. Liu, S. W. Hu, B. Y. Xu et al., "Microfluidic liquid-air dual-gradient chip for synergic effect bio-evaluation of air pollutant," *Talanta*, vol. 182, pp. 202–209, 2018.

[71] D. Huh, "A human breathing lung-on-a-chip," *Annals of the American Thoracic Society*, vol. 12, Supplement 1, pp. S42–S44, 2015.

[72] A. Jain, R. Barrile, A. van der Meer et al., "Primary human lung alveolus-on-a-chip model of intravascular thrombosis for assessment of therapeutics," *Clinical Pharmacology & Therapeutics*, vol. 103, no. 2, pp. 332–340, 2018.

[73] X. Yang, K. Li, X. Zhang et al., "Nanofiber membrane supported lung-on-a-chip microdevice for anti-cancer drug testing," *Lab on a Chip*, vol. 18, no. 3, pp. 486–495, 2018.

[74] J. Jia'en Li, S. Muralikrishnan, C.-T. Ng, L.-Y. L. Yung, and B.-H. Bay, "Nanoparticle-induced pulmonary toxicity," *Experimental Biology and Medicine*, vol. 235, no. 9, pp. 1025–1033, 2010.

[75] M. Zhang, C. Xu, L. Jiang, and J. Qin, "A 3D human lung-on-a-chip model for nanotoxicity testing," *Toxicology Research*, vol. 7, no. 6, pp. 1048–1060, 2018.

[76] H. Moghadas, M. S. Saidi, N. Kashaninejad, and N. T. Nguyen, "Challenge in particle delivery to cells in a microfluidic device," *Drug Delivery and Translational Research*, vol. 8, no. 3, pp. 830–842, 2018.

[77] K.-Y. Shim, D. Lee, J. Han, N.-T. Nguyen, S. Park, and J. H. Sung, "Microfluidic gut-on-a-chip with three-dimensional villi structure," *Biomedical Microdevices*, vol. 19, no. 2, p. 37, 2017.

[78] X. He, D. O. Mishchuk, J. Shah, B. C. Weimer, and C. M. Slupsky, "Cross-talk between E. coli strains and a human colorectal adenocarcinoma- derived cell line," *Scientific Reports*, vol. 3, no. 1, p. 3416, 2013.

[79] H. J. Kim, D. Huh, G. Hamilton, and D. E. Ingber, "Human gut-on-a-chip inhabited by microbial flora that experiences intestinal peristalsis-like motions and flow," *Lab on a Chip*, vol. 12, no. 12, pp. 2165–2174, 2012.

[80] W. Shin, L. A. Hackley, and H. J. Kim, ""Good fences make good neighbors": how does the human gut microchip unravel mechanism of intestinal inflammation?," *Gut Microbes*, vol. 11, no. 3, pp. 581–586, 2020.

[81] F. P. Guengerich, "Cytochrome P450 and chemical toxicology," *Chemical Research in Toxicology*, vol. 21, no. 1, pp. 70–83, 2008.

[82] H. J. Kim and D. E. Ingber, "Gut-on-a-chip microenvironment induces human intestinal cells to undergo villus differentiation," *Integrative Biology*, vol. 5, no. 9, pp. 1130–1140, 2013.

[83] H. J. Kim, H. Li, J. J. Collins, and D. E. Ingber, "Contributions of microbiome and mechanical deformation to intestinal bacterial overgrowth and inflammation in a human gut-on-a-chip," *Proceedings of the National Academy of Sciences of the United States of America*, vol. 113, no. 1, pp. E7–E15, 2016.

[84] S. Jalili-Firoozinezhad, R. Prantil-Baun, A. Jiang et al., "Modeling radiation injury-induced cell death and countermeasure drug responses in a human gut-on-a-chip," *Cell Death & Disease*, vol. 9, no. 2, p. 223, 2018.

[85] R. Villenave, S. Q. Wales, T. Hamkins-Indik et al., "Human gut-on-a-chip supports polarized infection of coxsackie B1 virus in vitro," *PLoS One*, vol. 12, no. 2, article e0169412, 2017.

[86] J. R. Spence, C. N. Mayhew, S. A. Rankin et al., "Directed differentiation of human pluripotent stem cells into intestinal tissue in vitro," *Nature*, vol. 470, no. 7332, pp. 105–109, 2011.

[87] M. Kasendra, A. Tovaglieri, A. Sontheimer-Phelps et al., "Development of a primary human Small Intestine-on-a-Chip using biopsy- derived organoids," *Scientific Reports*, vol. 8, no. 1, p. 2871, 2018.

[88] M. J. Workman, J. P. Gleeson, E. J. Troisi et al., "Enhanced utilization of induced pluripotent stem cell–derived human intestinal organoids using microengineered chips," *Cellular and Molecular Gastroenterology and Hepatology*, vol. 5, no. 4, pp. 669–677.e2, 2018.

[89] S. P. Claus, S. L. Ellero, B. Berger et al., "Colonization-induced host-gut microbial metabolic interaction," *mBio*, vol. 2, no. 2, 2011.

[90] D.-H. Yoo, I. S. Kim, T. K. van le, I. H. Jung, H. H. Yoo, and D. H. Kim, "Gut microbiota-mediated drug interactions between lovastatin and antibiotics," *Drug Metabolism and Disposition*, vol. 42, no. 9, pp. 1508–1513, 2014.

[91] A. Sharma, M. M. Buschmann, and J. A. Gilbert, "Pharmacomicrobiomics: the holy grail to variability in drug response?," *Clinical Pharmacology & Therapeutics*, vol. 106, no. 2, pp. 317–328, 2019.

[92] M. Renouf and S. Hendrich, "Bacteroides uniformis is a putative bacterial species associated with the degradation of the isoflavone genistein in human feces," *The Journal of Nutrition*, vol. 141, no. 6, pp. 1120–1126, 2011.

[93] Y. Guo, Z. Li, W. Su, L. Wang, Y. Zhu, and J. Qin, "A biomimetic human gut-on-a-chip for modeling drug metabolism in intestine," *Artificial Organs*, vol. 42, no. 12, pp. 1196–1205, 2018.

[94] L. R. Madden, T. V. Nguyen, S. Garcia-Mojica et al., "Bioprinted 3D primary human intestinal tissues model aspects of native physiology and ADME/Tox functions," *iScience*, vol. 2, pp. 156–167, 2018.

[95] H.-Y. Tan, S. Trier, U. L. Rahbek, M. Dufva, J. P. Kutter, and T. L. Andresen, "A multi-chamber microfluidic intestinal barrier model using Caco-2 cells for drug transport studies," *PLoS One*, vol. 13, no. 5, article e0197101, 2018.

[96] M. Hiraoka, "Mechanisms of drug-induced cardiac toxicity," in *Electrical Diseases of the Heart*, I. Gussak, C. Antzelevitch, A. A. M. Wilde, P. A. Friedman, M. J. Ackerman, and W. K. Shen, Eds., pp. 691–704, Springer, London, UK, 2008.

[97] H. Savoji, M. H. Mohammadi, N. Rafatian et al., "Cardiovascular disease models: a game changing paradigm in drug discovery and screening," *Biomaterials*, vol. 198, pp. 3–26, 2019.

[98] N. Annabi, K. Tsang, S. M. Mithieux et al., "Highly elastic micropatterned hydrogel for engineering functional cardiac tissue," *Advanced Functional Materials*, vol. 23, no. 39, pp. 4950–4959, 2013.

[99] F. Fu, L. Shang, Z. Chen, Y. Yu, and Y. Zhao, "Bioinspired living structural color hydrogels," *Science Robotics*, vol. 3, no. 16, 2018.

[100] K.-i. Kamei, Y. Kato, Y. Hirai et al., "Integrated heart/cancer on a chip to reproduce the side effects of anti-cancer drugs in vitro," *RSC Advances*, vol. 7, no. 58, pp. 36777–36786, 2017.

[101] A. Marsano, C. Conficconi, M. Lemme et al., "Beating heart on a chip: a novel microfluidic platform to generate functional 3D cardiac microtissues," *Lab on a Chip*, vol. 16, no. 3, pp. 599–610, 2016.

[102] M. R. Gwinn and V. Vallyathan, "Nanoparticles: health effects—pros and cons," *Environmental Health Perspectives*, vol. 114, no. 12, pp. 1818–1825, 2006.

[103] S. Ahn, H. A. M. Ardoña, J. U. Lind et al., "Mussel-inspired 3D fiber scaffolds for heart-on-a-chip toxicity studies of engineered nanomaterials," *Analytical and Bioanalytical Chemistry*, vol. 410, no. 24, pp. 6141–6154, 2018.

[104] F. Fu, Z. Chen, Z. Zhao et al., "Bio-inspired self-healing structural color hydrogel," *Proceedings of the National Academy of Sciences*, vol. 114, no. 23, pp. 5900–5905, 2017.

[105] M. Yang, H. Chan, G. Zhao et al., "Self-assembly of nanoparticles into biomimetic capsid-like nanoshells," *Nature Chemistry*, vol. 9, no. 3, pp. 287–294, 2017.

[106] B. Bharti, A. L. Fameau, M. Rubinstein, and O. D. Velev, "Nanocapillarity-mediated magnetic assembly of nanoparticles into ultraflexible filaments and reconfigurable networks," *Nature Materials*, vol. 14, no. 11, pp. 1104–1109, 2015.

[107] A. R. Studart, "Additive manufacturing of biologically-inspired materials," *Chemical Society Reviews*, vol. 45, no. 2, pp. 359–376, 2016.

[108] M. Wufuer, G. H. Lee, W. Hur et al., "Skin-on-a-chip model simulating inflammation, edema and drug-based treatment," *Scientific Reports*, vol. 6, no. 1, article 37471, 2016.

[109] S. Lee, S. P. Jin, Y. K. Kim, G. Y. Sung, J. H. Chung, and J. H. Sung, "Construction of 3D multicellular microfluidic chip for an in vitro skin model," *Biomedical Microdevices*, vol. 19, no. 2, p. 22, 2017.

[110] A. L. M. Ruela, A. G. Perissinato, M. E. . S. Lino, P. S. Mudrik, and G. R. Pereira, "Evaluation of skin absorption of drugs from topical and transdermal formulations," *Brazilian Journal of Pharmaceutical Sciences*, vol. 52, no. 3, pp. 527–544, 2016.

[111] M.-A. Bolzinger, S. Briançon, J. Pelletier, and Y. Chevalier, "Penetration of drugs through skin, a complex rate-controlling membrane," *Current Opinion in Colloid & Interface Science*, vol. 17, no. 3, pp. 156–165, 2012.

[112] H. Y. Lim, J. Kim, H. J. Song et al., "Development of wrinkled skin-on-a-chip (WSOC) by cyclic uniaxial stretching," *Journal of Industrial and Engineering Chemistry*, vol. 68, pp. 238–245, 2018.

[113] N. Mori, Y. Morimoto, and S. Takeuchi, "Skin integrated with perfusable vascular channels on a chip," *Biomaterials*, vol. 116, pp. 48–56, 2017.

[114] J. J. Kim, F. Ellett, C. N. Thomas et al., "A microscale, full-thickness, human skin on a chip assay simulating neutrophil responses to skin infection and antibiotic treatments," *Lab on a Chip*, vol. 19, no. 18, pp. 3094–3103, 2019.

[115] S.-F. Ng, J. J. Rouse, F. D. Sanderson, V. Meidan, and G. M. Eccleston, "Validation of a static Franz diffusion cell system for in vitro permeation studies," *AAPS PharmSciTech*, vol. 11, no. 3, pp. 1432–1441, 2010.

[116] B. Lukács, Á. Bajza, D. Kocsis et al., "Skin-on-a-chip device for ex vivo monitoring of transdermal delivery of drugs—design, fabrication, and testing," *Pharmaceutics*, vol. 11, no. 9, p. 445, 2019.

[117] M. Alberti, Y. Dancik, G. Sriram et al., "Multi-chamber microfluidic platform for high-precision skin permeation testing," *Lab on a Chip*, vol. 17, no. 9, pp. 1625–1634, 2017.

[118] Q. Ramadan and F. C. W. Ting, "In vitro micro-physiological immune-competent model of the human skin," *Lab on a Chip*, vol. 16, no. 10, pp. 1899–1908, 2016.

[119] F. Alexander, S. Eggert, and J. Wiest, "Skin-on-a-chip: transepithelial electrical resistance and extracellular acidification measurements through an automated air-liquid interface," *Genes*, vol. 9, no. 2, p. 114, 2018.

[120] P. Tucci, G. Porta, M. Agostini et al., "Metabolic effects of TiO_2 nanoparticles, a common component of sunscreens and cosmetics, on human keratinocytes," *Cell Death & Disease*, vol. 4, no. 3, article e549, 2013.

[121] S. McCormick, L. E. Smith, A. M. Holmes et al., "Multiparameter toxicity screening on a chip: effects of UV radiation and titanium dioxide nanoparticles on HaCaT cells," *Biomicrofluidics*, vol. 13, no. 4, article 044112, 2019.

[122] N. Hakimi, R. Cheng, L. Leng et al., "Handheld skin printer: in situ formation of planar biomaterials and tissues," *Lab on a Chip*, vol. 18, no. 10, pp. 1440–1451, 2018.

[123] S. Biglari, T. Y. L. le, R. P. Tan et al., "Simulating inflammation in a wound microenvironment using a dermal wound-on-a-chip model," *Advanced Healthcare Materials*, vol. 8, no. 1, article 1801307, 2019.

[124] D. Pamies, T. Hartung, and H. T. Hogberg, "Biological and medical applications of a brain-on-a-chip," *Experimental Biology and Medicine*, vol. 239, no. 9, pp. 1096–1107, 2014.

[125] J. Park, B. K. Lee, G. S. Jeong, J. K. Hyun, C. J. Lee, and S. H. Lee, "Three-dimensional brain-on-a-chip with an interstitial level of flow and its application as an in vitro model of Alzheimer's disease," *Lab on a Chip*, vol. 15, no. 1, pp. 141–150, 2015.

[126] Y. I. Wang, H. E. Abaci, and M. L. Shuler, "Microfluidic blood-brain barrier model provides in vivo-like barrier properties for drug permeability screening," *Biotechnology and Bioengineering*, vol. 114, no. 1, pp. 184–194, 2017.

[127] G.-F. Chen, T. H. Xu, Y. Yan et al., "Amyloid beta: structure, biology and structure-based therapeutic development," *Acta Pharmacologica Sinica*, vol. 38, no. 9, pp. 1205–1235, 2017.

[128] M. Tajes, E. Ramos-Fernández, X. Weng-Jiang et al., "The blood-brain barrier: structure, function and therapeutic approaches to cross it," *Molecular Membrane Biology*, vol. 31, no. 5, pp. 152–167, 2014.

[129] J. A. Brown, V. Pensabene, D. A. Markov et al., "Recreating blood-brain barrier physiology and structure on chip: a novel neurovascular microfluidic bioreactor," *Biomicrofluidics*, vol. 9, no. 5, article 054124, 2015.

[130] G. Adriani, D. Ma, A. Pavesi, R. D. Kamm, and E. L. K. Goh, "A 3D neurovascular microfluidic model consisting of neurons, astrocytes and cerebral endothelial cells as a blood-brain barrier," *Lab on a Chip*, vol. 17, no. 3, pp. 448–459, 2017.

[131] N. R. Wevers, D. G. Kasi, T. Gray et al., "A perfused human blood–brain barrier on-a-chip for high-throughput assessment of barrier function and antibody transport," *Fluids and Barriers of the CNS*, vol. 15, no. 1, p. 23, 2018.

[132] A. Adeyinka and L. Pierre, *Organophosphates*, StatPearls: Treasure Island, 2019.

[133] Y. Koo, B. T. Hawkins, and Y. Yun, "Three-dimensional (3D) tetra-culture brain on chip platform for organophosphate toxicity screening," *Scientific Reports*, vol. 8, no. 1, p. 2841, 2018.

[134] J. Shah, H. Enright, D. Lam et al., *Evaluating the organophosphate NIMP on a 3D-brain-on-a-chip system*, Lawrence Livermore National Lab.(LLNL), 2019.

[135] Y. Fan, D. T. Nguyen, Y. Akay, F. Xu, and M. Akay, "Engineering a brain cancer chip for high-throughput drug screening," *Scientific Reports*, vol. 6, no. 1, article 25062, 2016.

[136] L.-D. Ma, Y. T. Wang, J. R. Wang et al., "Design and fabrication of a liver-on-a-chip platform for convenient, highly efficient, and safe in situ perfusion culture of 3D hepatic spheroids," *Lab on a Chip*, vol. 18, no. 17, pp. 2547–2562, 2018.

[137] Y. Liu, K. Hu, and Y. Wang, "Primary hepatocytes cultured on a fiber-embedded PDMS chip to study drug metabolism," *Polymers*, vol. 9, no. 12, p. 215, 2017.

[138] A. A. Poloznikov, A. A. Zakhariants, S. V. Nikulin et al., "Structure-activity relationship for branched oxyquinoline HIF activators: effect of modifications to phenylacetamide "tail"," *Biochimie*, vol. 133, pp. 74–79, 2017.

[139] J. Theobald, M. A. Abu el Maaty, N. Kusterer et al., "In vitro metabolic activation of vitamin D3 by using a multi-compartment microfluidic liver-kidney organ on chip platform," *Scientific Reports*, vol. 9, no. 1, p. 4616, 2019.

[140] D. W. Lee, S. K. Ha, I. Choi, and J. H. Sung, "3D gut-liver chip with a PK model for prediction of first-pass metabolism," *Biomedical Microdevices*, vol. 19, no. 4, p. 100, 2017.

[141] A. Skardal, M. Devarasetty, S. Forsythe, A. Atala, and S. Soker, "A reductionist metastasis-on-a-chip platform for in vitro tumor progression modeling and drug screening," *Biotechnology and Bioengineering*, vol. 113, no. 9, pp. 2020–2032, 2016.

[142] D. Onozato, M. Yamashita, A. Nakanishi et al., "Generation of intestinal organoids suitable for pharmacokinetic studies from human induced pluripotent stem cells," *Drug Metabolism and Disposition*, vol. 46, no. 11, pp. 1572–1580, 2018.

[143] O. Kilic, D. Pamies, E. Lavell et al., "Brain-on-a-chip model enables analysis of human neuronal differentiation and chemotaxis," *Lab on a Chip*, vol. 16, no. 21, pp. 4152–4162, 2016.

[144] T. D. Brown, M. Nowak, A. V. Bayles et al., "A microfluidic model of human brain (μHuB) for assessment of blood brain barrier," *Bioengineering & Translational Medicine*, vol. 4, no. 2, article e10126, 2019.